

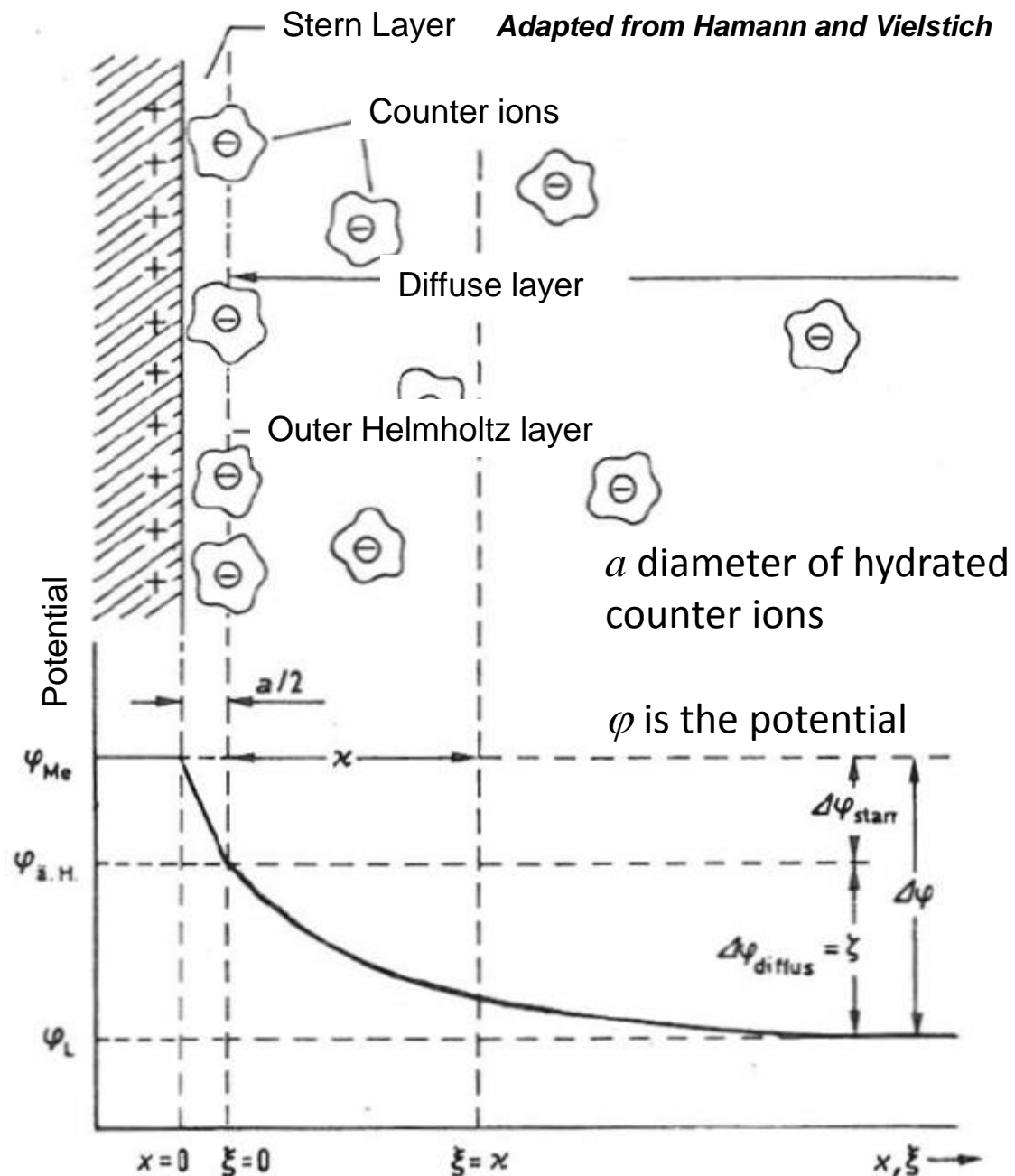
Electro kinetic Phenomena

- Electro-osmosis
- Electrophoresis
- Gel electrophoresis, polymer dynamics in gels

Electric Double Layer

In aqueous solutions we have to deal with a situations where (usually) every surfaces is charged. Not only the constituents (proteins, molecules, DNA, metals or any other surface) but also the water molecules are carrying charge. Water dissociates into H_3O^+ and OH^- and at $\text{pH}=7$: there are around $10^{-7}\text{M} \Leftrightarrow 10^{17}$ of both ions present in solution per litre.

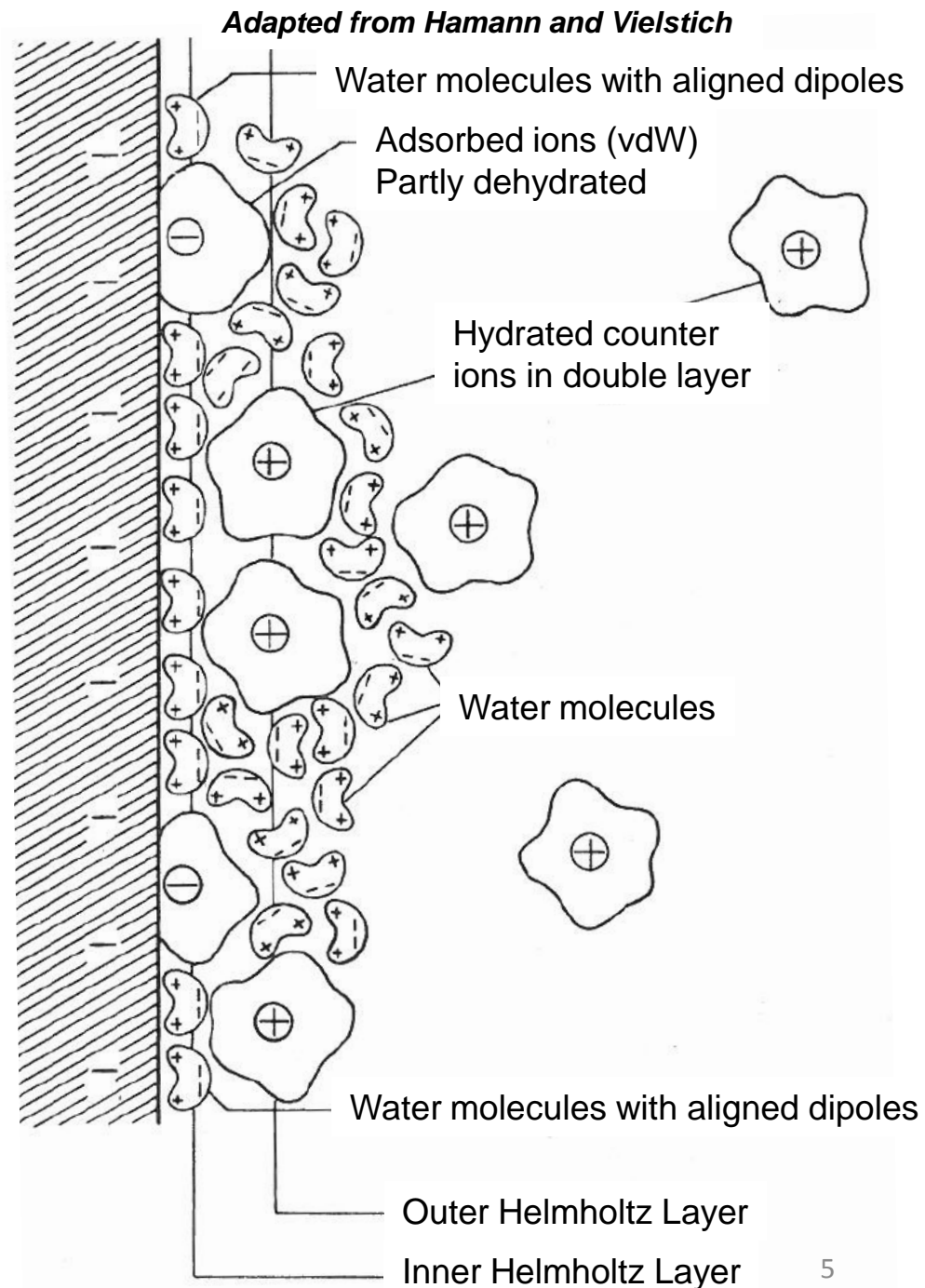
Interactions - van der Waals, hydrophobic, chemical and Coulomb, give rise to a structure close to any charged surface, composed of ions and water, known as the **electric double layer (EDL)**. The EDL determines the behaviour of charged polymers or biological molecules in aqueous solutions.



Full Electric Double Layer

One of the complications of the structure of the EDL is the complex structure of the polar water molecules which form a hydration shell around ions or macromolecules in aqueous solution. In close proximity to any surface other interactions like the van der Waals hydrophobic or chemical interactions can disrupt the hydration layer and give rise to the complex structure of the EDL.

It is useful to remember that in a realistic situation the exact structure of the electric double layer will be determined by ALL molecular interactions. The ions closest or adsorbed on the surface are often regarded as bound, however they are still in equilibrium with the surrounding medium. The EDL can be decomposed into the **Outer Helmholtz** or **Stern** layer and the inner Helmholtz layer. The latter is composed of adsorbed ions that partly lost their hydration shell and may even carry the same charge as the surface. The composition of the EDL critically depends on the outside parameters like ion concentration, pH and temperature.



Debye length, Bjerrum length, and ionic strength

There are two important length scales that allow for assessment of the thickness of the electric double layer (EDL) of the typical distance between two like-charged ions in solution. The thickness of the EDL is roughly given by the Debye screening length that we derived in the first part of the lectures from the linearization of the Poisson-Boltzmann equation (SI units):

$$l_D \equiv \lambda_D = \left(\frac{e^2}{\epsilon_0 \epsilon k_B T} \sum_i z_i c_i \right)^{-1/2} \quad \text{for monovalent salt } \lambda_D = \left(\frac{\epsilon_0 \epsilon k_B T}{e^2 c_0} \right)^{1/2}$$

The Debye length is determined by the properties of the solution that the EDL is submerged in. It is interesting to consider the relation to the Bjerrum length that we also introduced in the discussion on electrostatic interactions and the Poisson-Boltzmann equation. In SI units the Bjerrum length is :

$$l_B \equiv \frac{e^2}{4\pi\epsilon_0\epsilon k_B T} \quad \text{and thus } \lambda_D = (4\pi l_B c_0)^{-1/2}$$

As room temperature, in water, l_B is approximately 0.7 nm. It is interesting to note that for water l_B is not temperature dependent as the product of the relative dielectric constant and temperature ϵT is insensitive to T .

Often the term ionic strength I is used in the literature. I is defined by grouping the ions and their respective concentrations c_i together:

$$I \equiv \frac{1}{2} \sum_i z_i^2 c_i$$

Inclusion of the finite ion size in Debye-Huckel model

Until now we assumed that ions are point-like charges. However, it is possible to include the size of ions into the Debye-Huckel theory. This model is known as restricted primitive model of electrolytes. The potential around an ion with diameter $2a$ and charge e is given by

$$\psi(r) = \frac{e}{4\pi\epsilon_0\epsilon} \frac{e^{-(r-2a)/\lambda_D}}{r(1+2a/\lambda_D)} \quad \text{for } r > 2a$$

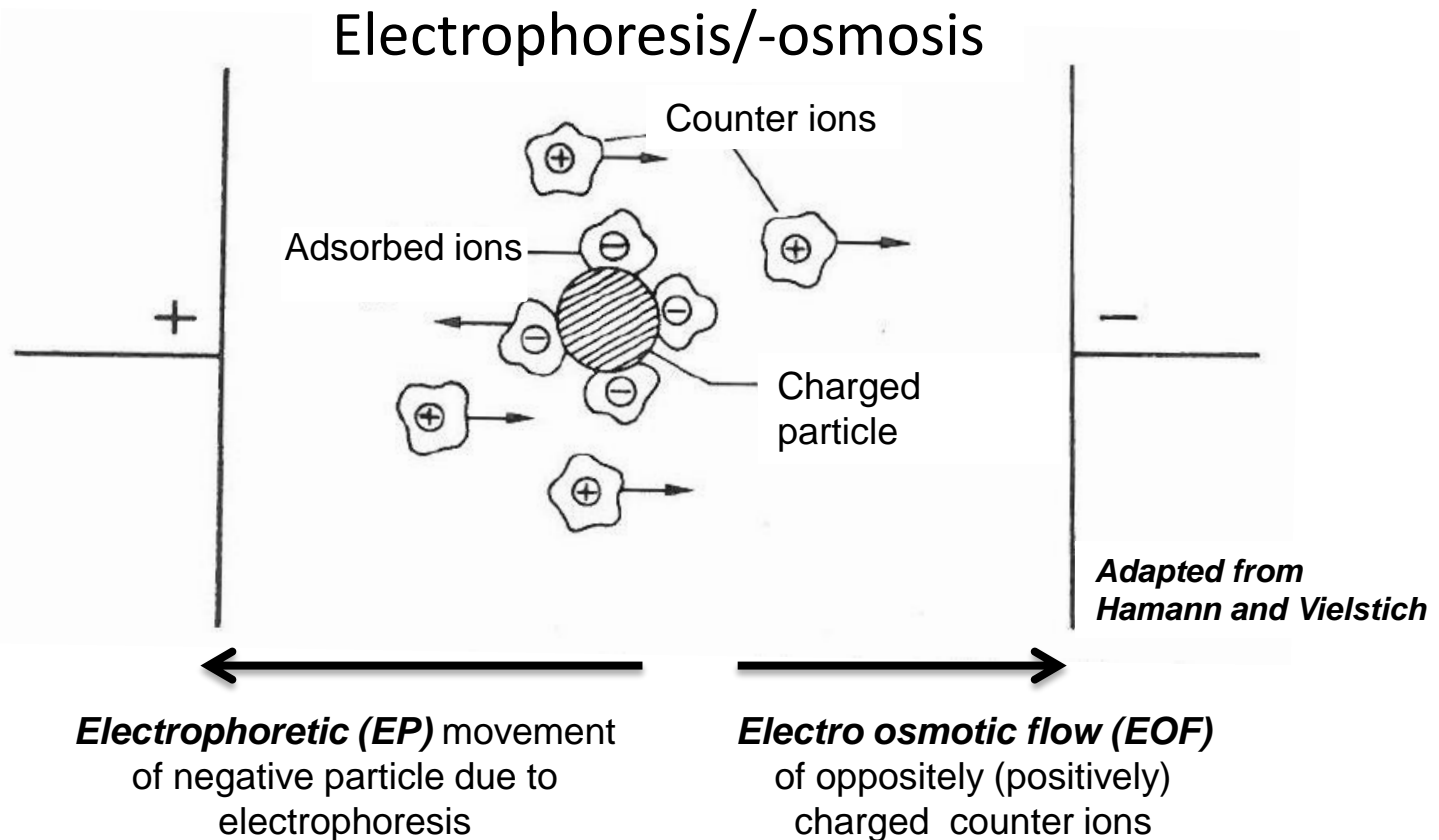
and for $0 < r < 2a$

$$\psi(r) = \frac{e}{4\pi\epsilon_0\epsilon r} - \frac{e}{4\pi\epsilon_0\epsilon\lambda_D(1+2a/\lambda_D)}$$

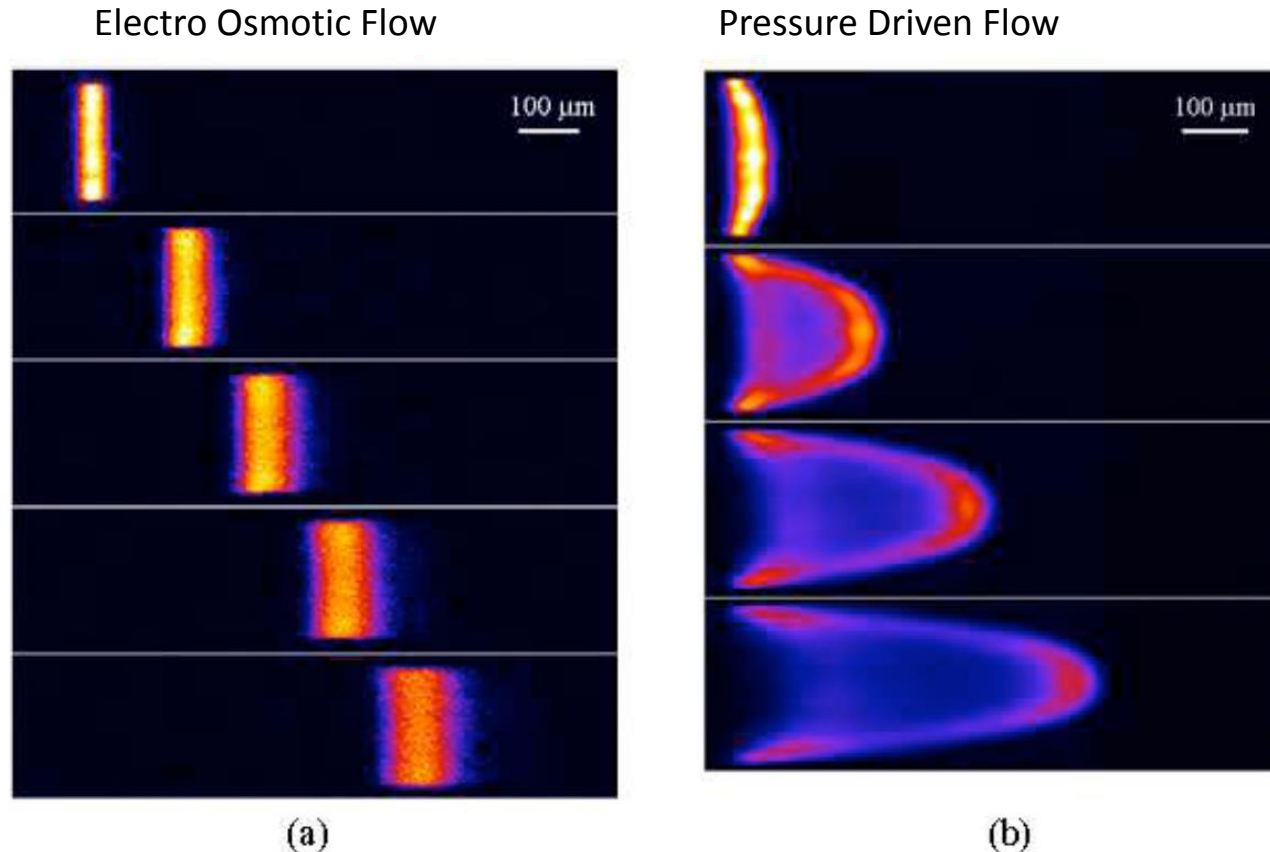
The result is a correction of the potential at distance of $2a$, ions touching, that increases the surface potential. It leads to an effective shift of the decay of the potential to distances of twice the ion radius. The distance dependence is the same as for the screened Coulomb potential. For point-like particles ($a=0$) we recover the Debye-Huckel solution.

Electrokinetic Effects

The EDL is one of the key elements for all our following discussions. Surfaces i.e. particles that are hydrophilic are usually charged in aqueous solutions. We will now discuss two closely related electro-kinetic phenomena, ***electrophoresis and electro-osmosis***, which are due to an applied electric field to the water-particle-ion system. We will discuss both electro-kinetic effects in parallel as an understanding is only possible taking into account both effects, taking into account the action of the ions on the charged surface and the water and vice-versa. .



EOF: Visualization of electro-osmotic flow



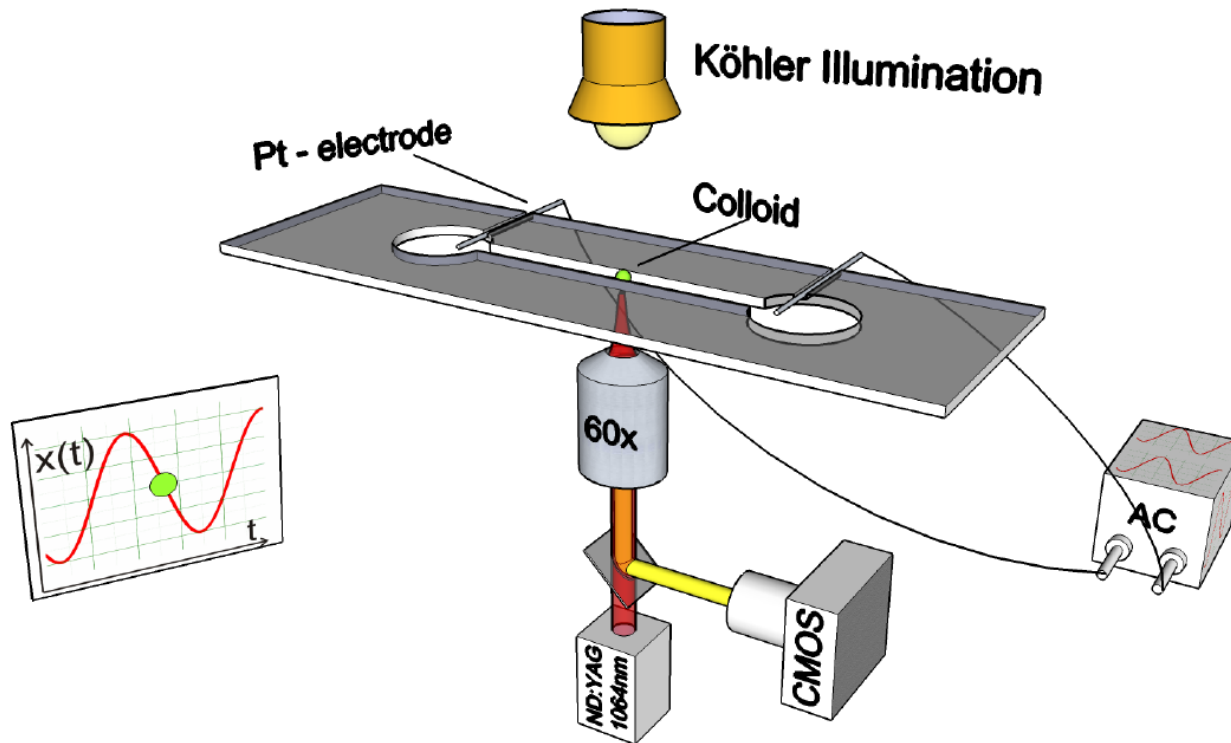
Visualization performed using a molecular tagging technique (caged fluorescence visualization) and shows the reduced sample dispersion for (a) EOF in a capillary with a rectangular cross section 200 μm wide and 9 mm deep; (b) pressure-driven flow in a rectangular cross-section 250 μm wide and 70 μm deep.

<http://microfluidics.stanford.edu/Projects/Archive/caged.htm>

http://www.damtp.cam.ac.uk/user/gold/teaching_biophysicsIII.html

Optical Tweezers: Single particle electrophoresis

Otto (2008)



We will start with an investigation of single particle electrophoresis. In order to study the electrophoretic mobility, of a single particle, optical tweezers are ideal candidates as they not only allow to follow the movement of the particle in the electric field but also can determine the forces acting on the particle. This is a unique feature allowing for a complete understanding of the system.

Here, we will more discuss an experimental realization that uses several of the approaches we discussed earlier in the course. The position of the particle will be monitored by single particle tracking with video microscopy, while the forces are determined by analysis of the power spectrum. The main trick employed here is to move the particle with an alternating field allowing to determine the motion of the particle even when the amplitude is smaller than Brownian fluctuations.

Oscillation of charged particle in AC-field

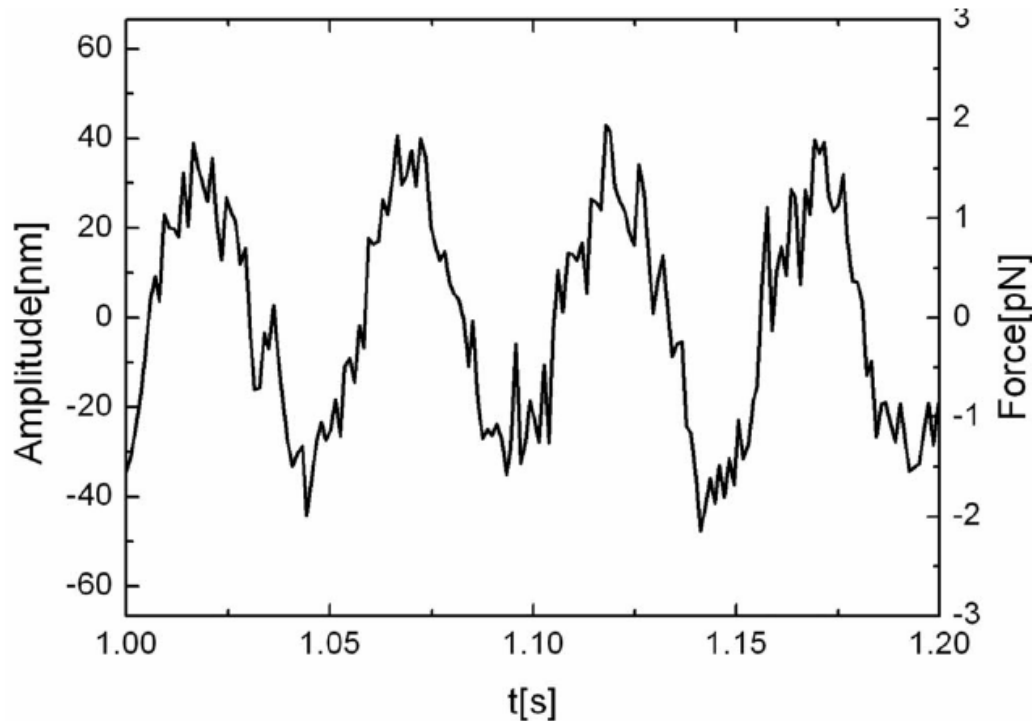


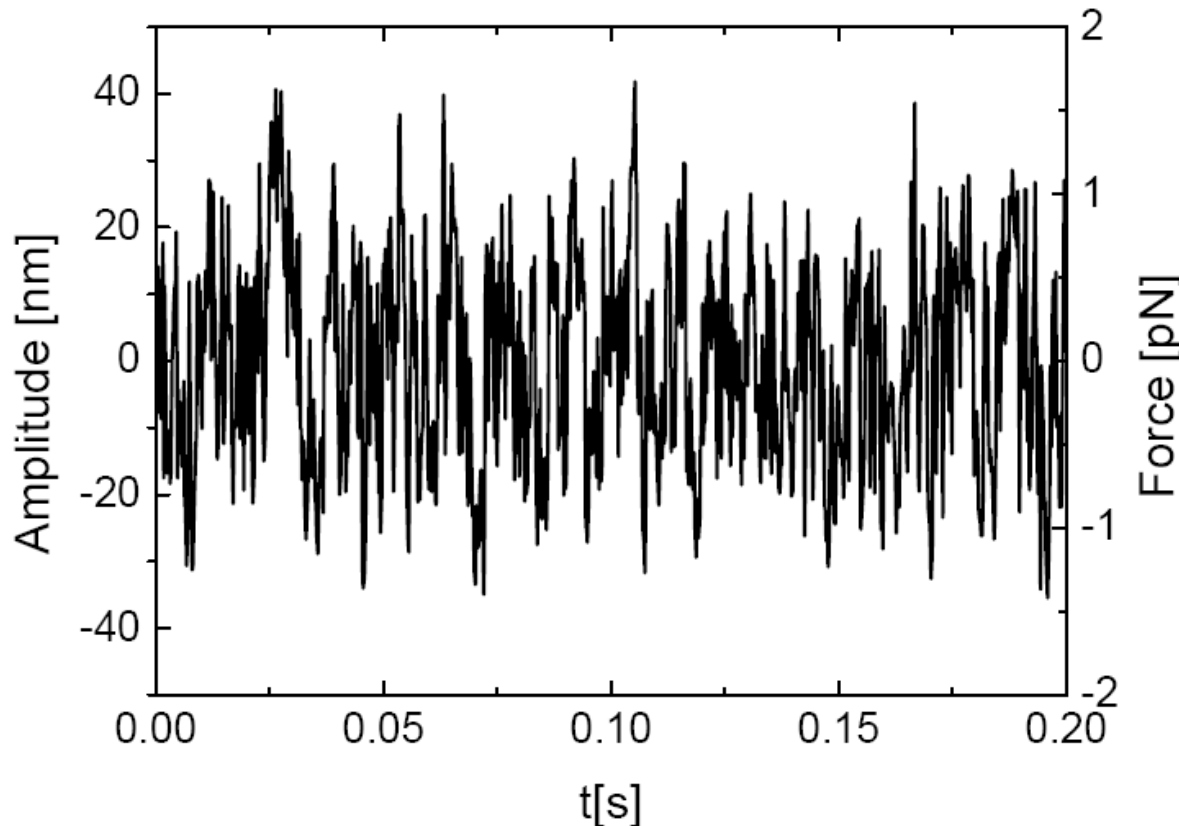
FIG. 4. Amplitude and force as a function of time of a $2.23\ \mu\text{m}$ PS colloid moving in an ac field of $E=63\ \text{V/cm}$ at $f=20\ \text{Hz}$ in de-ionized water.

For a typical measurement, the particle is subject to an electric field with applied voltages of up to 60 V. One annoying complication of these high voltages is the electrochemical decomposition of water into H_2 and O_2 at the electrodes. However, over short time scales (few seconds) the oscillatory motion of the particle due to the electrophoretic force can be detected giving rise to a nice oscillation. The Brownian fluctuations of the particle in the trap are readily visible even at these relatively high forces. We can detect forces around 1-2 pN easily.

The decomposition of water limits the applicability of high voltages in this type of measurement. One solution is to use again the frequency analysis using the Fourier transforms we discussed earlier in the context of force calibration.

*Optical Tweezers: Detect forces in fN – range **

Otto (2008)

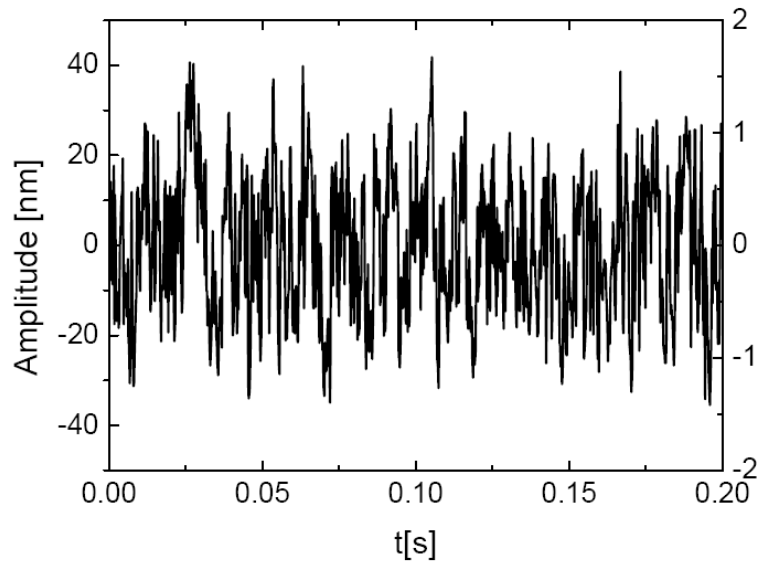


Applying lower voltages and thus lower electric fields pushes the movement of the particle below the fluctuations of the thermal fluctuations in the trap.

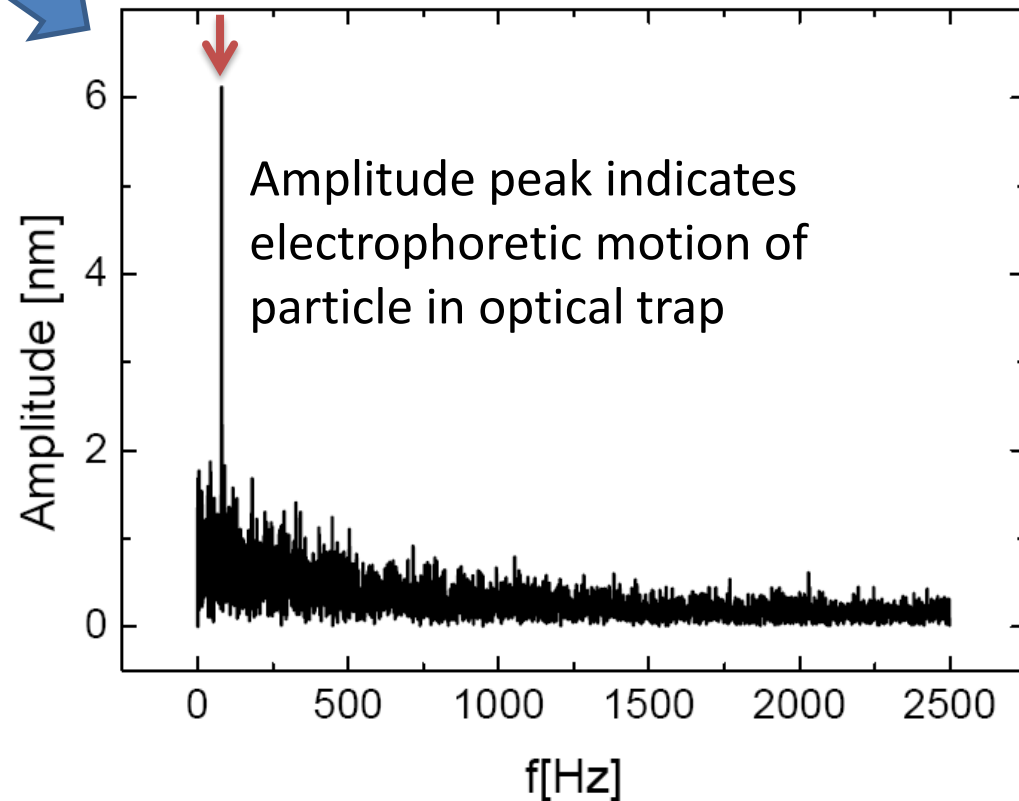
However, due to the well-defined frequency we should be able to determine the amplitude of the motion by analysing the data on the left using the amplitude spectrum. We would expect to observe a clear peak at the frequency given by the AC voltage.

*Detect forces in fN – range **

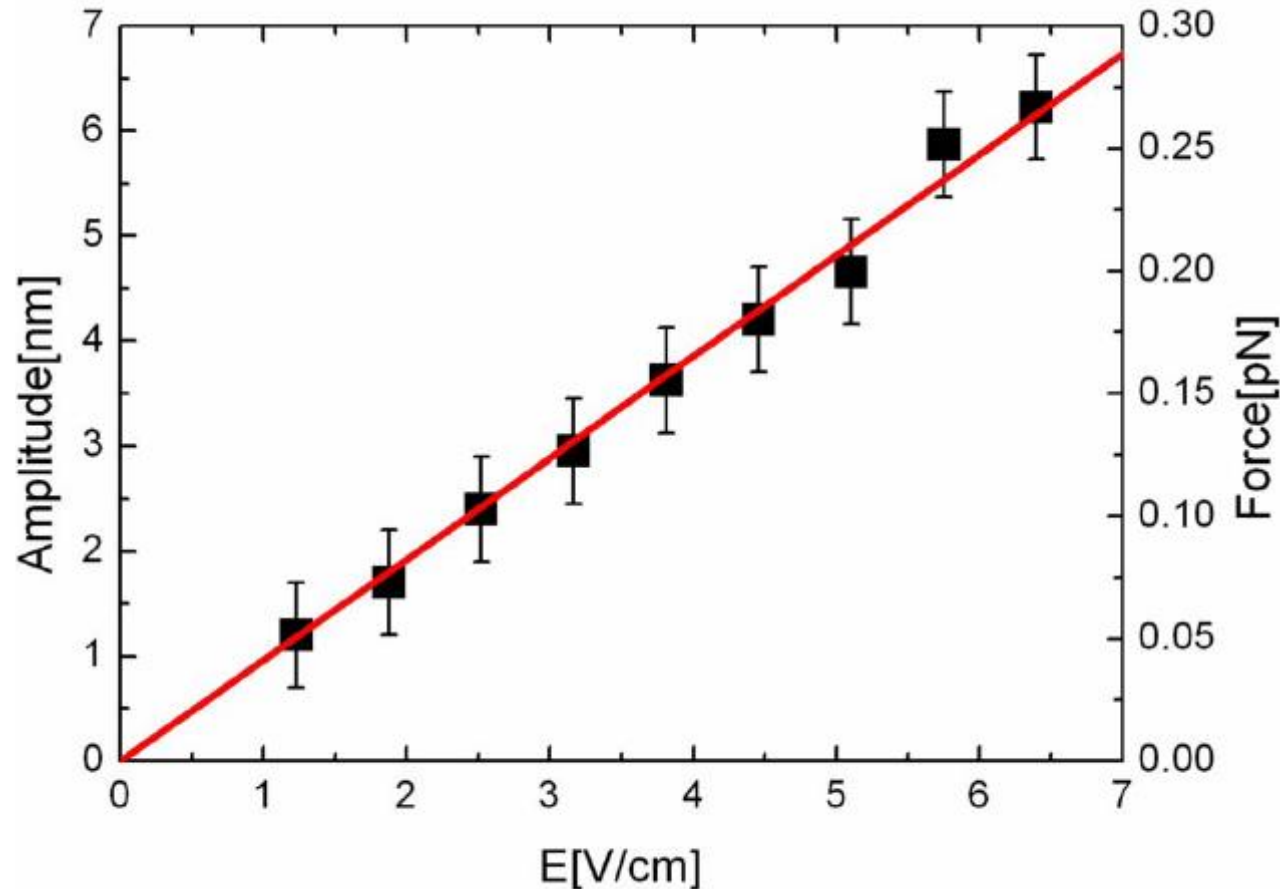
[Otto \(2008\)](#)



Fourier transform - Amplitude



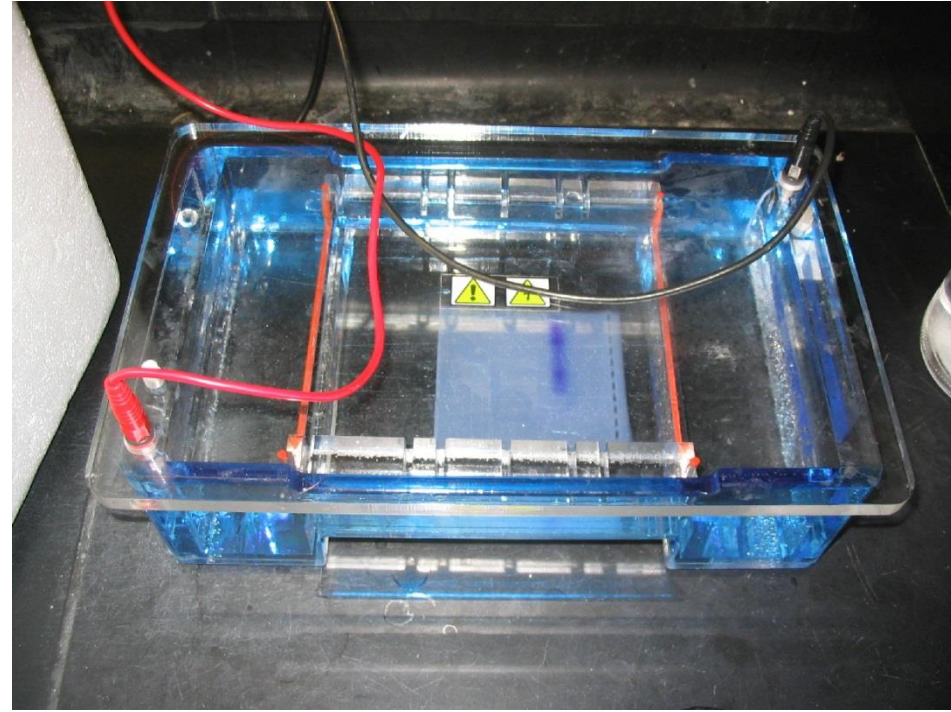
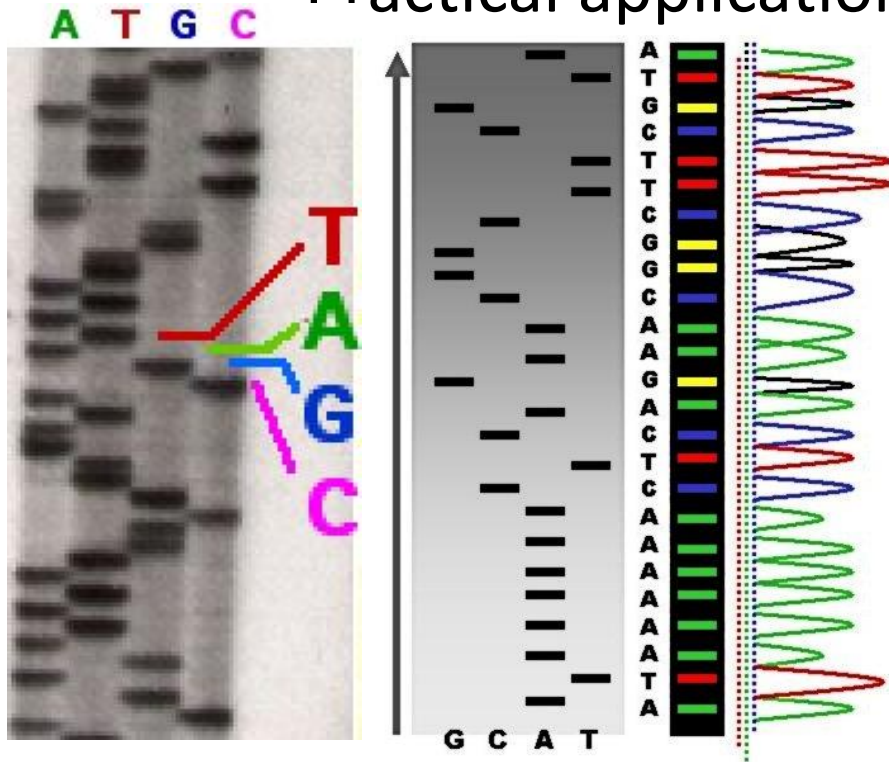
Electrophoretic Force depends linearly on Voltage



Otto (2008)

With this simple approach we can easily detect 50 femto Newton forces on the particles. One obvious expectation would be that the maximum force should depend linearly on the applied voltage (electric field) and this is exactly what we find. The reason for the high resolution despite the considerable Brownian fluctuations is that we average over many periods in our signal and thus see even smallest amplitudes in the amplitude spectrum.

Practical application: Gel Electrophoresis



<http://Wikipedia.org>

http://www-che.syr.edu/faculty/boddy_group/pages/electrophoresis.jpg

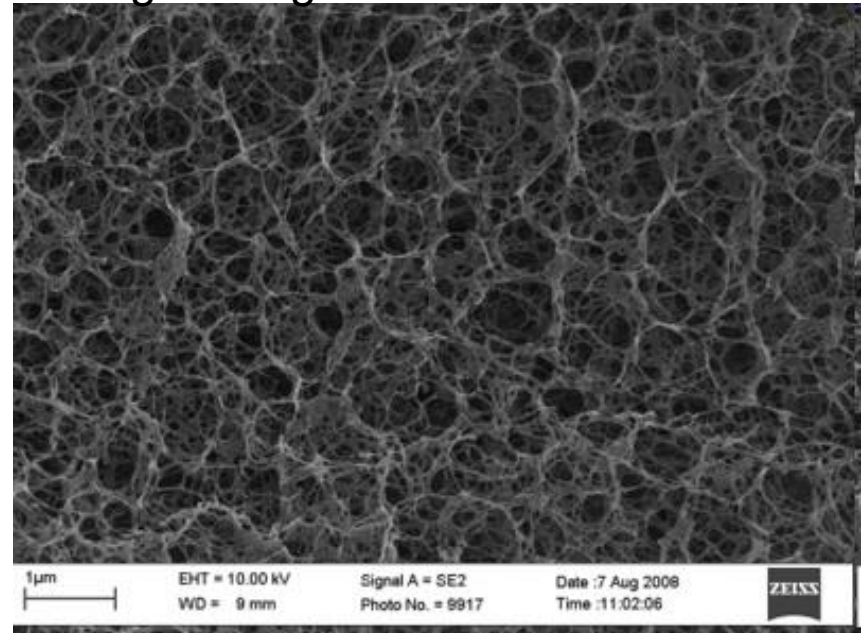
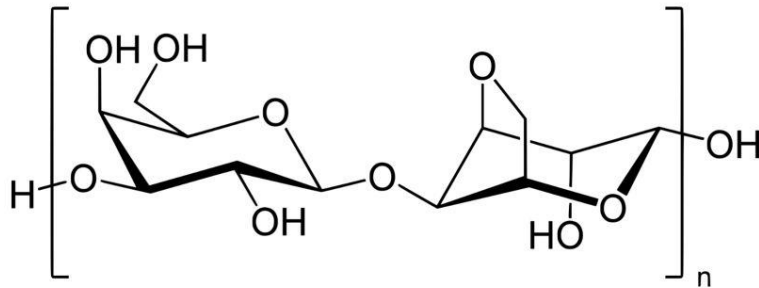
After the brief discussion on electrokinetic effects, we will now introduce **gel electrophoresis**. Gel electrophoresis is one of the most important techniques for the characterization of biomolecules (proteins, DNA, RNA) based on electrophoretic movement of polymers in a matrix of almost uncharged molecules forming a porous structure also called “**gel**”. The main purpose is to sort molecules by their molecular weight employing their charge. Due to the presence of the gel we do not have to take into account complications arising from electro-osmotic flows as the gels fibers effectively stop any major electrically driven fluid flows in the system.

http://www.damtp.cam.ac.uk/user/gold/teaching_biophysicsIII.html

One example for a gel: Agarose

Agarose gel in dried condition

*Agarose monomer**



In order to stop electro-osmotic flows and enable sorting of polymers by their molecular mass (length) one can form entangled polymer gels. After mixing Agarose monomers heating them to around 100°C and cooling them down to room temperature, they form a network of small pores as shown in the electron micrograph above. The density and distance of the polymers forming the mesh of pores can be easily tuned by the amount of agarose in the solution. The mesh can be regarded as very similar to concentrated polymer solutions.

The movement of polymers in this mesh can be interpreted as driven diffusion due to an externally applied electric field. The mobility of polyelectrolytes is controlled by the effective pore diameters and is tuned with regards to the length of the polymers to be sorted.

Polymer Dynamics in Gel Electrophoresis

- **Rouse** – polymer is string of N beads with radius R , is moving freely through the chain (“free draining”, solvent not relevant)
Friction coefficient: $N\gamma$

Curve-linear diffusion coefficient: $D_R = k_B T / N\gamma$

- Rouse time $\tau_R \Leftrightarrow$ time polymer diffuses over distance equal to its end-to-end distance R_N

- For any chain one gets:
$$\tau_R = \frac{1}{6\pi^2} \frac{\gamma b^2}{k_B T} N^{1+2\nu} \approx \tau_0 N^{1+2\nu}$$

- Characteristic time for monomer in an ideal chain ($\nu=0.5$):

$$\tau_0 \approx \frac{\gamma b^2}{k_B T} \Rightarrow \tau_R \approx N^2 \tau_0 \text{ for an ideal chain with } \nu = 0.5$$

- Problems with Rouse model include: unrealistic hydrodynamics, no knots

Polymer Dynamics

- **Zimm** – similar to Rouse model but solvent moves with chain (no slip on chain), long range hydrodynamic interactions, so we have now typical size of segments b and viscosity of solvent η . The total friction coefficient of the chain is then given by the diameter of the chain R and depends on the fluid viscosity.
- Stokes friction (neglecting all pre-factors of order 1 as usual):

$$\gamma \approx \eta R$$

- With Stokes-Einstein we can then write down the Zimm diffusion coefficient:

$$D_Z = \frac{k_B T}{\eta R} \approx \frac{k_B T}{\eta b N^\nu}$$

- Remember: The exponent ν is depending on chain, $\nu=0.5$ ideal, $\nu=0.588 \approx 3/5$ self avoiding chain (Flory exponent– see Cicuta Soft matter course), $\nu=1/2$ ideal, $\nu=1/3$ for collapsed chains

- Consequently the Zimm relaxation time is then τ_Z :

$$\tau_Z \approx \frac{R^2}{D_Z} \approx \frac{\eta}{k_B T} R^3 \approx \frac{\eta b^3}{k_B T} N^{3\nu} \approx \tau_0 N^{3\nu}$$

- Main difference to Rouse is the weaker dependence on N .
- Rouse model works well in polymer melts and gels while Zimm is better for describing polymers in dilute solution.

Polymer Dynamics

- Sub-chains behave in the same way as the entire chain
- There are N relaxation modes of the chain

$$\tau_p = \tau_0 \left(\frac{N}{p} \right)^2 \quad \text{with } p = 1, 2, \dots, N$$

- Mean square displacement of a segment with p monomers:

$$\langle |\mathbf{r}_j(\tau_p) - \mathbf{r}_j(0)|^2 \rangle \approx b^2 \frac{N}{p} \approx b^2 \left(\frac{\tau_p}{\tau_0} \right)^{\frac{1}{2}}$$

- Mean square displacement of a monomer in chain with $N \gg 1$ for times $t < \tau_R$

$$\langle |\mathbf{r}_j(t) - \mathbf{r}_j(0)|^2 \rangle \approx b^2 \left(\frac{t}{\tau_0} \right)^{\frac{1}{2}} \quad \text{for } \tau_0 < t < \tau_R$$

Polymer Dynamics

- Now compare to free diffusion (Fick)

$$\langle |\mathbf{r}_j(t) - \mathbf{r}_j(0)|^2 \rangle \approx b^2 \left(\frac{t}{\tau_0} \right)^{\frac{1}{2}} \quad \text{for } \tau_0 < t < \tau_R$$

$$\langle |\mathbf{r}(t) - \mathbf{r}(0)|^2 \rangle = 6Dt$$

- Conclusion: Rouse mean-square displacement is sub-diffusive
- Within Zimm model we get a slightly different answer in the exponent:

$$\langle |\mathbf{r}_j(t) - \mathbf{r}_j(0)|^2 \rangle \approx b^2 \left(\frac{t}{\tau_0} \right)^{\frac{2}{3}} \quad \text{for } \tau_0 < t < \tau_Z$$

Polymer Dynamics

Both Zimm and Rouse models assume that the chain is free to move, completely independent of the others. In a gel the chain cannot move freely and is entangled in the gel fibres. The chain cannot cross the gel fibres. A very similar situation is found in high density polymer solutions.

- Idea (Sir Sam Edwards):
chains are confined in a tube made of the fibres, tube has radius:

$$r_t \approx b\sqrt{N_e} \text{ with } N_e \text{ Number of monomers per entanglement}$$

and r_t is the entanglement length

- Coarse grained chain length is $R_0 \approx r_t \sqrt{\frac{N}{N_e}} \approx b\sqrt{N}$
- Coarse grained contour length: $\langle L \rangle \approx r_t \frac{N}{N_e} \approx \frac{b^2 N}{r_t} \approx \frac{bN}{\sqrt{N_e}}$

Polymer Dynamics

- Simplified picture in gel:

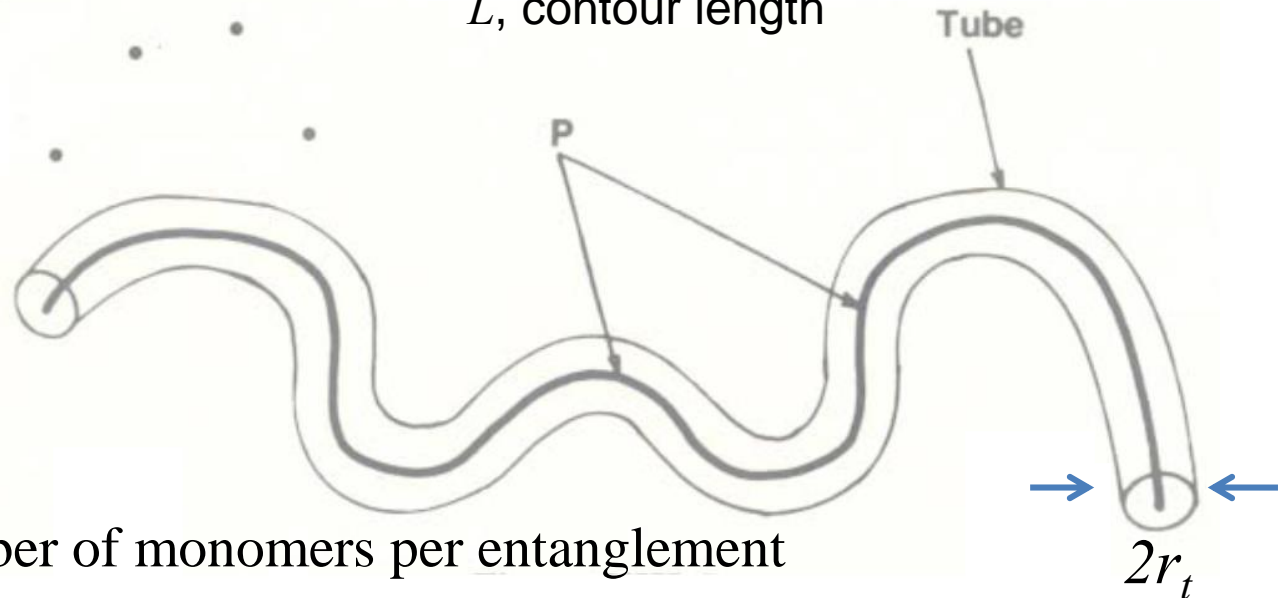


R_0 , contour length in Edwards tube

$$R_0 \approx r_t \sqrt{\frac{N}{N_e}} \approx b\sqrt{N}$$

$$\langle L \rangle \approx r_t \frac{N}{N_e} \approx \frac{b^2 N}{r_t} \approx \frac{bN}{\sqrt{N_e}}$$

L , contour length



$r_t \approx b\sqrt{N_e}$ with N_e Number of monomers per entanglement
and r_t is the entanglement length

Diffusion in Tube: “Reptation”

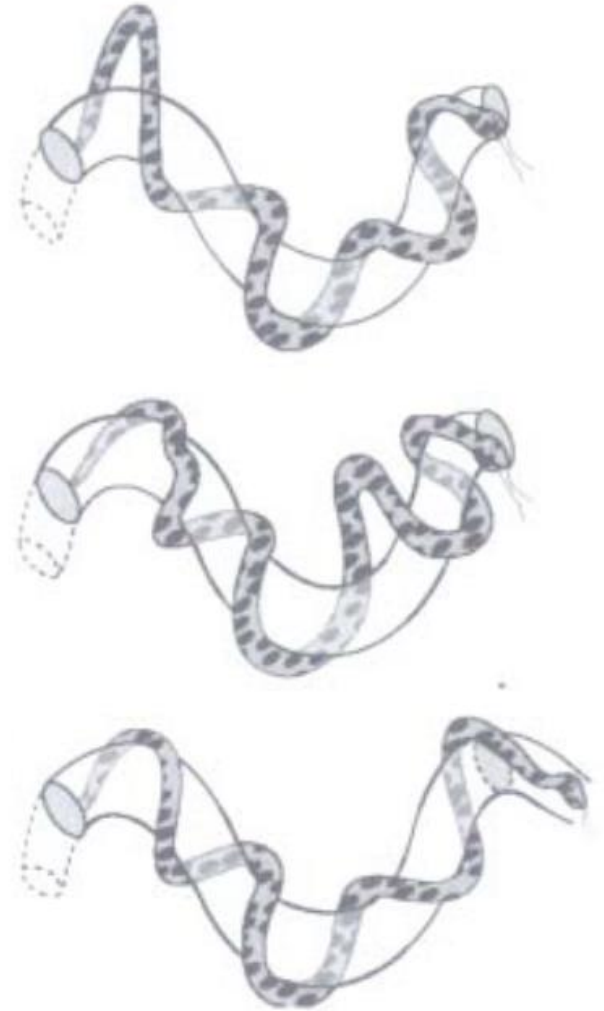
We can now use the models we discussed before to understand the diffusion in the gel. The diffusion coefficient in the tube is just given by the Rouse model $D_R = D_C = k_B T / N \gamma$.

The reptation time is the time to diffuse along the complete tube length

$$\tau_{\text{rep}} \approx \frac{\langle L \rangle^2}{D_c} \approx \frac{\gamma b^2 N^3}{kT N_e} = \frac{\gamma b^2}{kT} N_e^2 \left(\frac{N}{N_e} \right)^3$$

The lower time limit for reptation is given for the Rouse mode with $N=N_e$

$$\tau_e \approx \frac{\gamma b^2}{k_B T} N_e^2$$

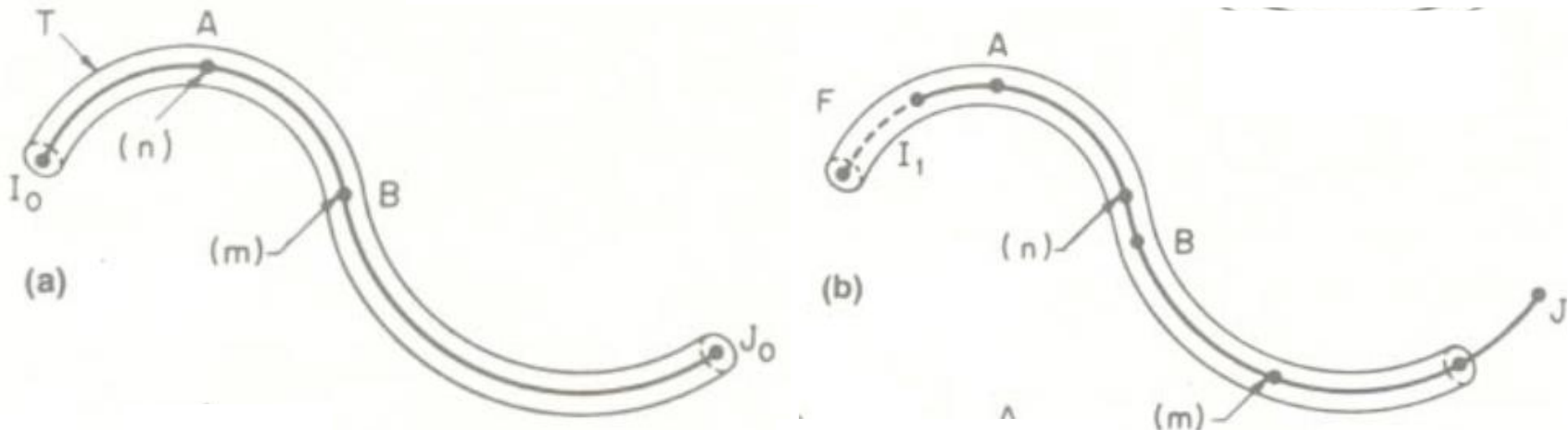


Longer Timescales

1. For $t < \tau_e$, Rouse diffusion:
$$\langle |\mathbf{r}_j(t) - \mathbf{r}_j(0)|^2 \rangle \approx b^2 \left(\frac{t}{\tau_0} \right)^{\frac{1}{2}}$$
2. For $\tau_e < t < \tau_R$, motion confined in tube \Leftrightarrow displacement only along the tube, this is slower than unrestricted Rouse motion (as expected)
$$\langle |s_j(t) - s_j(0)|^2 \rangle \approx b^2 \left(\frac{t}{\tau_0} \right)^{\frac{1}{2}} \approx r_t^2 \left(\frac{t}{\tau_e} \right)^{\frac{1}{2}}$$

The tube itself is a random walk with step length $a \sim r_t$

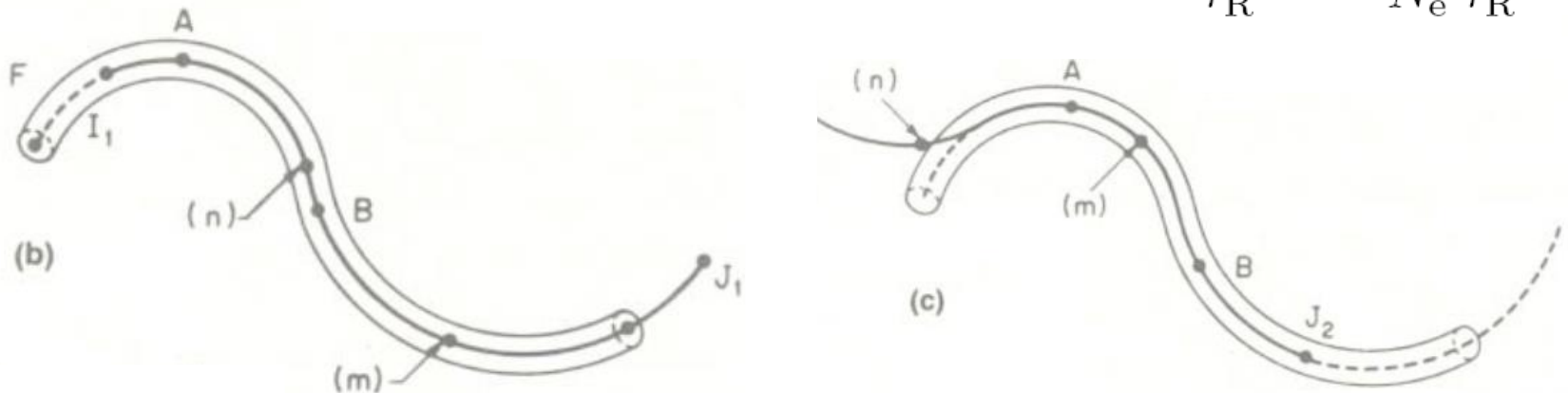
$$\langle |\mathbf{r}(t) - \mathbf{r}(0)|^2 \rangle \approx r_t \sqrt{\langle |s_j(t) - s_j(0)|^2 \rangle} \approx r_t^2 \left(\frac{t}{\tau_e} \right)^{\frac{1}{4}}$$



Timescales in Gels

3. For $\tau_R < t < \tau_{rep}$, motion of all segments is correlated, polymer diffuses along the tube

$$\langle |s(t) - s(0)|^2 \rangle \approx D_c t \approx b^2 N \frac{t}{\tau_R} \approx r_t^2 \frac{N}{N_e} \frac{t}{\tau_R}$$



Random walk of tube is now

$$\langle |\mathbf{r}(t) - \mathbf{r}(0)|^2 \rangle \approx r_t \sqrt{\langle |s_j(t) - s_j(0)|^2 \rangle} \approx r_t^2 \left(\frac{N}{N_e} \right)^{\frac{1}{2}} \left(\frac{t}{\tau_R} \right)^{\frac{1}{2}}$$

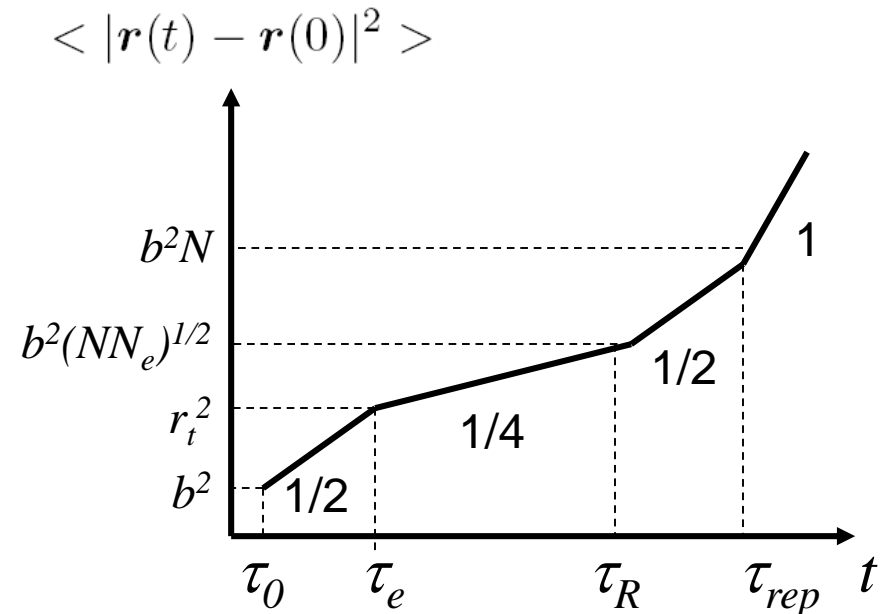
4. For times much longer than the reptation time $t > \tau_{rep}$, free diffusion is recovered with the diffusion coefficient D_g in the gel

$$\langle |\mathbf{r}(t) - \mathbf{r}(0)|^2 \rangle = 6D_g t$$

Timescales in Gels

Four different regimes

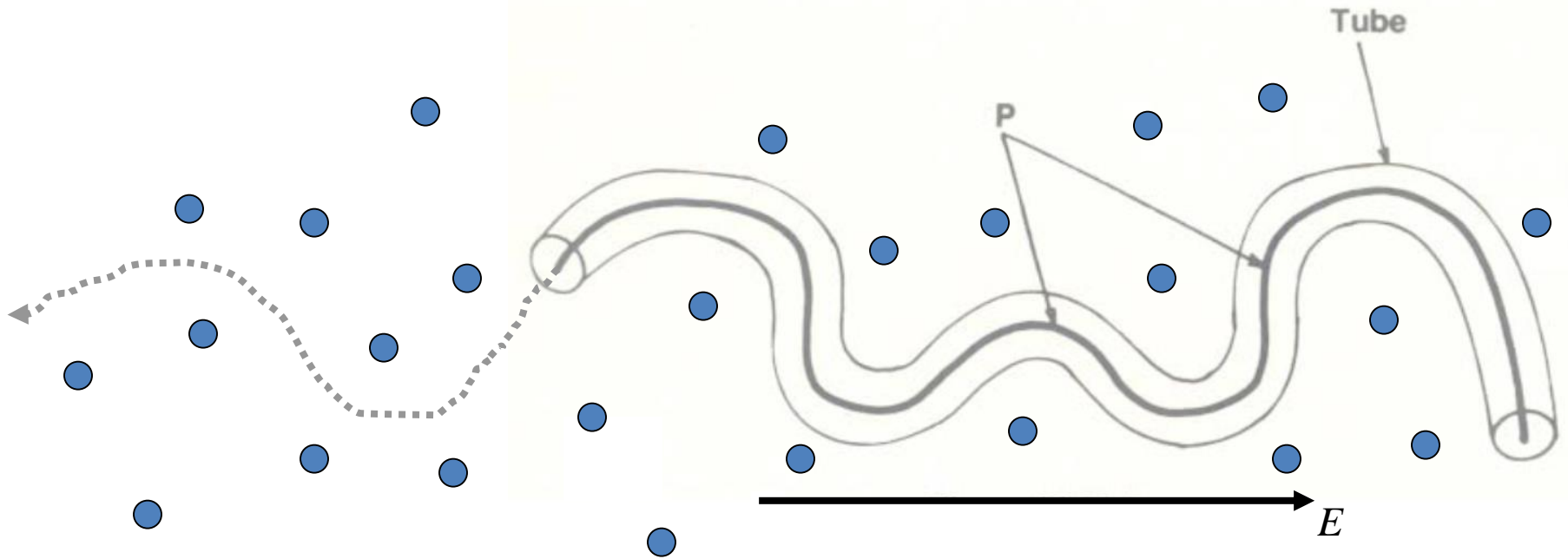
1. For $\tau_0 < t < \tau_e$ $\langle |\mathbf{r}(t) - \mathbf{r}(0)|^2 \rangle \sim t^{\frac{1}{2}}$
2. For $\tau_e < t < \tau_R$ $\langle |\mathbf{r}(t) - \mathbf{r}(0)|^2 \rangle \sim t^{\frac{1}{4}}$
3. For $\tau_R < t < \tau_{rep}$ $\langle |\mathbf{r}(t) - \mathbf{r}(0)|^2 \rangle \sim t^{\frac{1}{2}}$
4. For $t > \tau_{rep}$ $\langle |\mathbf{r}(t) - \mathbf{r}(0)|^2 \rangle \sim t^1$



Polymers behave like simple liquids only when probed on time scales larger than the reptation time. On very short timescales polymer dynamics is slowed because of the connectivity of the chain segments (Rouse, Zimm), on intermediate time scales the slow-down arises from the entangled nature of the chains (reptation tube disengagement). For long time scales the diffusion is now dependent on the length of the chain N , which allows for separation of polymers with the same zeta-potential by their length.

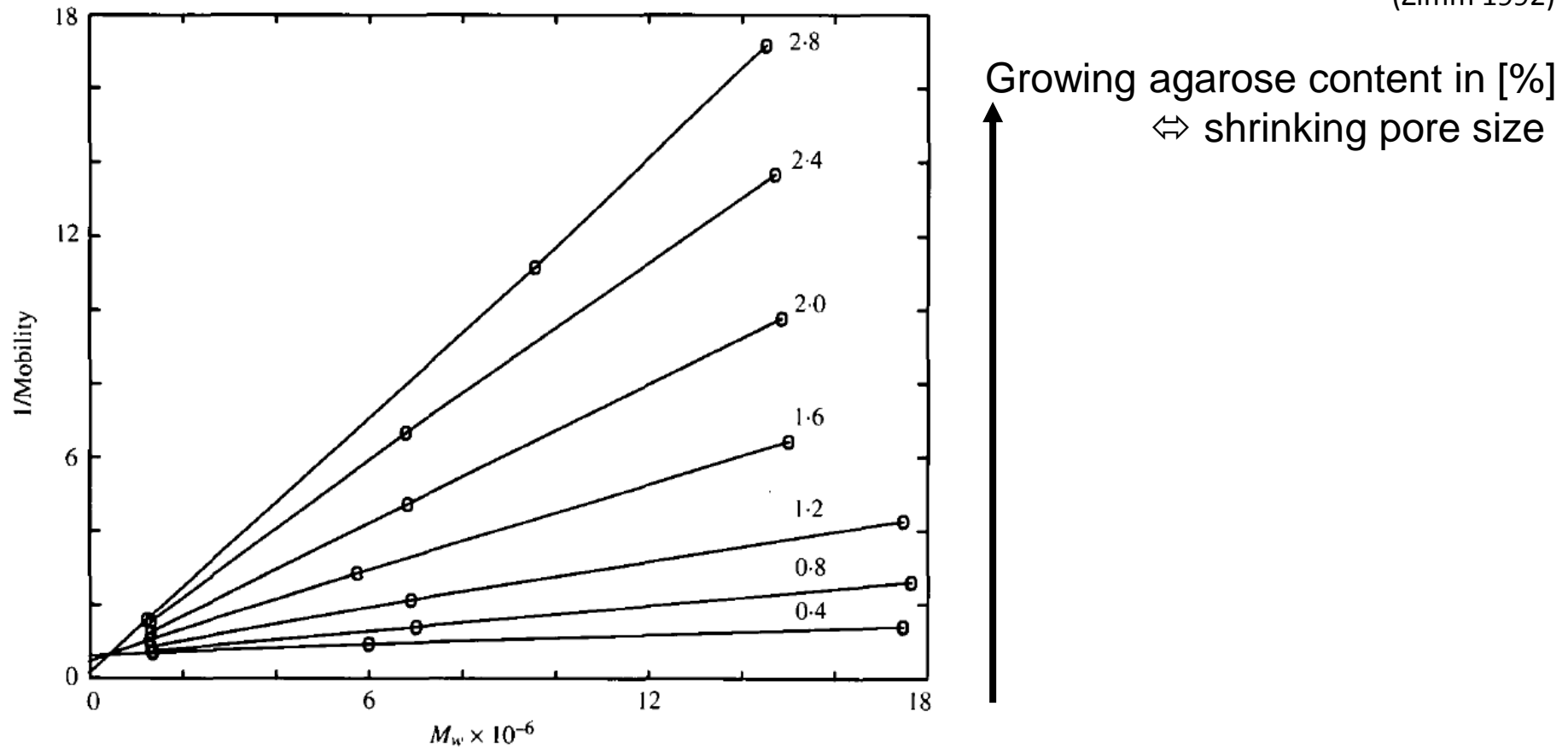
Gel Electrophoresis (EP)

- Reptation time is time to diffuse along its own length
- For experiments much longer than reptation time free diffusion (Fick) is recovered now with diffusion constant depending on length of the polymer



DNA mobility in gel depends on DNA length

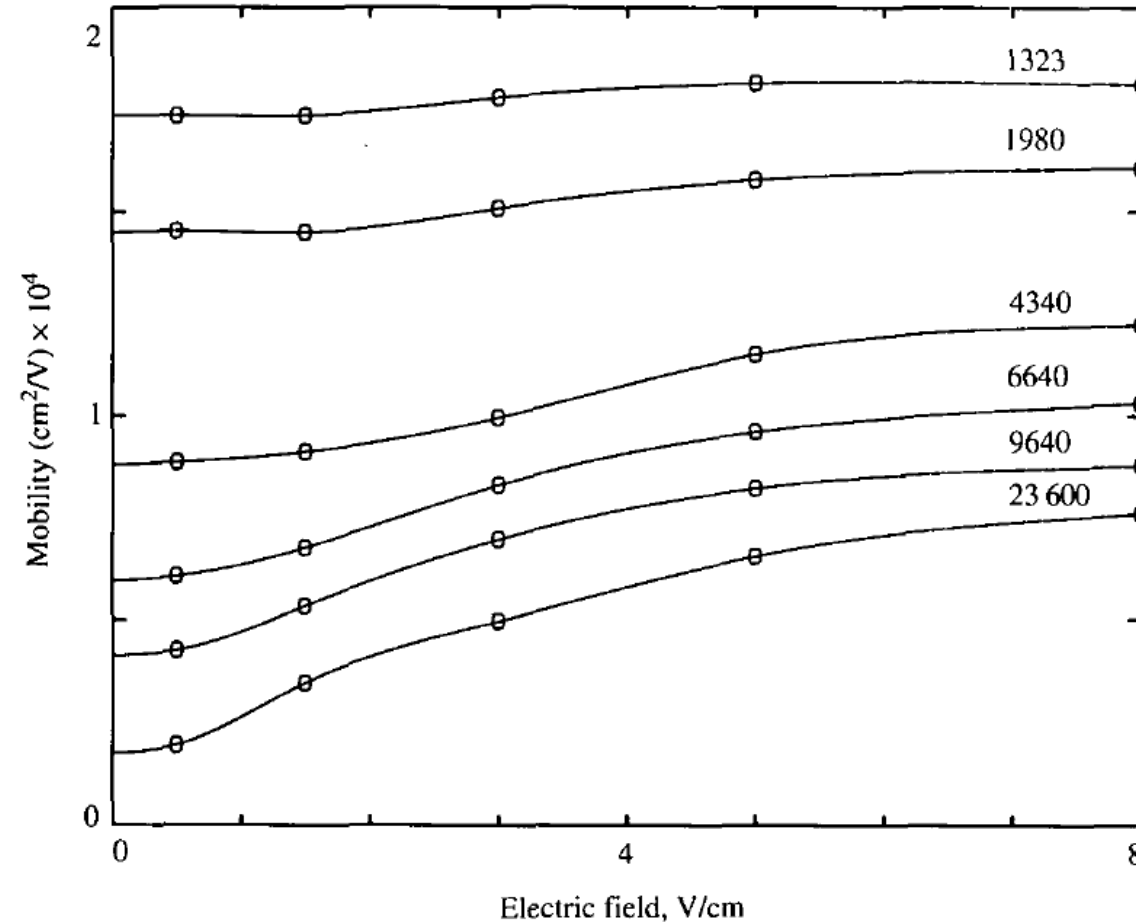
(Zimm 1992)



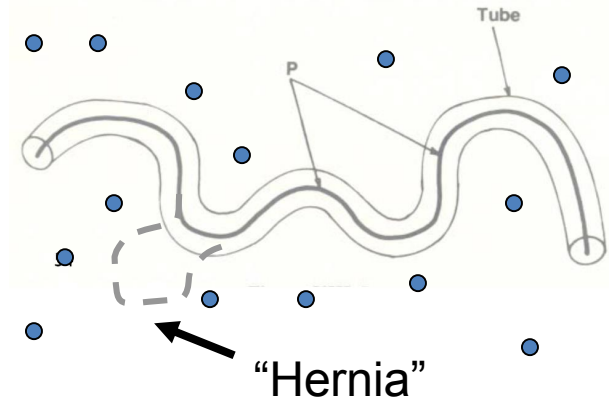
After discussing the dynamics in a gel we can now look at the experimental data. We would expect that the mobility depends also on distance of gel fibres (size of the pores the DNA has to migrate through), which is clearly observed in the range of molecular weights shown above. We would also expect that the drift velocity should inversely depend on the DNA length, which we find is true for this range of molecular weight.

Electric Field Dependence

(Zimm 1992
Viovy 2000)



DNA length increases
(lines guides to the eye only)



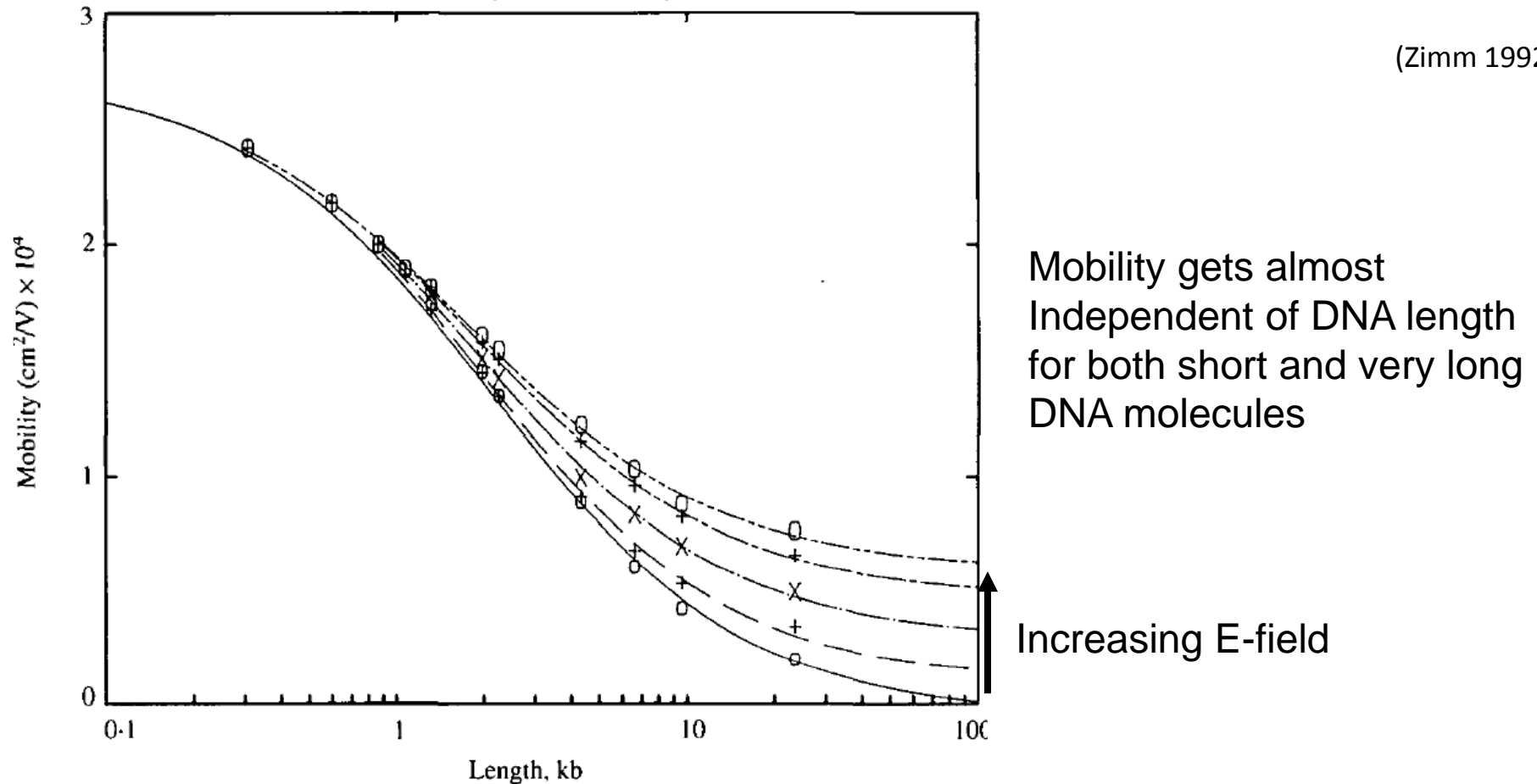
Condition for reptation model

$$\varepsilon = \frac{Eqb}{k_B T} \ll 1$$

At low electric fields the mobility is almost independent of the magnitude of the field. However, for fields bigger than 1V/cm nonlinearities occur, for longer DNA molecules more pronounced than for shorter ones. In this regime the reptation model breaks down due to “herniating” of the chains ⇔ force on segments high enough to pull segments out of the reptation tube.

Validity of Reptation Model in Gel EP

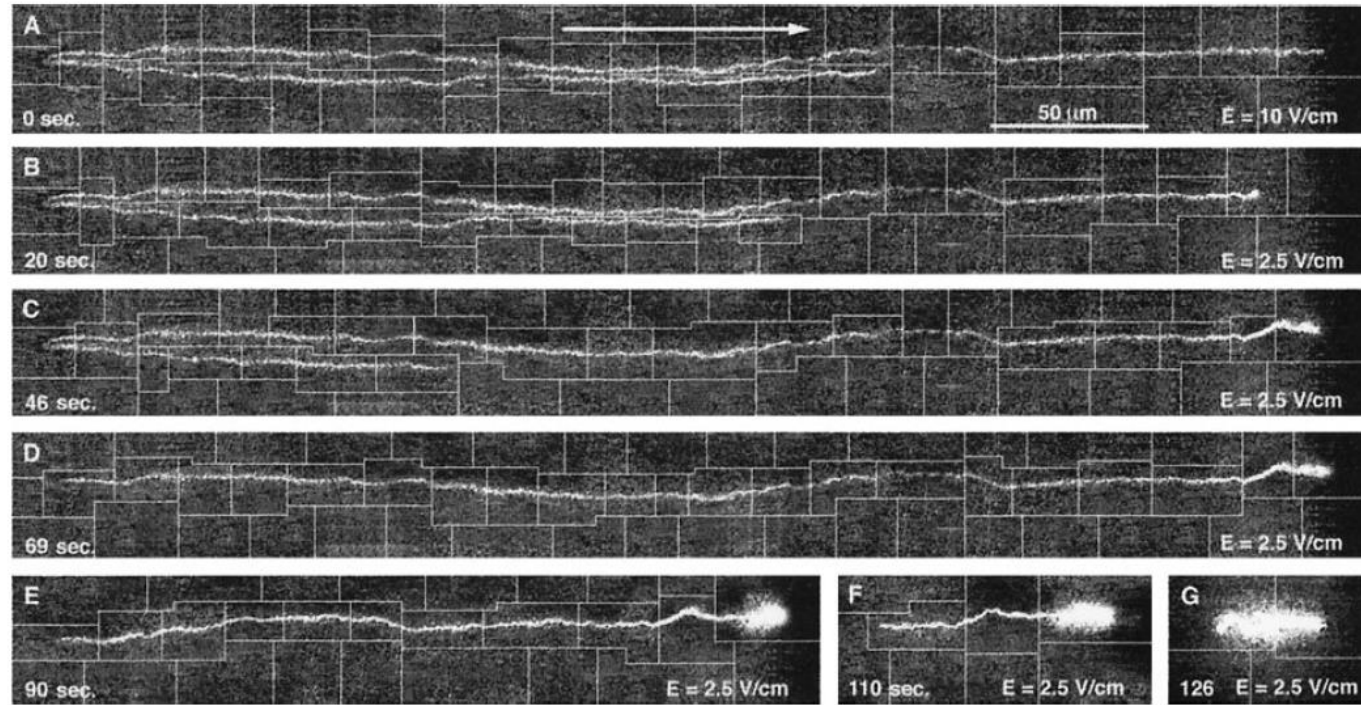
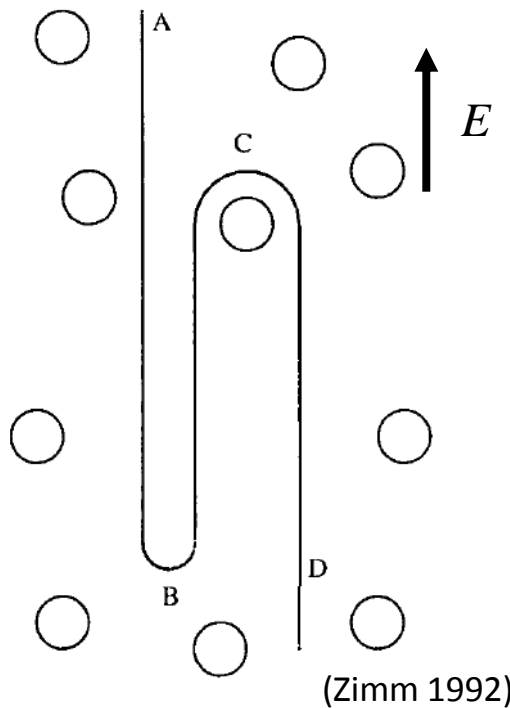
(Zimm 1992)



The reptation model for gel electrophoresis works if the length of polymers is much longer than the Debye screening length. Typically, the DNA should be longer than several persistence lengths. Another important condition is that the chains have to be longer than the typical pore diameter in the gel, otherwise they can freely move through the gaps. Finally, for very long polymers, the reptation model also breaks down as trapping and knots become very important for the mobility and a simple, driven diffusive motion is not a good description any more.

Separation of long DNA

(Gurrieri 1999)

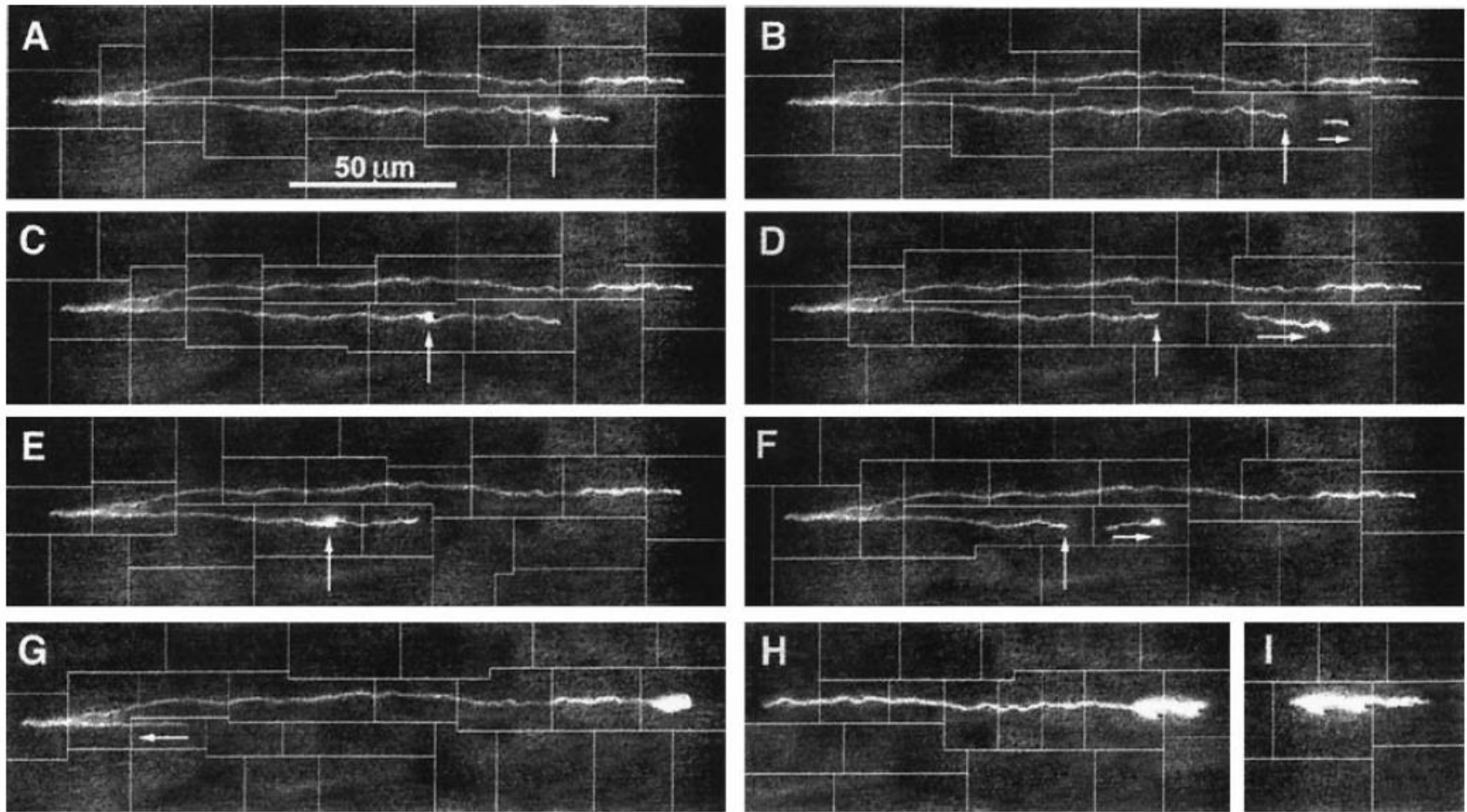


Due to the formation of “hernia” DNA can get trapped around gel fibres. Especially for very long DNA this can lead to fully stretched molecules. If this happens the simple reptation model has to be extended. By labelling the DNA molecule with fluorescent dyes this can be studied with single molecule fluorescence. Molecule can get trapped in the gel by either being wrapped around a gel fiber or by forming an entropic coil in a larger void. These effects can lead to difficulties for separation of long molecules: using DC current. By applying time-dependent electric fields one can exploit the trapping effects one can separate long molecules. Pulsed field gel electrophoresis can be used for separating 10s of kilo to mega-base long strands.

http://www.damtp.cam.ac.uk/user/gold/teaching_biophysicsIII.html

Cutting long DNA molecules in Gels

(Gurrieri 1999)

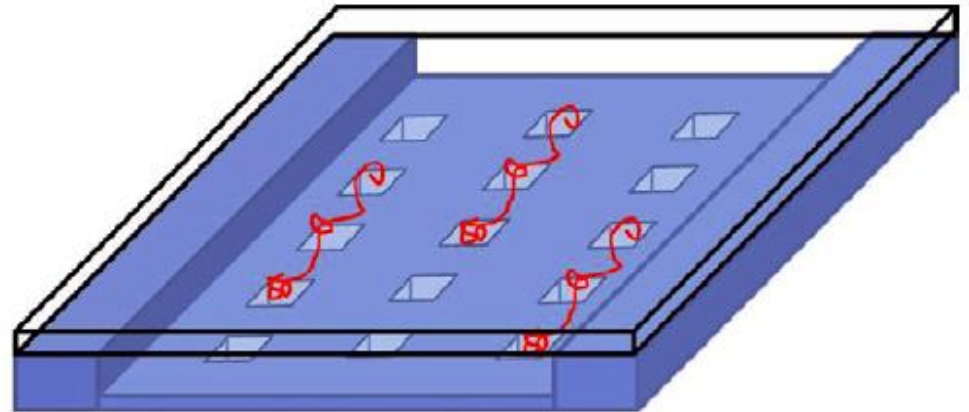
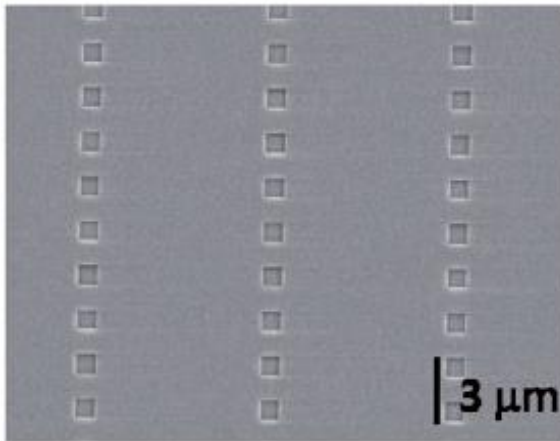


Both the wrapping around gel fibres and the trapping can be also manipulated. If a molecule is trapped around a single fibre with roughly equal arm length. It is possible to cut one part of the strand by applying a short and intense laser pulse. This imbalances the force and the starts moving again until it coils up again in the next void in the gel

http://www.damtp.cam.ac.uk/user/gold/teaching_biophysicsIII.html

Entropic trapping of DNA

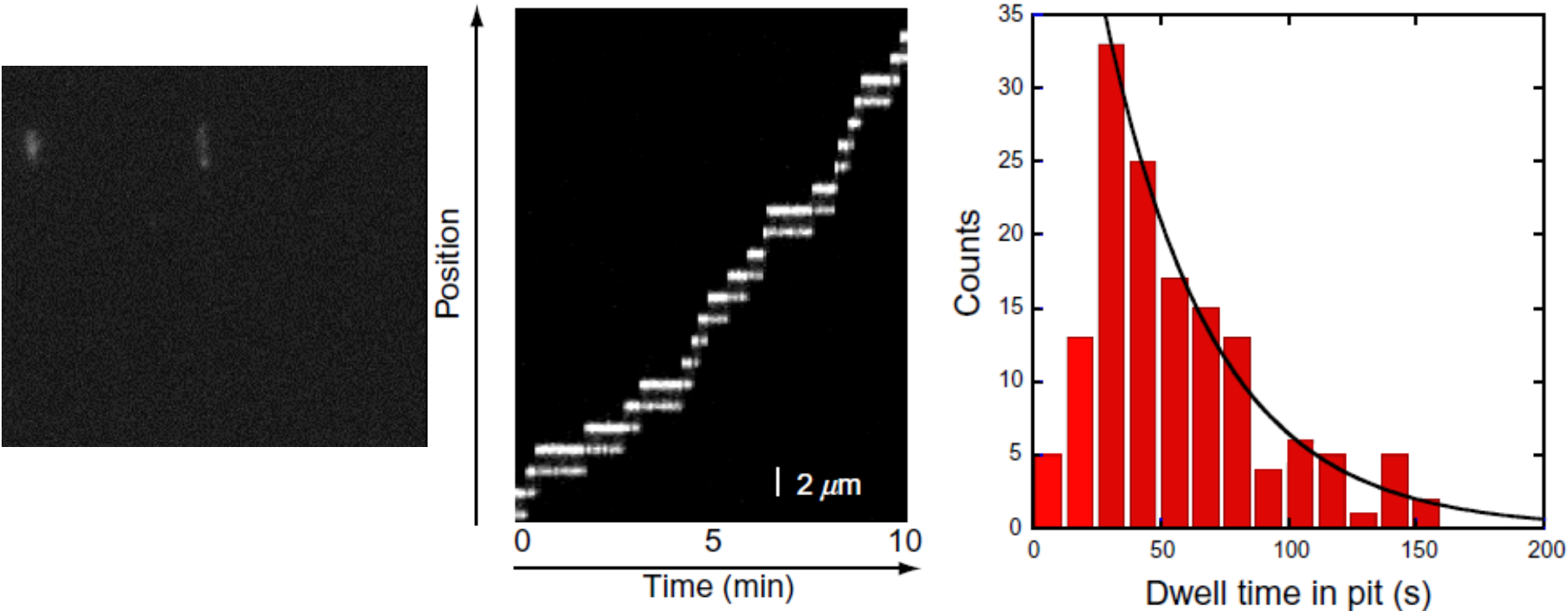
(Del Bonis-O'Donnell 2009)



The trapping of the DNA in voids in the gel can be also investigated in artificially created nanofluidic channel geometries. Small pits with diameters of a few hundred nanometers can be created by standard nanotechnology. The structures can be made in silica channels allowing for optical access and thus imaging the motion of the DNA molecules. By varying either the molecule length or the size of the pit one can establish different types of motion of the DNA molecules when it is driven by an applied pressure. In order to cross from one pit to the next the DNA has to stretch out and thus there is an entropic barrier slowing down the movement. The waiting times can be quantified by simply analysing video data.

Entropic barrier leads to exponentially distributed dwell times

(Del Bonis-O'Donnell 2009)



The trapping of the DNA in voids in the gel can also be investigated in artificially created nanofluidic channel geometries. Small pits with diameters of a few hundred nanometers can be created by standard nanotechnology. The structures can be made in silica channels allowing for optical access and thus imaging the motion of the DNA molecules. By varying either the molecule length or the size of the pit one can establish different types of motion of the DNA molecules when it is driven by an applied pressure. In order to cross from one pit to the next the DNA has to stretch out and thus there is an entropic barrier slowing down the movement. The waiting times can be quantified by simply analysing video data.

Entropic Forces and Single Molecules

(Craighead et al. 2002)

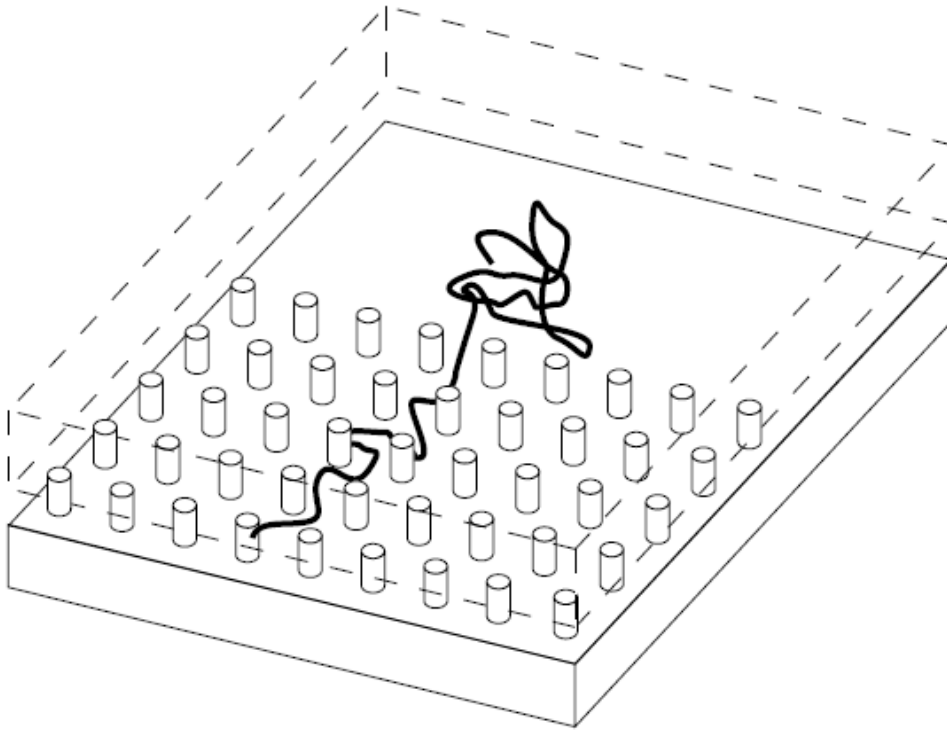


FIG. 1. The fluidic device consists of a quasi-two-dimensional gap between a floor and ceiling approximately 60 nm in height. Some regions of the device are populated with nanopillars.

Following our discussion of gel electrophoresis we briefly mentioned the trapping of long DNA molecules in voids in the gel or in artificial geometries. Especially the role of entropy and the involved forces can be studied in another, more controlled geometry derived from nanotechnology, so called nanofluidic devices.

The aim is to follow the pathway of a single DNA molecule when it is partly trapped in a region with low entropy and at the same time is exposed to a region of high entropy as shown in the scheme on the right. Following the recoiling of the molecule will allow us to determine the entropic forces acting on the molecule.

Entropic Forces and Single Molecules

(Craighead et al. 2002)

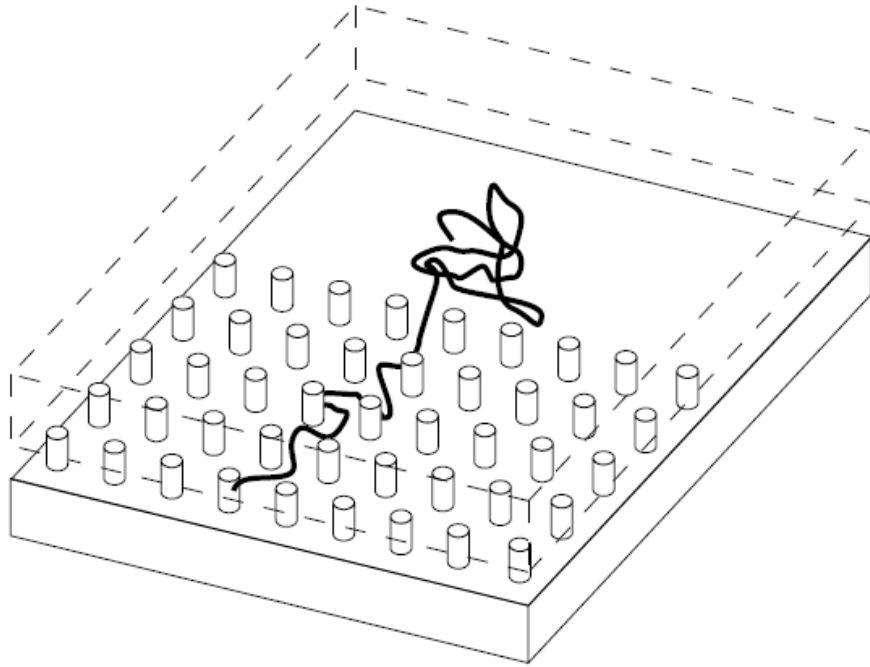
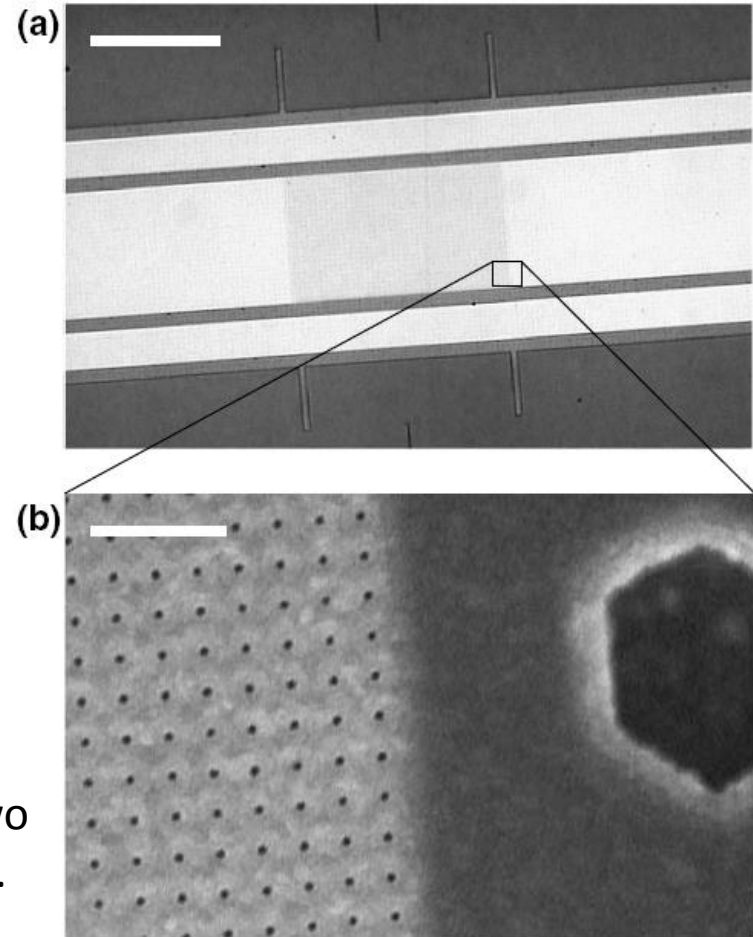


FIG. 1. The fluidic device consists of a quasi-two-dimensional gap between a floor and ceiling approximately 60 nm in height. Some regions of the device are populated with nanopillars.

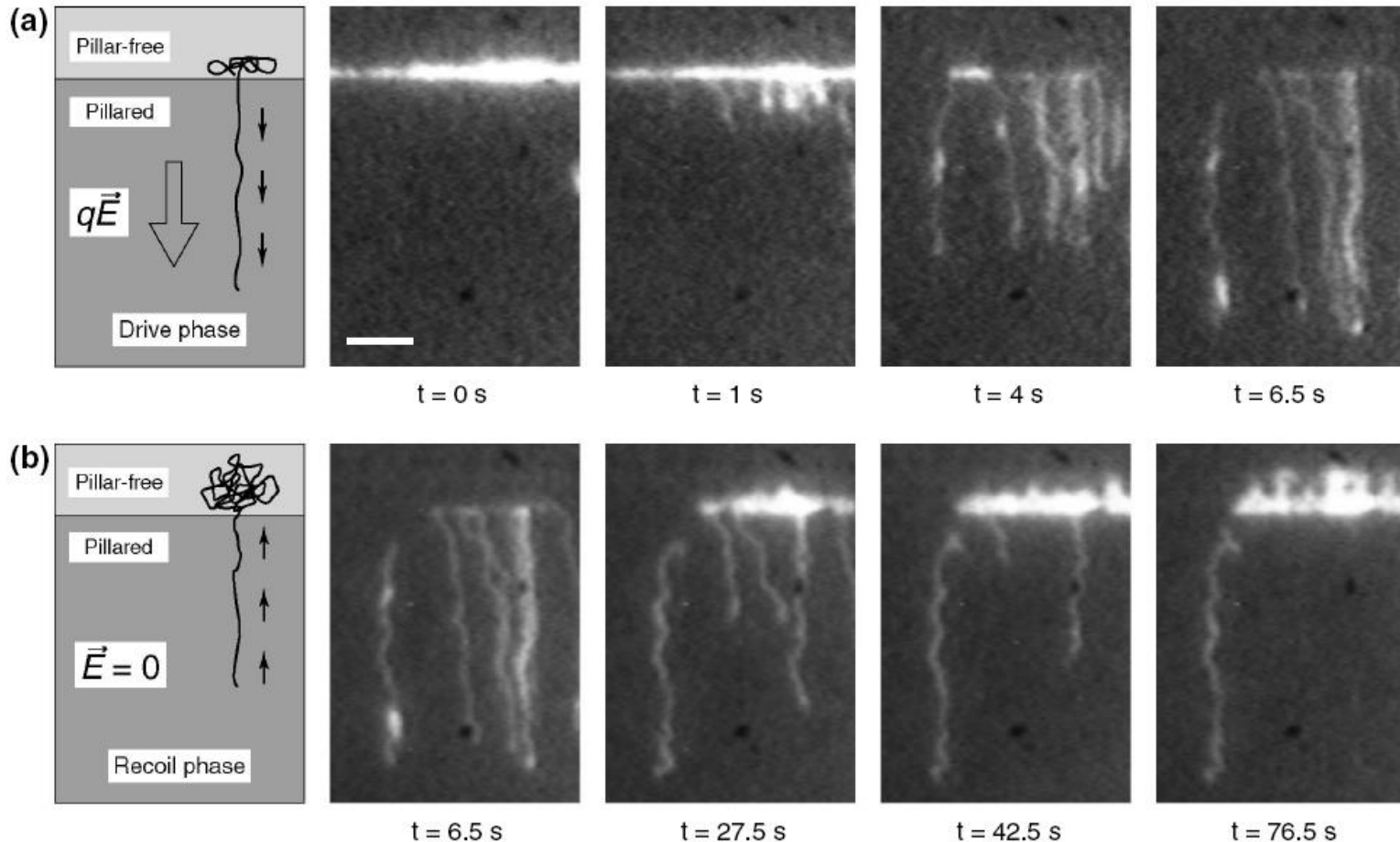
The „Nanofluidic“ device is made by „glueing“ two pieces of glass together with a distance of 60 nm.

The pillars are separated by 160 nm, have an effective diameter of 35 nm, which yields an effective distance of 115 nm, which is roughly equal to two persistence lengths of each DNA molecule. All surfaces are negatively charged to reduce sticking of the DNA to the surfaces, this can be ensured by keeping the pH above 6 where glass (SiO_x) is negatively charged.



Entropic Forces and Single Molecules

(Craighead et al. 2002)



At the beginning of the experiment, DNA in solution is pulled into the pillar region by applying an electric field. The DNA is labeled with a fluorescent dye which makes it visible and easy to trace. The data shows that if part of the molecule is in the pillar-free region it recoils, otherwise it stays in the pillar region.

Entropic Recoiling of DNA reveals Entropic Force

(Craighead et al. 2002)

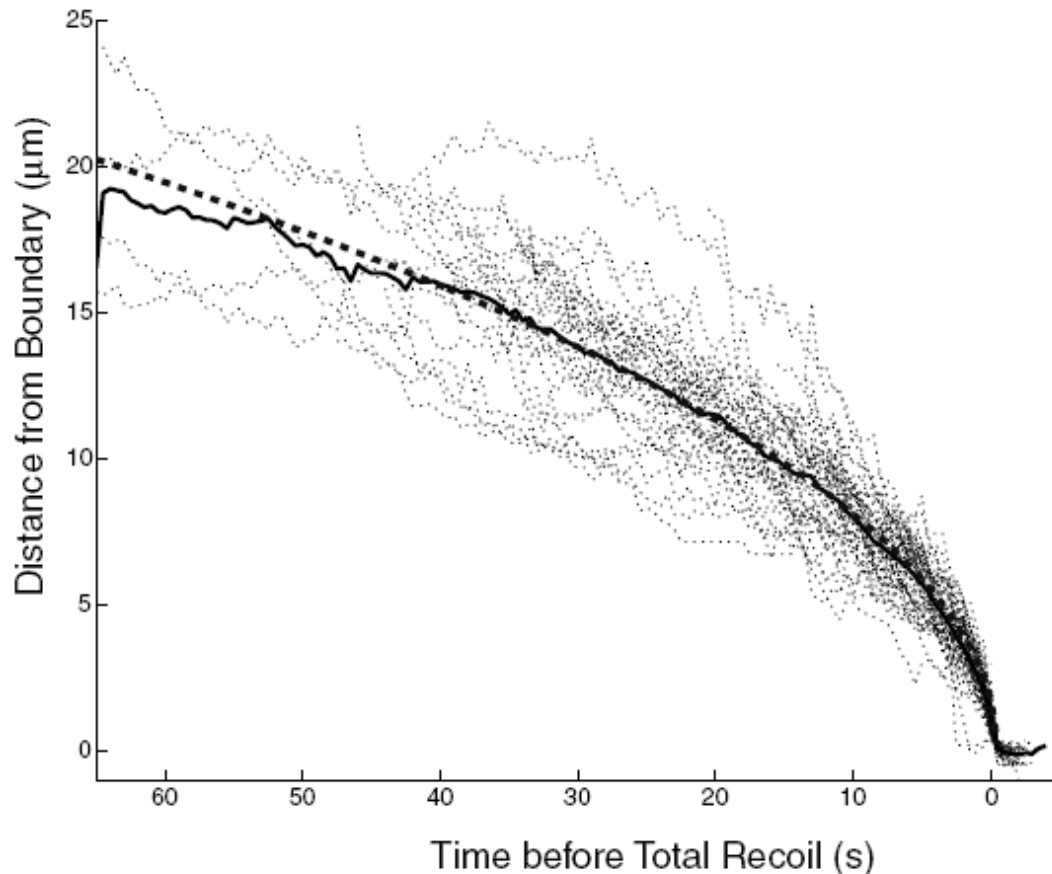


FIG. 4. The distal-end position for 56 recoil events as a function of time. The t values have been shifted so that $t_0 = 0$ for all events. The thin dashed lines show the position data for the individual events. The solid black line is the average of these traces. The heavy dotted line is a fit to the data using Eq. (3).

Following the trajectories of several molecules one can see that the curve follows a square root dependence. The spread in the data is what is expected for single molecule data in environments where $k_B T$ is the dominating energy scale.

These experiments allow to establish that entropy is a local quantity which affects the retraction only if a finite party of the molecule is in the high entropy region. However, the equilibrium position at infinite times would lead to all molecules ending up in the high entropy region. However, the diffusion in the pillar region is very slow on the time scale of the experiments and thus is not observed.

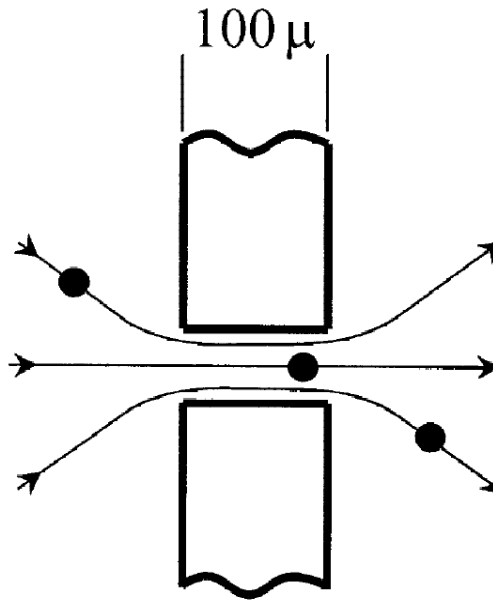
Solid-State Nanopores

- Resistive-pulse technique
- DNA translocation dynamics

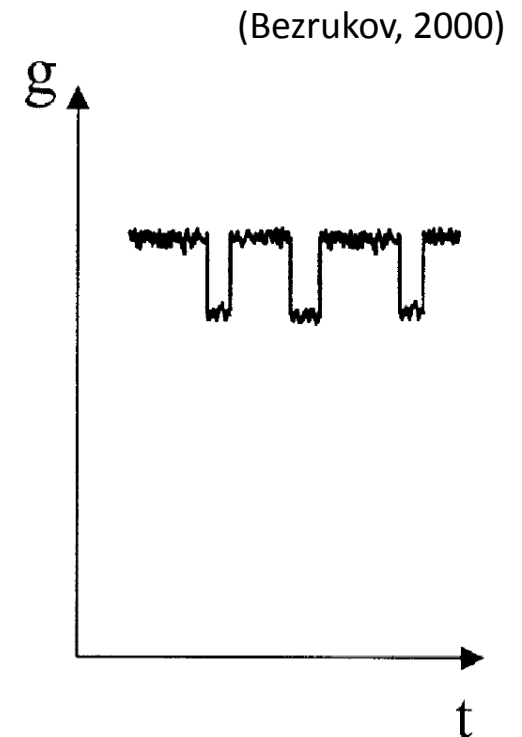
Resistive-Pulse Technique

The resistive-pulse technique was developed with the aim to develop a label-free counting technique for particles in (aqueous) solution. The main advantage of this technique is that it is possible to detect any analyte without labeling (chemically) altering the particles or molecules. Historically, this was first used for the counting of blood cells in samples (1953 patented by Coulter) and since then developed into a major technique for sizing and counting particles and cells.

Main idea: use orifice in glass with a diameter of tens of microns detecting particles down to several tenths of a micron by pressure driven flow. Typical applications include blood cell counting (1958) or bacterial cell counting, with special emphasis on cell-volume distributions.



Orifice in glass



- Tenths of micron diameter capillary
- particles with dimensions down to 60 nm can be detected
 - Virus counting
 - Bacteriophage particles (1977)

Nanopore Fabrication

(Dekker, 2007)

Detection limit obviously depends on the diameter of the orifice that is used. In the last decade the technique was further developed with the goal to count and analyze single polymers (DNA, RNA, proteins, etc.) in solution.

Ideally detect not only the presence of the molecule but also the structure: bends, kinks, bound proteins, ...

Obvious challenge: the typical diameter of double-stranded DNA is only ~2 nm so standard technology is not good enough to control the orifice diameter. In the following we will call the orifice “nanopore”. For spatial resolution along the molecules one would also require the nanopore as short as possible. One solution is silicon-based nanotechnology.

Step 1: Create free-standing membrane

Material: Silicon Nitride low stress SiN_x

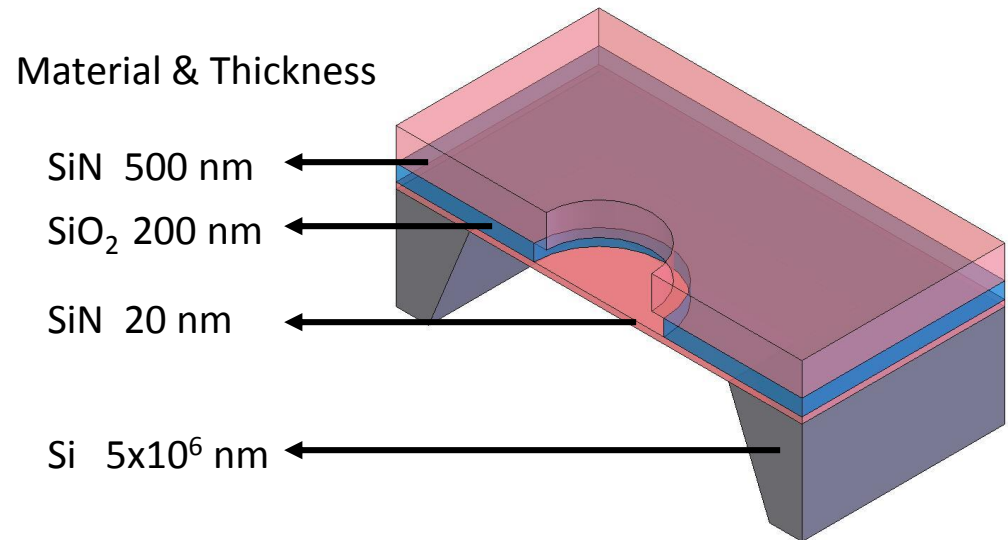
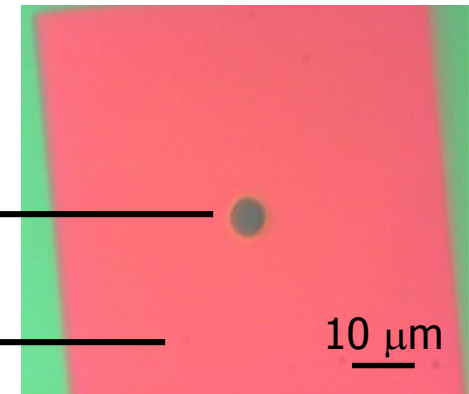


Image with light microscope
in reflection

Free standing membrane
with 20 nm thickness

Free standing membrane
with 720 nm thickness



Nanopore Fabrication

(Dekker, 2007)

Detection limit obviously depends on the diameter of the orifice that is used. In the last decade the technique was further developed with the goal to count and analyze single polymers (DNA, RNA, proteins, etc.) in solution.

Ideally detect not only the presence of the molecule but also the structure: bends, kinks, bound proteins, ...

Obvious challenge: the typical diameter of double-stranded DNA is only ~ 2 nm so standard technology is not good enough to control the orifice diameter. In the following we will call the orifice “nanopore”. For spatial resolution along the molecules one would also require the nanopore as short as possible. One solution is silicon-based nanotechnology.

Step 2: Drill small hole in free standing membrane with focused electron beam

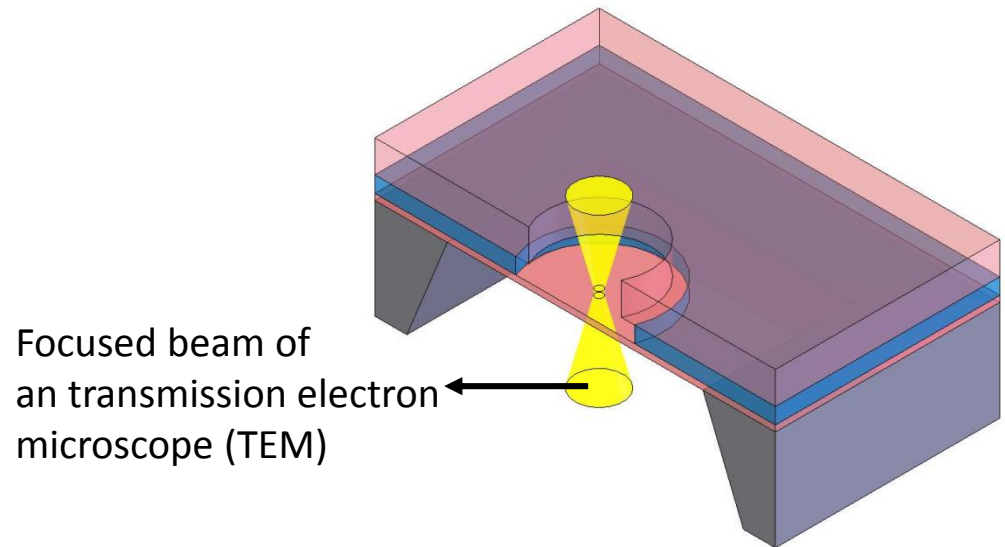
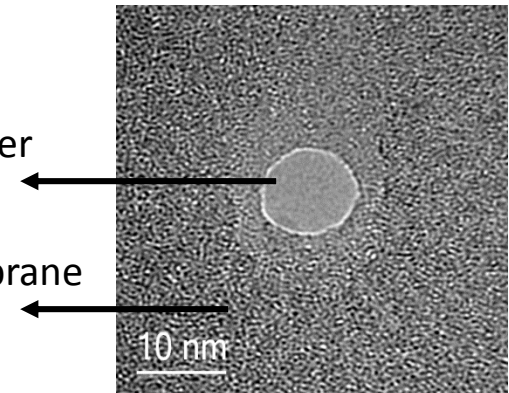


Image with transmission electron microscope

Nanopore with a diameter of ~ 10 nm

Free standing SiN_x membrane with thickness of 20 nm



Nanopore Fabrication

(Dekker, 2007)

Detection limit obviously depends on the diameter of the orifice that is used. In the last decade the technique was further developed with the goal to count and analyze single polymers (DNA, RNA, proteins, etc.) in solution.

Ideally detect not only the presence of the molecule but also the structure: bends, kinks, bound proteins, ...

Obvious challenge: the typical diameter of double-stranded DNA is only ~2 nm so standard technology is not good enough to control the orifice diameter. In the following we will call the orifice “nanopore”. For spatial resolution along the molecules one would also require the nanopore as short as possible. One solution is silicon-based nanotechnology.

Step 3: Adjust diameter of nanopore by using the glassy characteristics of SiN_x

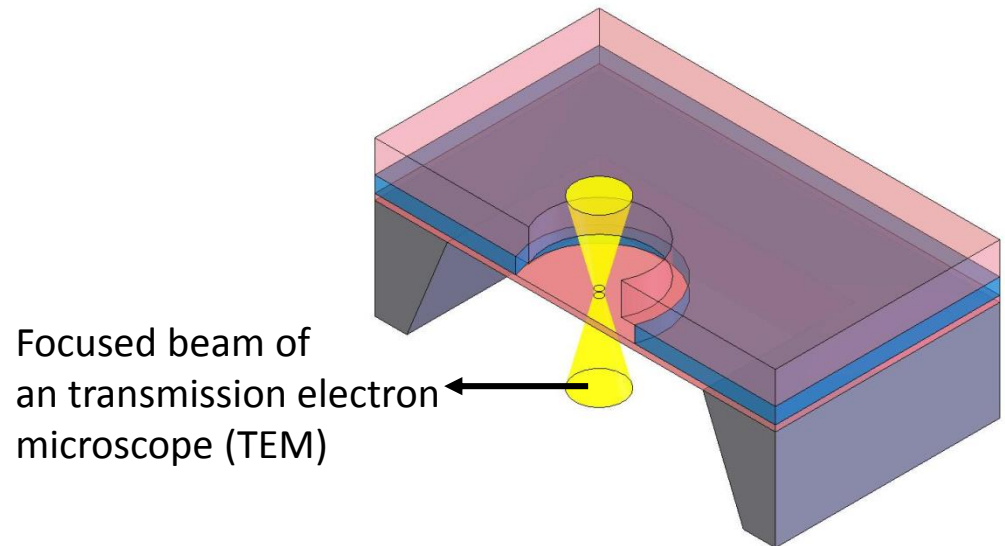
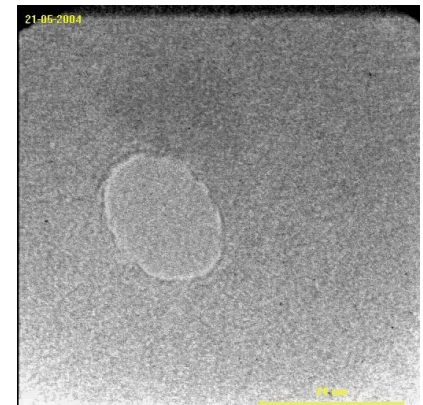


Image with transmission electron microscope

Initial nanopore is elliptical with a diameter of ~20 nm

Final nanopore is circular with a diameter of ~5 nm

Sculpting at the nm-scale!



Nanopore Fabrication

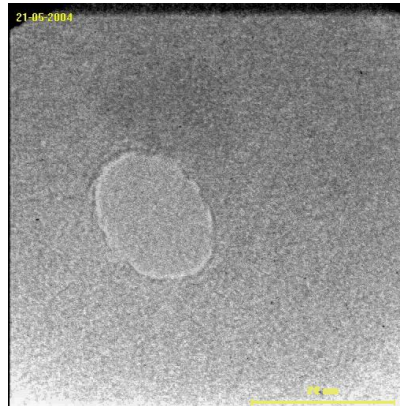
(Dekker, 2007)

Image with transmission electron microscope

Initial nanopore is elliptical with a diameter of ~ 20 nm

Final nanopore is circular with a diameter of ~ 5 nm

Sculpting at the nm-scale!



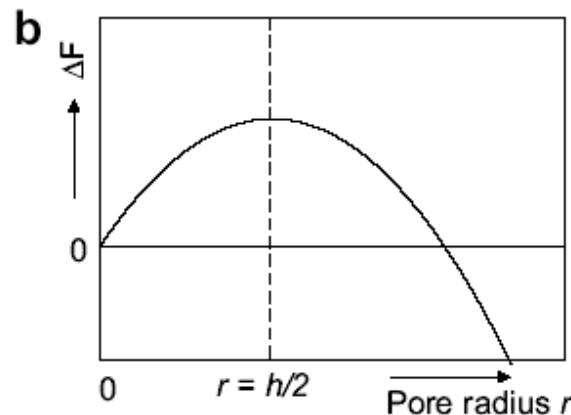
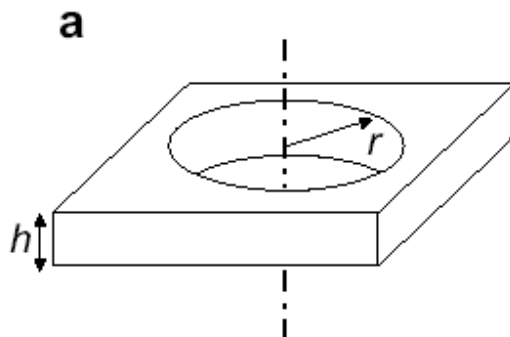
- SiNx is an amorphous (not crystalline) material
- Electron beam deposits energy into the sample
- Local temperature is increased and material can start to flow
- Surface tension wants to minimize free energy
- Free energy gain ΔF is just

$$\Delta F = \gamma \Delta A = 2\pi\gamma(rh - r^2)$$

γ surface tension

r pore radius

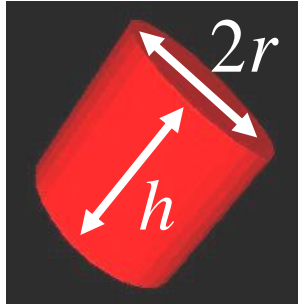
h pore length



Ionic Resistance of Nanopores

(Hille 2001)(Hall 1975)

The simplest model for a nanopore is a cylinder filled with liquid. You can then write down the resistance R_{pore} for the ionic current:



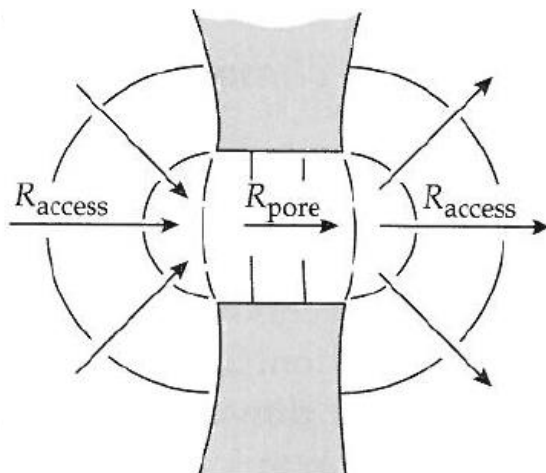
$$R_{\text{pore}} = \frac{1}{\sigma_{\text{KCl}}(T)} \left(\frac{h}{\pi r^2} \right)$$

h = membrane thickness

r = nanopore radius

$\sigma(T) = 1/\rho(T)$ conductivity

However, if the membrane thickness is in the range of the diameter of the nanopore we have to take into account the so-called access resistance, which is nothing else than the distortion of the electric field lines due to the mismatch in dielectric constant between membrane and ionic solution :



$$R_{\text{pore}} = \frac{1}{\sigma_{\text{KCl}}(T)} \left(\frac{h}{\pi r^2} \right)$$

$$R_{\text{access}} = \frac{1}{\sigma_{\text{KCl}}(T)} \left(\frac{1}{2r} \right) = 2 \times \frac{1}{\sigma_{\text{KCl}}(T)} \left(\frac{1}{4r} \right)$$

$$R_{\text{nanopore}} = \frac{1}{\sigma_{\text{KCl}}(T)} \left(\frac{h}{\pi r^2} + \frac{1}{2r} \right)$$

Understanding Access Resistance By Concentration Driven Diffusion

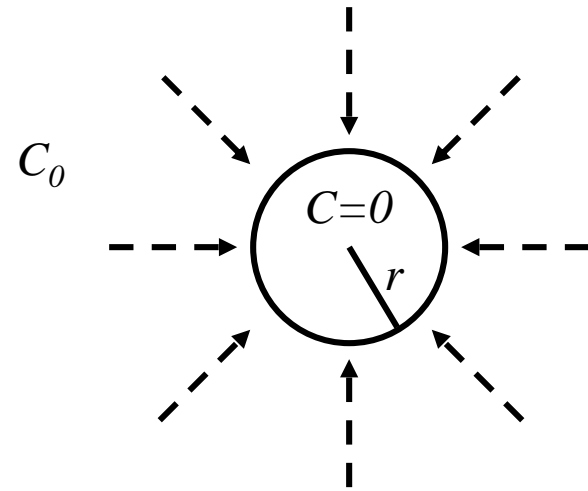
- Diffusive current I (particles per second) to a perfect spherical absorber with radius r is ($C=0$ at absorber and C_0 at infinity)

$$I = 4\pi DrC_0$$

- Thus for a hemisphere we get

$$I = 2\pi DrC_0$$

- It is interesting to note here that the diffusive current is proportional to r and not to r^2 . The reason is that as r increases the surface increases as r^2 but the gradient is getting smaller as $1/r$



Understanding Access Resistance

One of the simplest ways to understand origin of the access resistance can be obtained by looking at diffusive current driven by concentration gradients.

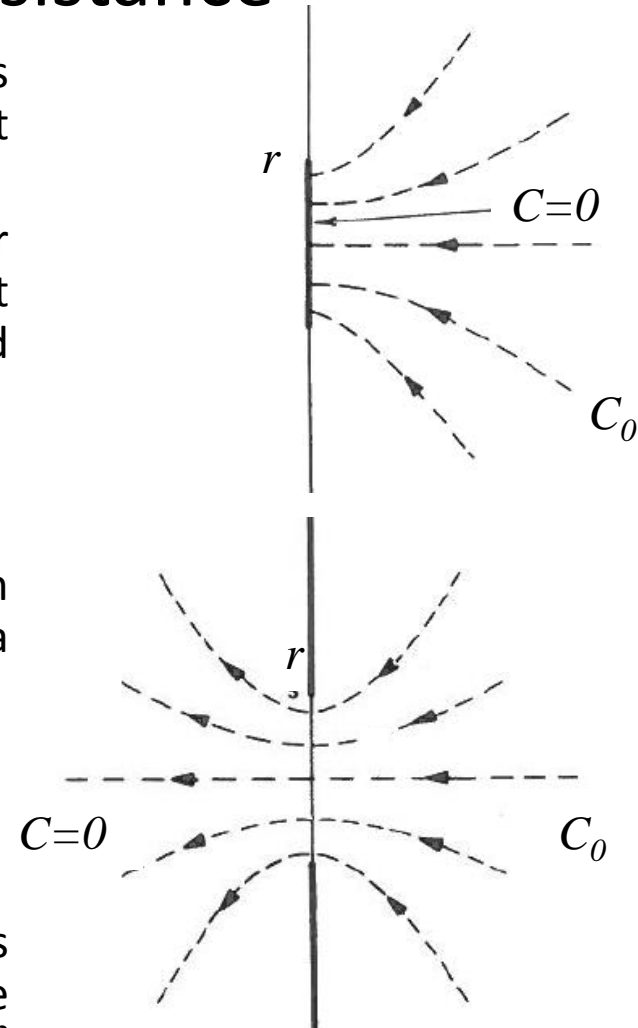
Assuming that there is a diffusive current I (particles per second) to a perfect disk like absorber with radius r is ($C=0$ at absorber and C_0 at infinity) one can calculate the current as

$$I = 4DrC_0$$

We can easily conclude that the diffusive current through a hole (assuming it is a perfect absorber) with radius r in a membrane of zero thickness is thus just half the above value

$$I = 2DrC_0$$

It is interesting to note here that the diffusive current is proportional to r and not to r^2 . The reason for the dependence on the radius is that as r increases the surface increases as r^2 but the gradient is getting smaller as $1/r$. This is absolutely equivalent to the situation in driven ionic current when the concentration gradient is replaced by the driving potential.



Access Resistance

- For driven ionic currents through nanopores we are able to simply rewrite the equations for the diffusion current on the preceding pages by changing concentration gradient into ΔV , diffusion constant D into ionic conductivity $\sigma(T)$ and thus write

Resistance of a hemisphere:

$$R = \frac{1}{2\pi\sigma(T)r} = \frac{\rho(T)}{2\pi r}$$

Resistance of a circular absorber:

$$R = \frac{1}{4\sigma(T)r} = \frac{\rho(T)}{4r}$$

Resistance of a circular pore:

$$R = \frac{1}{2\sigma(T)r} = \frac{\rho(T)}{2r}$$

- This explains the additional term in the nanopore resistance, could be also interpreted as enhanced length of the nanopore with implications for the spatial resolution of sensing applications

$$R_{\text{nanopore}} = \frac{1}{\sigma_{KCl}(T)} \left(\frac{h}{\pi r^2} + \frac{1}{2r} \right)$$

Diffusion Limited Ionic Currents

(Hille 2001)

The diffusion towards the nanopore entrance sets a limit to the ionic current flowing through a nanopore. For this discussion we are neglecting any potential drops in the solution surrounding the nanopore.

Assuming that we are in steady-state, we can estimate the diffusive current to a hemispherical pore mouth with radius of 5 nm is:

$$I = 2\pi DrC_0$$

$$I = 2\pi \cdot 5 \cdot 10^{-9} \text{ m} \cdot 2 \cdot 10^{-9} \text{ m}^2 \text{ s}^{-1} \cdot 0.1 \text{ mol/l}$$

$$I \approx 3.8 \cdot 10^9 \text{ ions / s} = 610 \text{ pA}$$

This indicates that nanopores at high bias voltage should be diffusion limited, which is not the case \Leftrightarrow there is a finite potential drop - due to the access resistance - outside of the nanopore delivering ions faster than diffusion.

For biological channels their radius is often below or around 1 nm:

$$I = 2\pi \cdot 5 \cdot 10^{-10} \text{ m} \cdot 2 \cdot 10^{-9} \text{ m}^2 \text{ s}^{-1} \cdot 0.1 \text{ mol l}^{-1} \approx 3.8 \cdot 10^8 \text{ ions / s} = 61 \text{ pA}$$

at typical membrane potentials of 100 mV this is larger than the current through most biological nanopores which indicates that small biological pores are usually not diffusion limited.

Diffusion constant and conductivity

(CRC Handbook 2000)

- For a given aqueous solution the diffusion constant of the ionic species D_+ and D_- , for the positive and negative ions respectively, is directly linked to the conductivity of the salt solution:

$$\sigma(T) = \frac{1}{\rho(T)} = \frac{z^2 e}{k_B T} (D_+ + D_-) n = z^2 e (\mu_+ + \mu_-) n$$

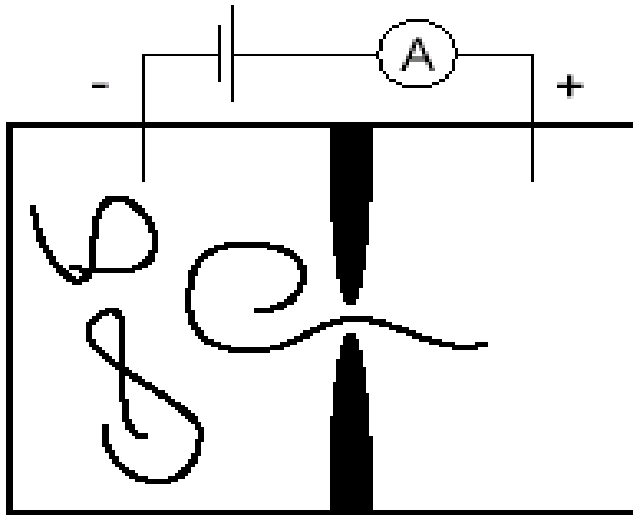
where μ_+ and μ_- are the mobility for the respective ionic species and n the ion concentration

- Some diffusion constants for ions in aqueous solution (infinite dilution, T=25C, $10^{-9}\text{m}^2/\text{s}$):

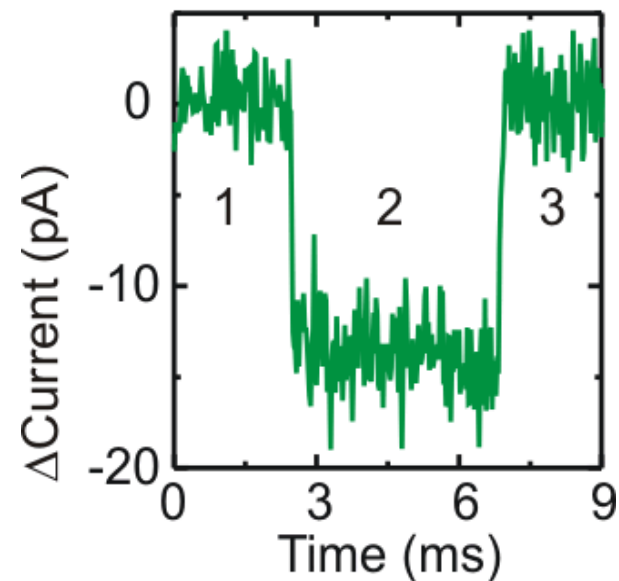
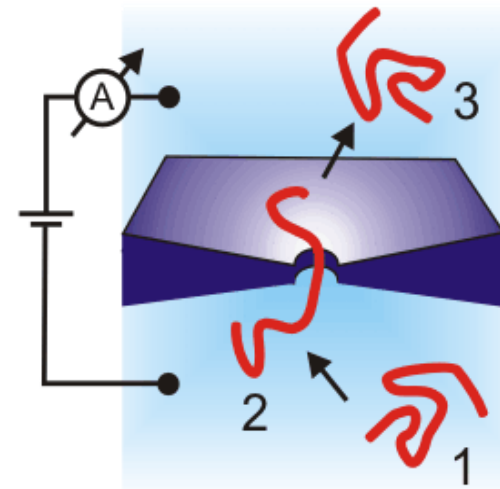
K+	1.957	Cl-	2.032
Na+	1.334	F-	1.475
Li+	1.029		
Cs+	2.056		
H+	9.311	OH-	5.273
Mg2+	0.706		

Nanopores as DNA Detectors

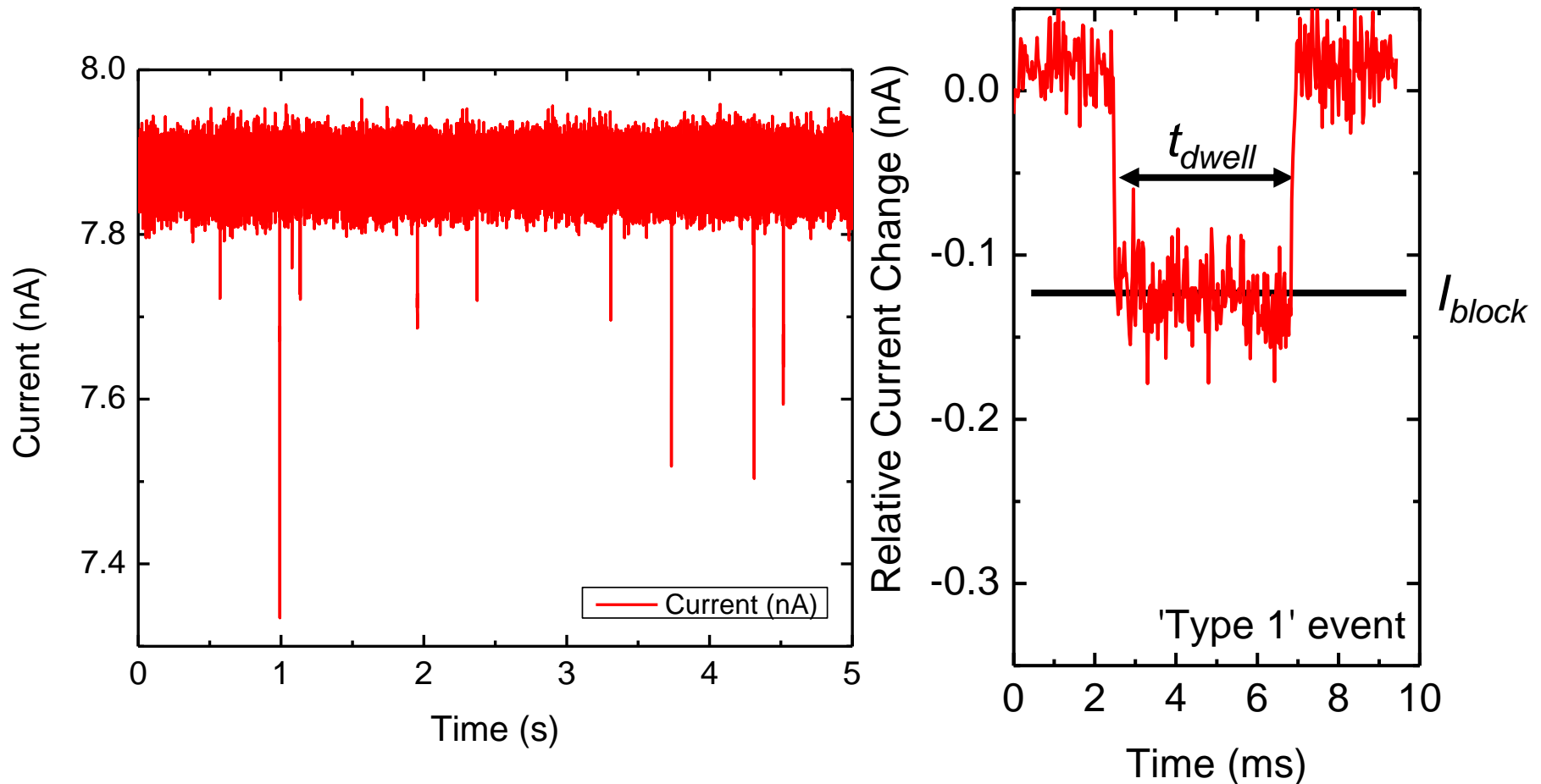
(Dekker, 2007)



- Reservoirs contain salt solution
- Connected by a nanopore
- DNA added on one side
- DNA is detected by ionic current



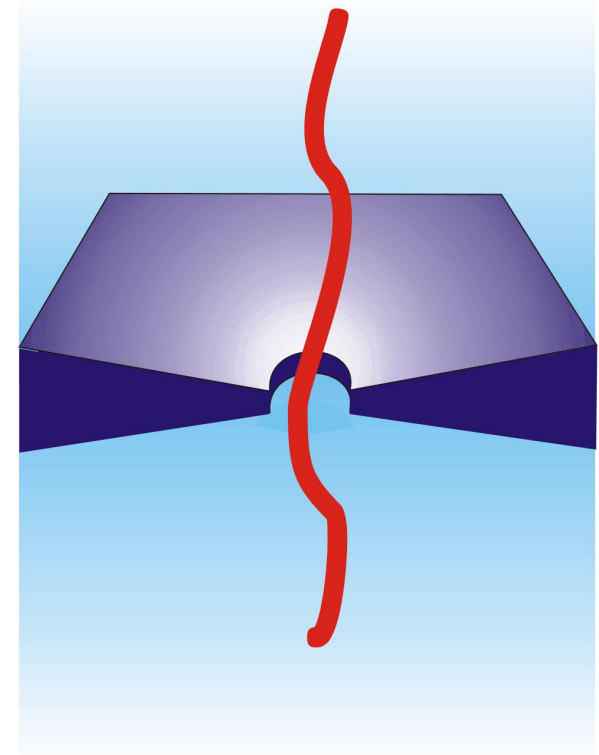
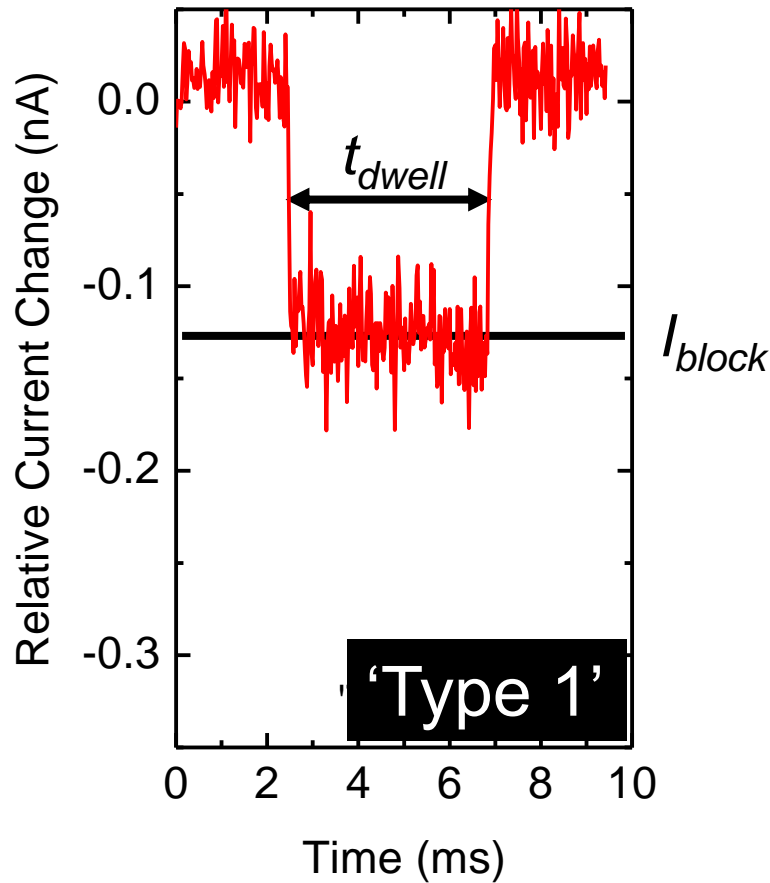
DNA Translocation



- DNA translocation measured in 1M KCl with nanopore of 10 nm diameter
- Current decreases, indicating DNA passing through the nanopore
- Microsecond time resolution allow for detection of event structure

Typical Events in Nanopores

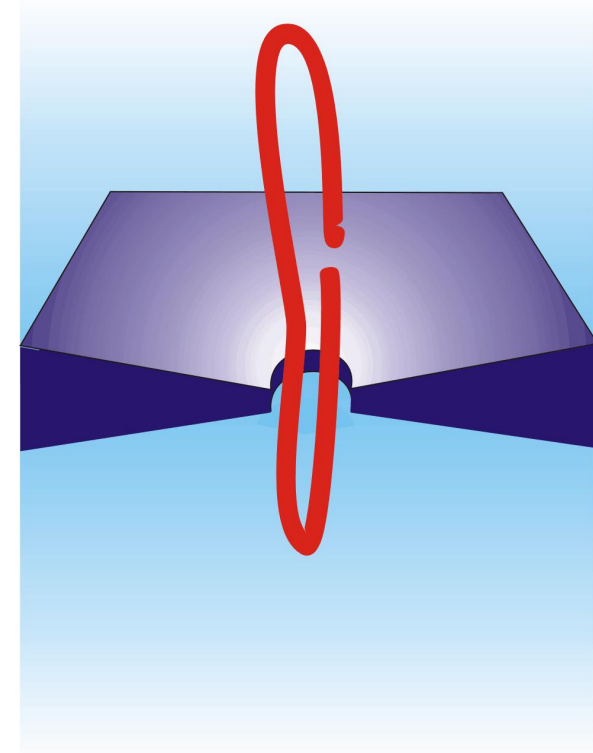
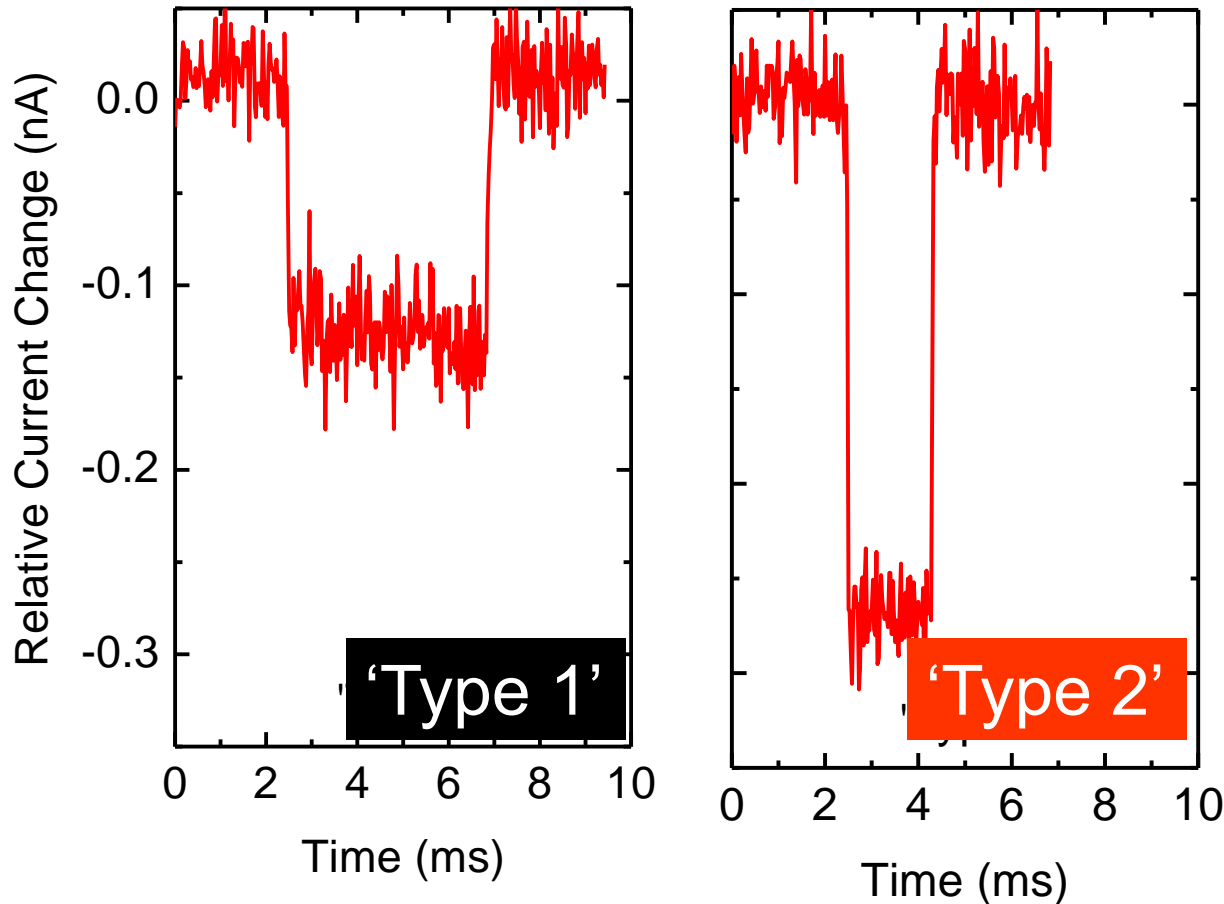
(Smeets et al. 2006)



- Linear translocation of the DNA through the nanopore
- Events are characterized by dwell time t_{dwell} and averaged current blockade level I_{block}

Typical Events in Nanopores

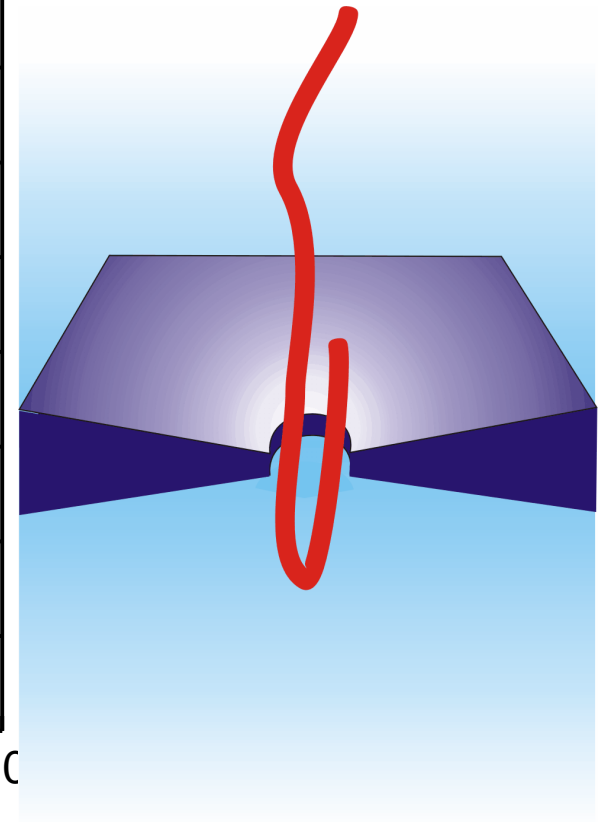
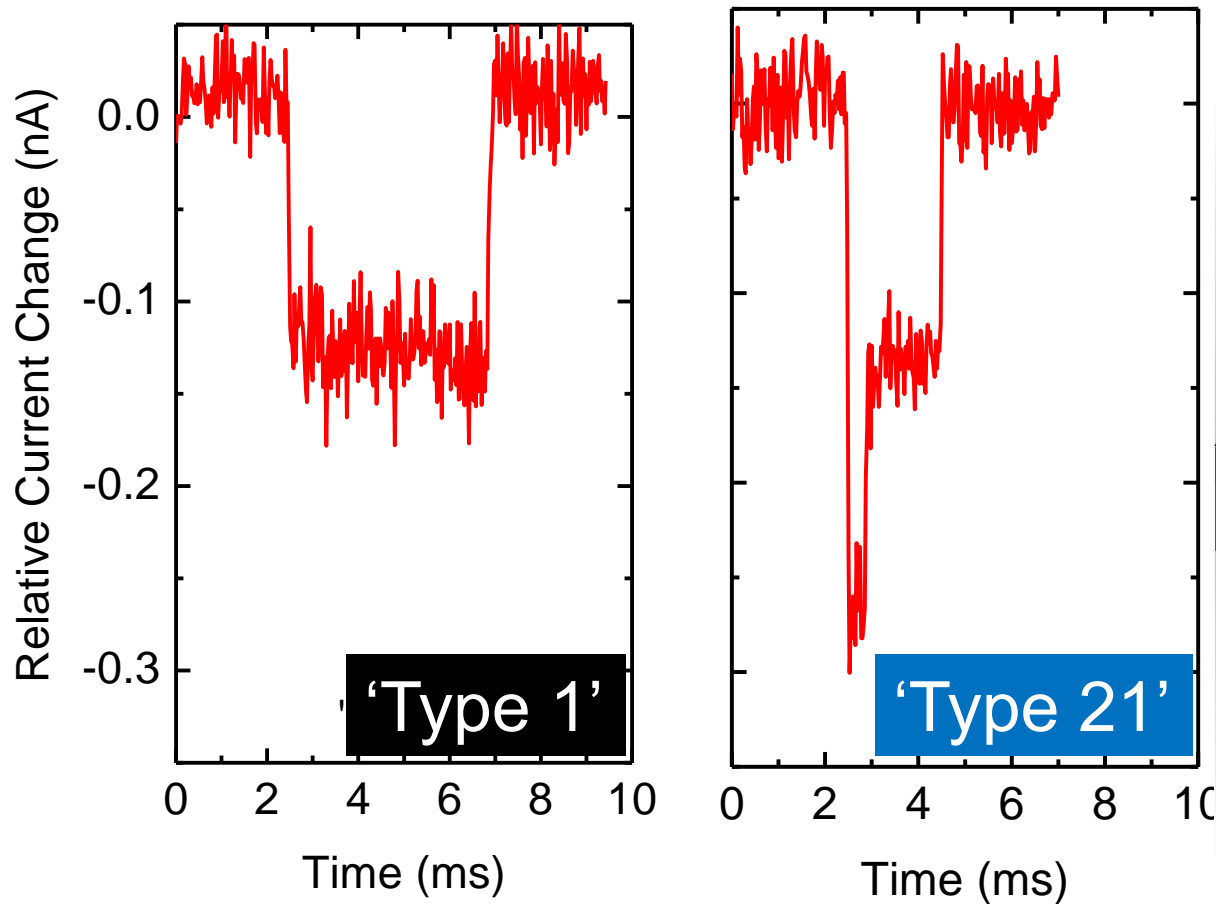
(Smeets et al. 2006)



- Doubling of the current blockade: DNA can be folded when going through the nanopore (diameter 10 nm)

Typical Events in Nanopores

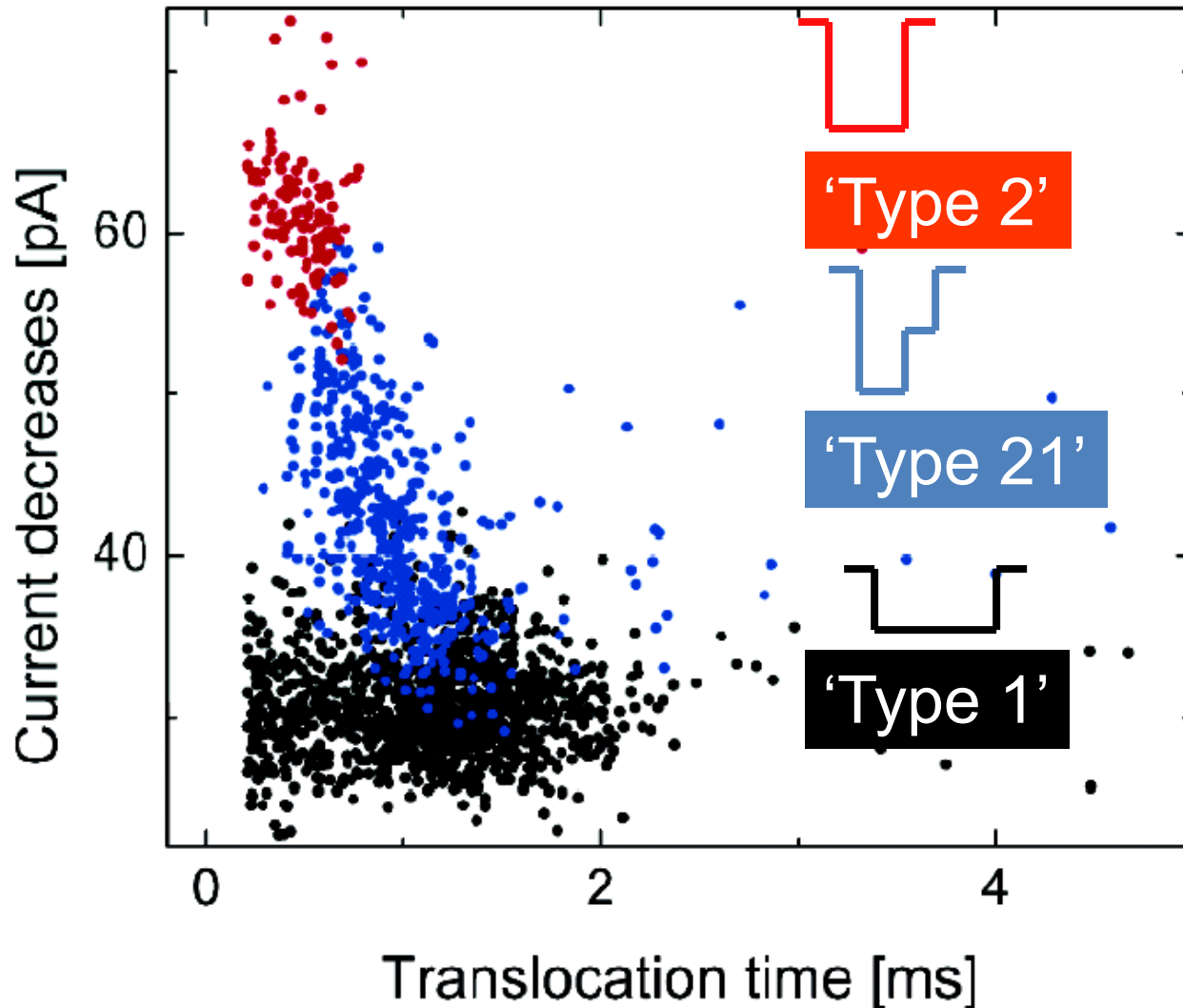
(Smeets et al. 2006)



- Combination of both events are also observed
- DNA can fold in nanopores with diameters of several nm

Analyzing DNA Translocations

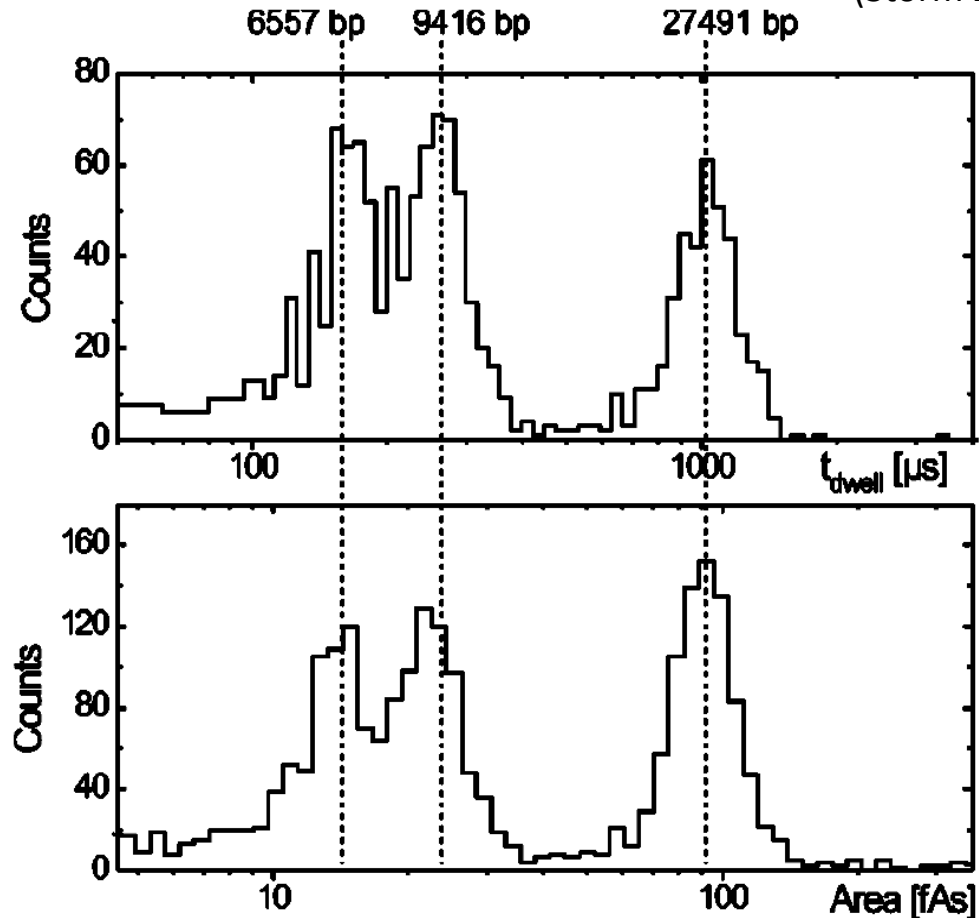
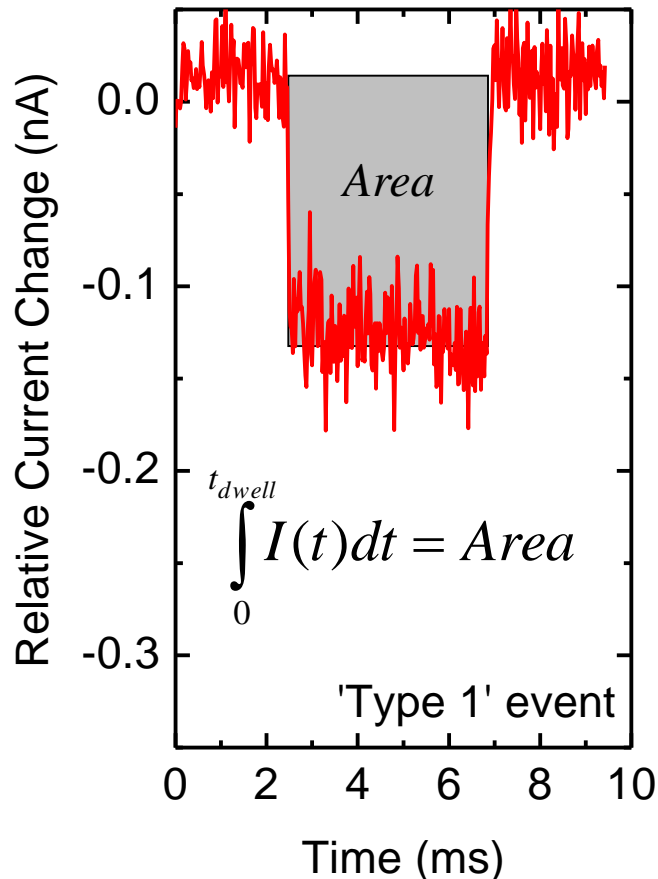
(Smeets et al. 2006)



- Each point represents one single-molecule measurement
- High throughput analysis is easily possible
- 'Type 2' twice the blockade of 'Type 1' and half the dwell time
- 'Type 21' lies in between, as expected
- Tertiary structure of DNA can be detected
⇔ folds and kinks, bound proteins, ...

Event area scales with DNA length

(Storm 2005)



- Integrated charge scales linearly with length of translocating DNA
- Prove that DNA is actually going through the nanopore

Polymer physics with Nanopores

(Storm 2005)

- Long DNA molecules are pulled through much faster than their Zimm relaxation time

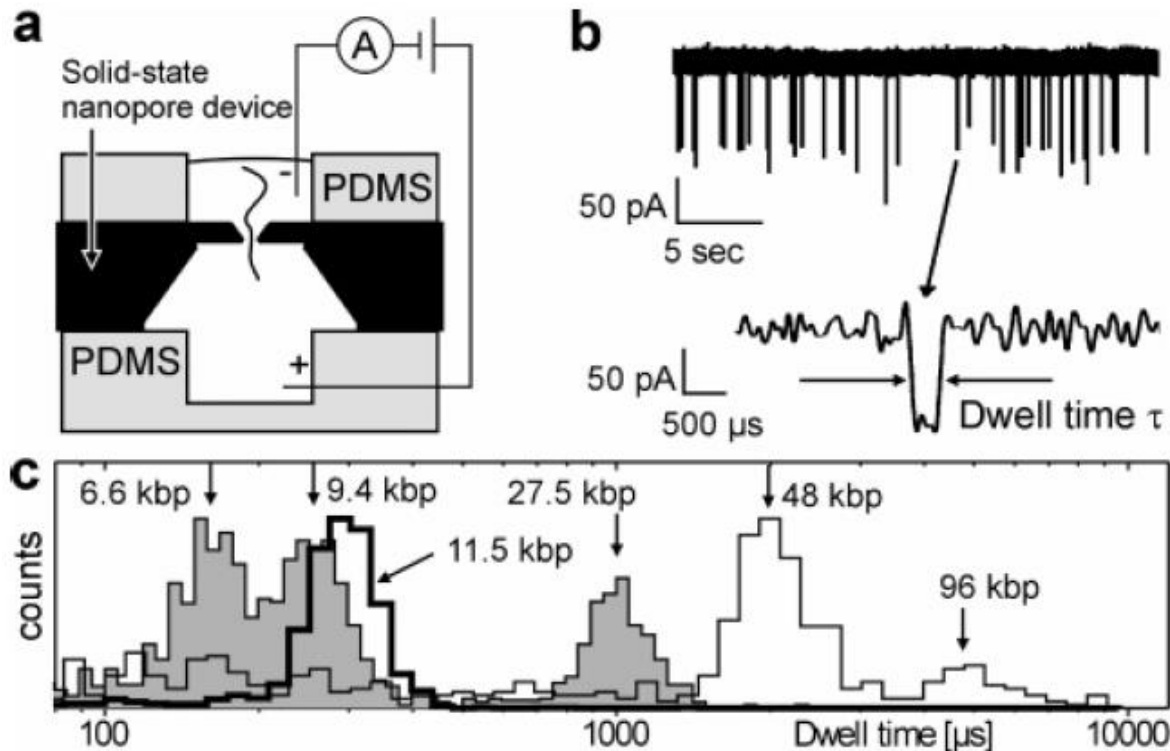
$$\tau_Z \approx \frac{R^2}{D_Z} \approx \frac{\eta}{k_B T} R^3 \approx \frac{\eta b^3}{k_B T} N^{3\nu} \approx \tau_0 N^{3\nu}$$

$$\tau_Z \approx \frac{0.001 \text{ Nsm}^{-2} (100 \times 10^{-9} \text{ m})^3}{k_B T} 160^{3 \times 0.588} \approx 2 \text{ s}$$

- Translocation time for 16 micron long DNA (48 kbp) $\sim 1 \text{ ms}$ \Leftrightarrow drag on polymer coil should be detectable in translocation time?

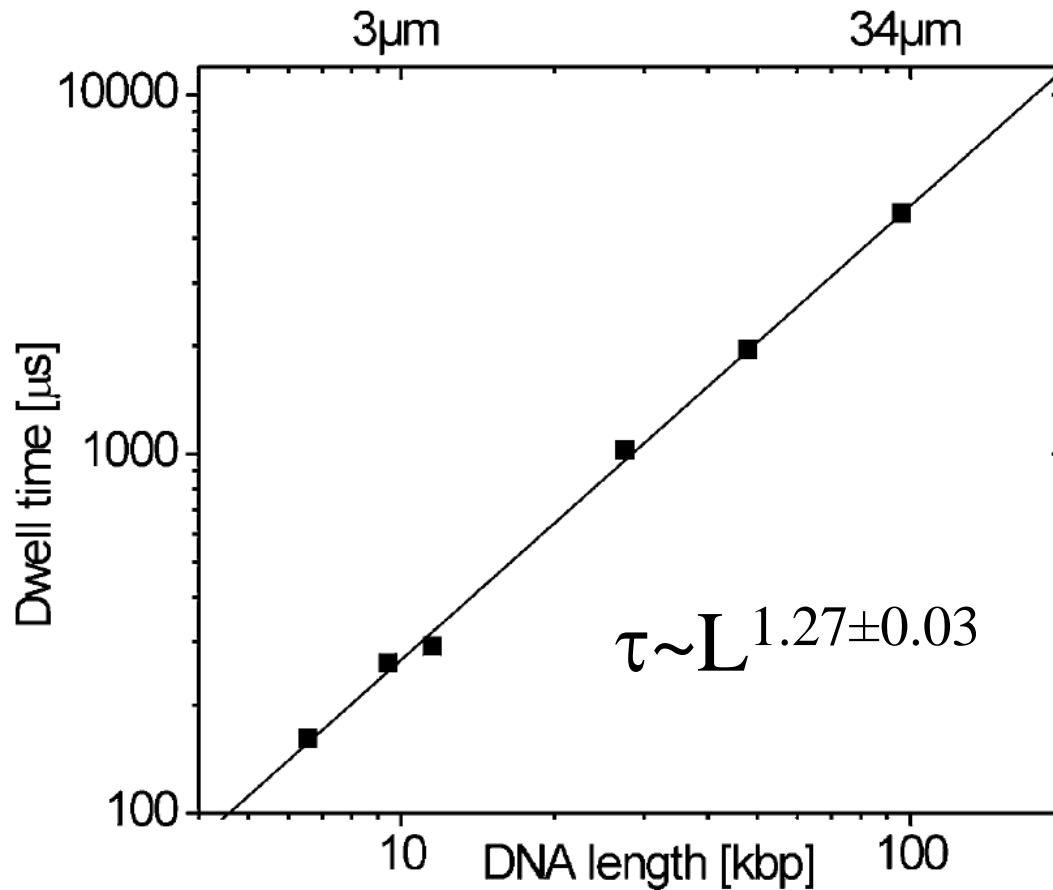
Experimental results: fast translocations

(Storm 2005)



- Fast translocation: dwell time τ larger than Zimm time τ_Z ,
- Polymer cannot reach a new equilibrium configuration during translocation of each segment b
- DNA length varied between 6.6 kbp and 96 kbp \Leftrightarrow length increased by factor of 16, τ increases 0.2 ms to 5 ms, factor of 25

Experimental results: fast translocations

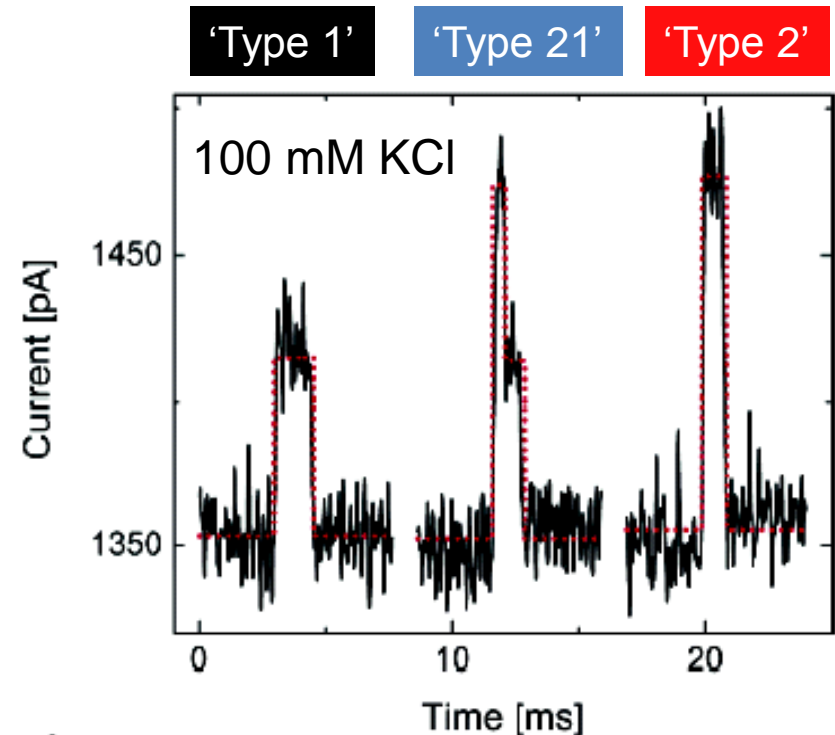
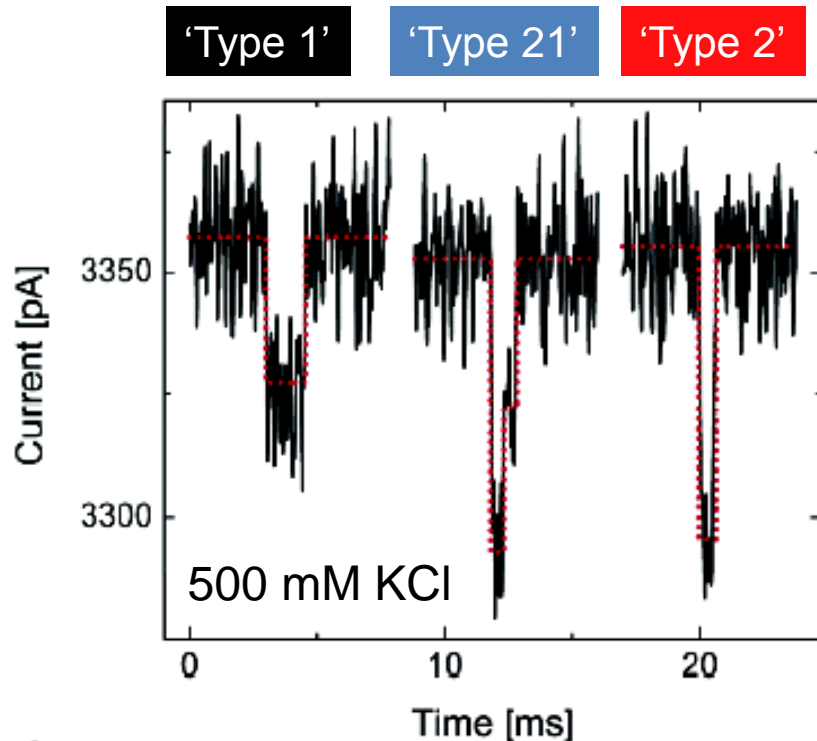


(Storm 2005)

- Translocation time scales with $L^{2\nu}$ with $\nu \sim 0.588$ the Flory exponent for dsDNA – very nice fit to calculations

Variation of Ionic Strength

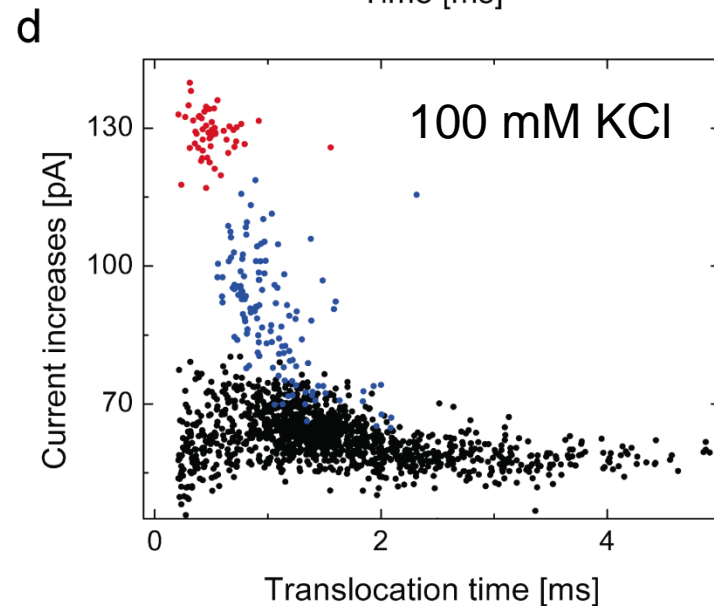
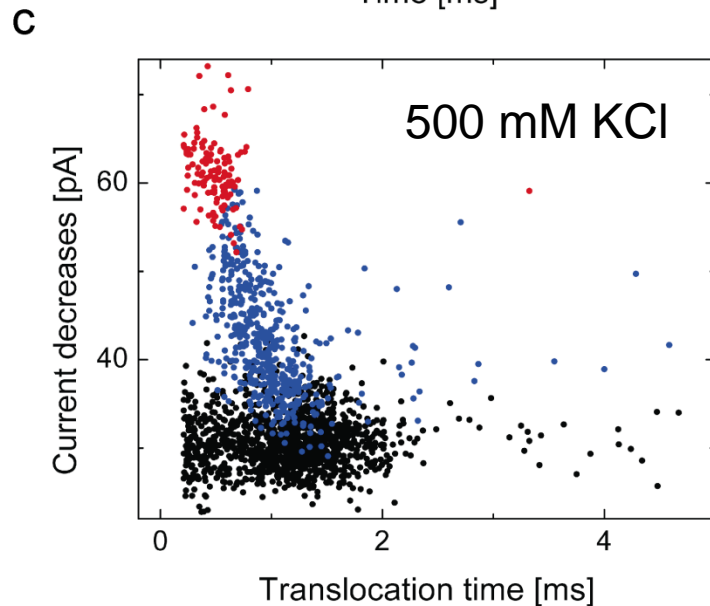
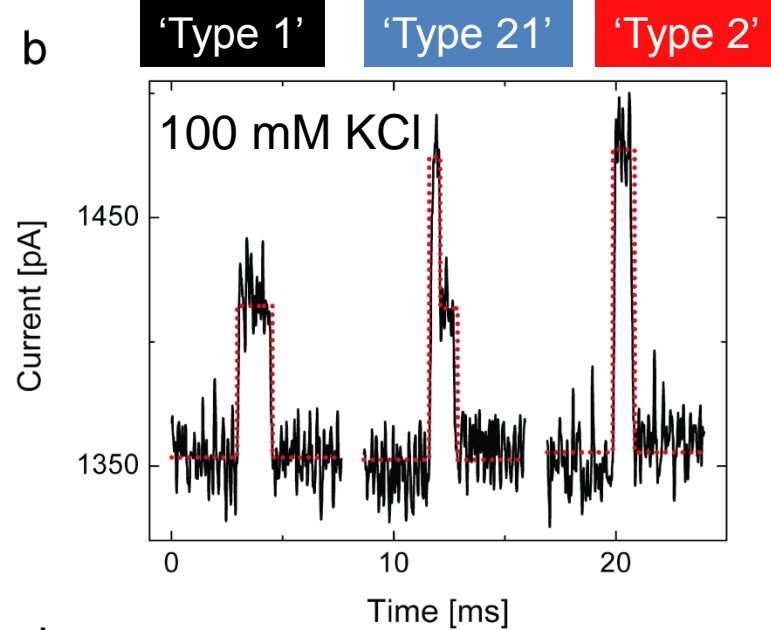
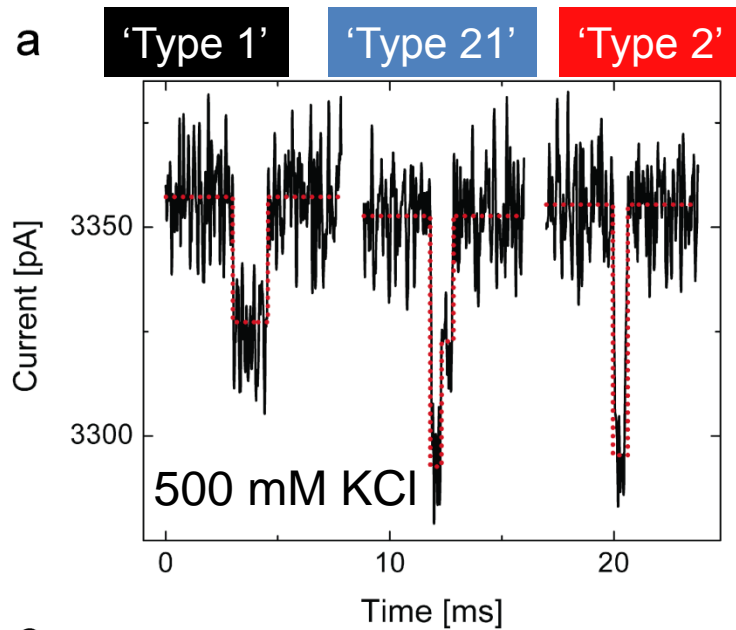
(Smeets et al. 2006)



- For salt concentrations larger than 400 mM ionic current through nanopore is DECREASED when DNA is in the nanopore
- For salt concentration smaller than 400 mM current through nanopore is INCREASED when DNA is in the nanopore
- DNA is a polyelectrolyte with charge and counterions

Variation of Ionic Strength

(Smeets et al. 2006)



Change in nanopore conductance ΔG

(Smeets et al. 2006)

$$\Delta G = \frac{e}{L_{pore}} \left(-\frac{\pi}{4} d_{DNA}^2 (\mu_K + \mu_{Cl}) n_{Bulk} + 2 \frac{\mu_K^*}{a} + 2 \frac{\mu_{DNA}}{a} \right)$$

Conductance reduction due
to DNA in Nanopore

Counter ions
on DNA

Conductance due to
the moving DNA

- Change in nanopore conductance ΔG due to DNA with diameter d_{DNA}
- DNA pushes ions out of the nanopore
- DNA counter ions are brought into nanopore
- Opposite effects depending on bulk concentration of ions n_{bulk}
- With μ_K and μ_{DNA} the mobility of counterions and DNA, respectively

Change in nanopore conductance ΔG

(Smeets et al. 2006)

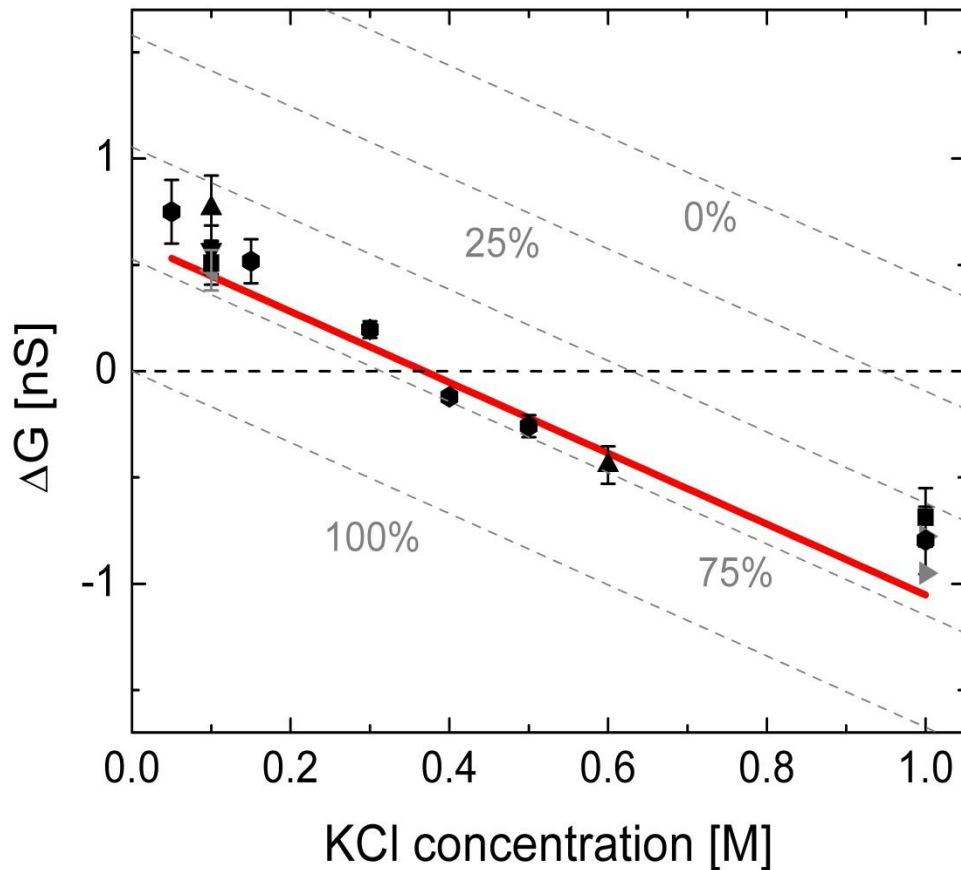
$$\Delta G = \frac{e}{L_{pore}} \left(-\frac{\pi}{4} d_{DNA}^2 (\mu_K + \mu_{Cl}) n_{Bulk} + \underbrace{\frac{2\mu_K^* + 2\mu_{DNA}}{a}} \right)$$

$$\Delta G = \frac{1}{L_{pore}} \left(-\frac{\pi}{4} d_{DNA}^2 (\mu_K + \mu_{Cl}) n_{Bulk} e + \frac{\mu_K q_{eff,DNA}}{a} \right)$$

- Our assumption: all of the counter ions are movable, however some have lower mobility
- Account for this by reducing DNA charge by “attaching” part of the potassium counter ions to the DNA backbone
- Mobility of potassium is higher than DNA mobility

Change in nanopore conductance ΔG

(Smeets et al. 2006)



$$\Delta G_{-} \sim \left(\frac{\pi}{4} d_{DNA}^2 (\mu_K + \mu_{Cl}) n_{KCl} \right)$$

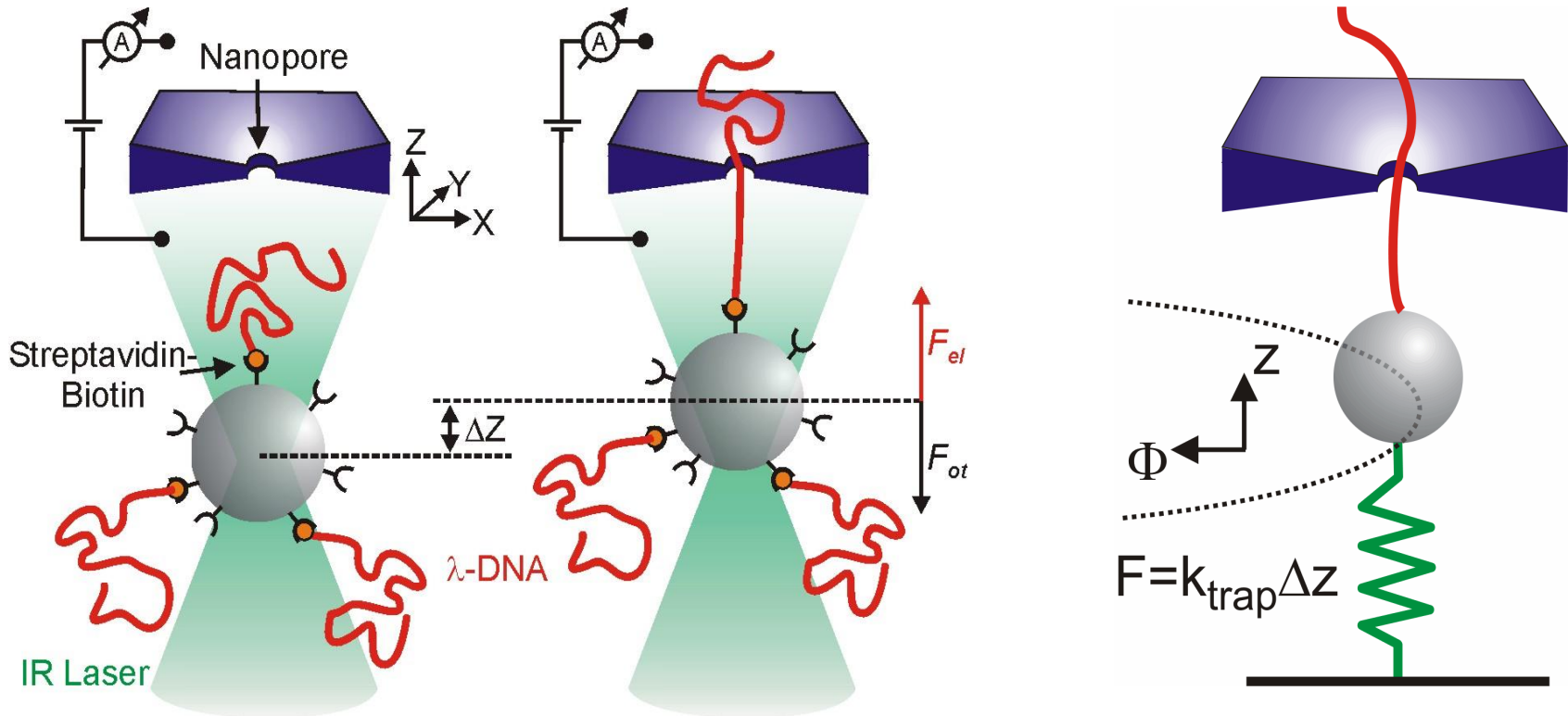
$$\Delta G_{+} \sim (\mu_K^* q_{l,DNA}^*) \rightarrow \mu_K q_{l,DNA}^*$$

$$q_{l,DNA}^* = 0.58 \pm 0.02 \frac{e}{bp}$$

- Simple model can be used to fit the data and extract the line charge density of DNA $q_{l,DNA}^*$
- Bare DNA has a line charge density of $2e/bp$

Optical Tweezers and Nanopores

(Keyser et al. 2006)

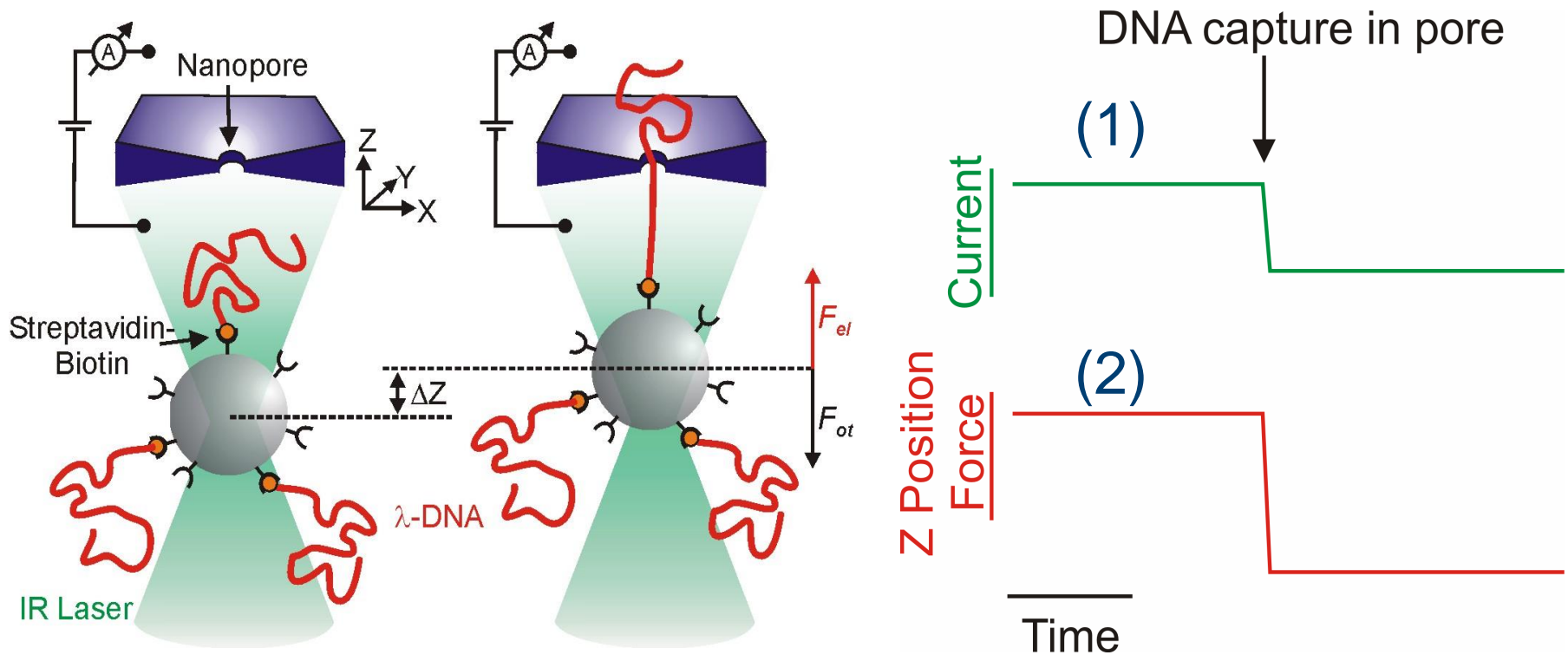


After discussing free DNA translocation experiments we can now Combine optical tweezers with nanopores and current detection we will now try to fully understand the physics governing the electrophoretic translocation through nanopores. The main variable we need for this is the force acting on the molecule in the nanopore. We will again employ optical tweezers, now in combination with a nanopore to measure translocation speed, force and position

http://www.damtp.cam.ac.uk/user/gold/teaching_biophysicsIII.html

Two measurements: current and force

(Keyser et al. 2006)



A single colloidal particle is coated with DNA and is held in close proximity to a nanopore in the focus of the optical trap. An applied electric potential will drive the DNA into the biased nanopore. When the DNA enters the nanopore we will see that both the ionic current through the nanopore as well as the position (force) or the particle will change at the same time:

(1) the current changes

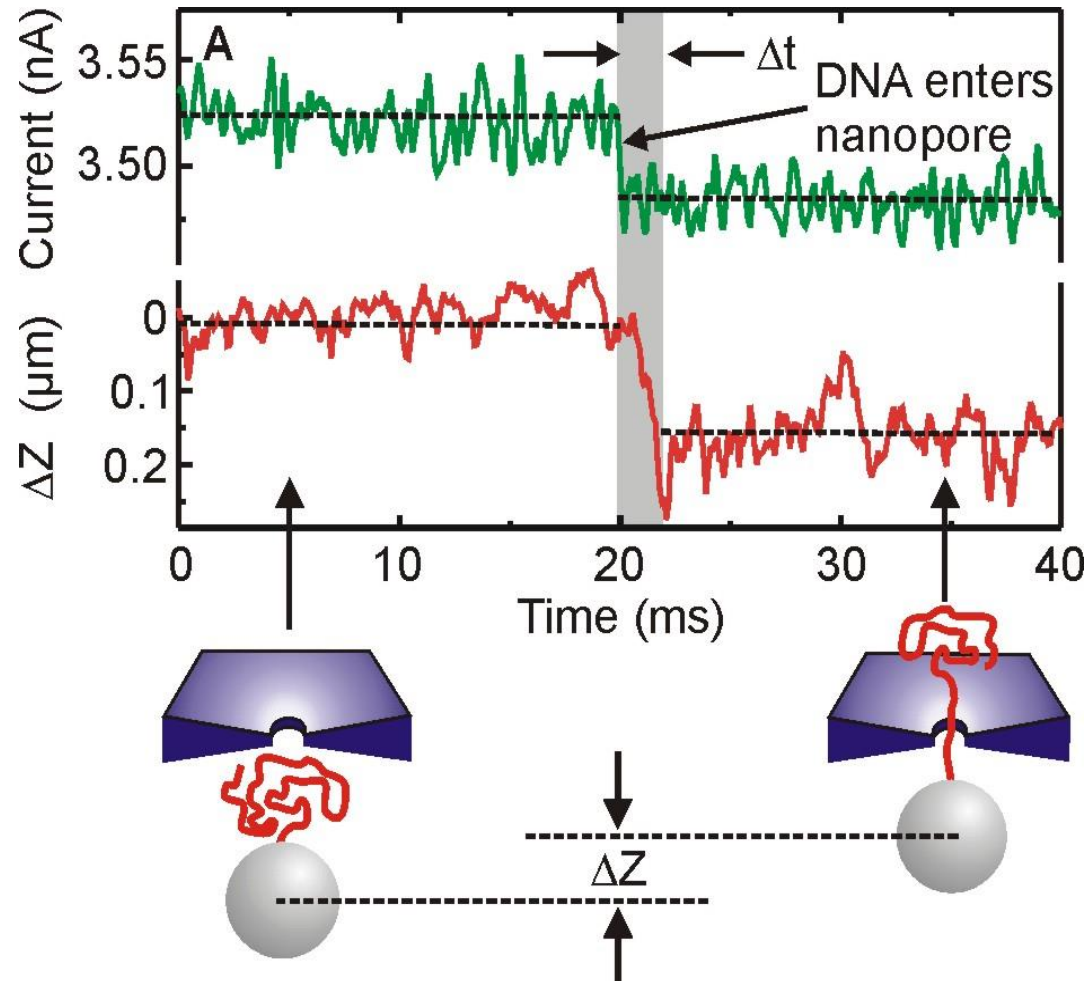


(2) the bead position changes

http://www.damtp.cam.ac.uk/user/gold/teaching_biophysicsIII.html

Time-Resolved Events

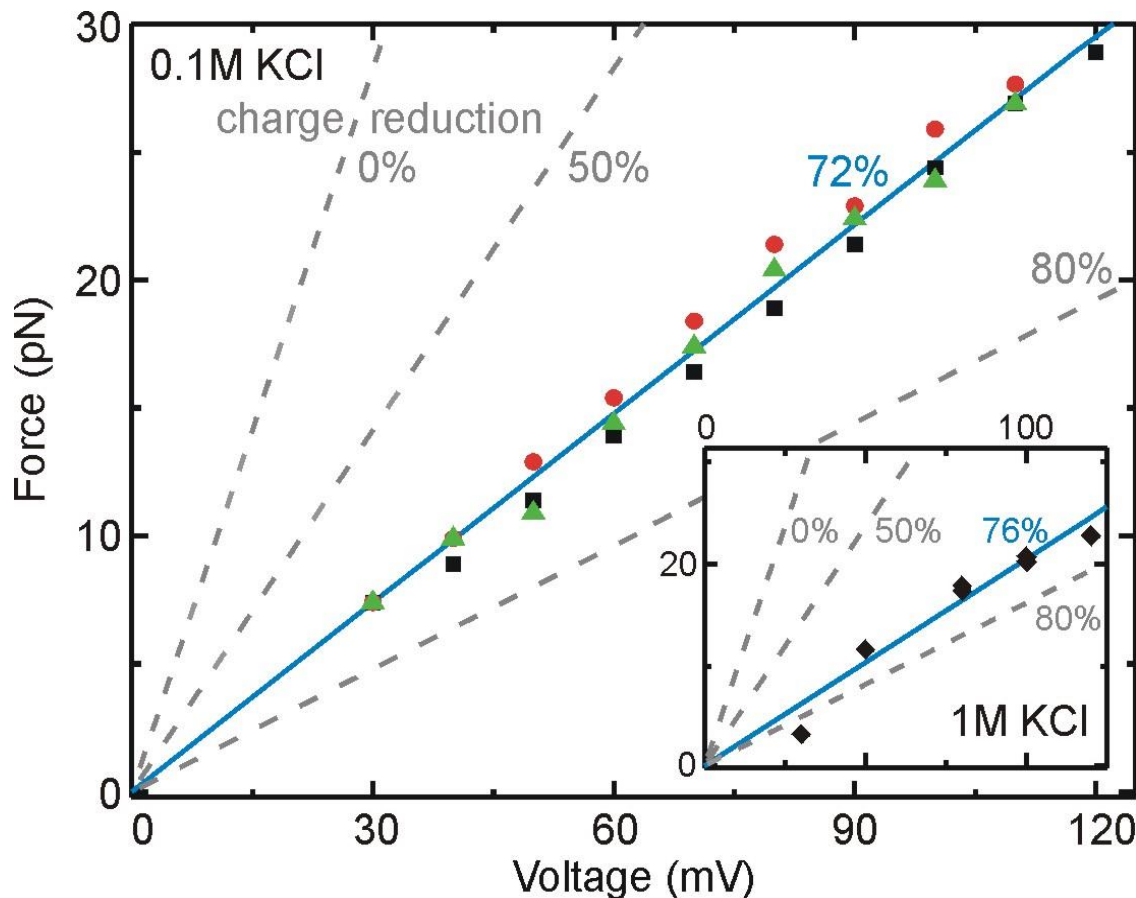
(Keyser et al. 2006)



- Conductance step indicates capture of DNA in nanopore
- Only when DNA is pulled taut the force changes
- Time to pull taut Δt is consistent with free translocation speed of DNA
- DNA is stalled in the nanopore and allows for force measurements on the molecule, and other things

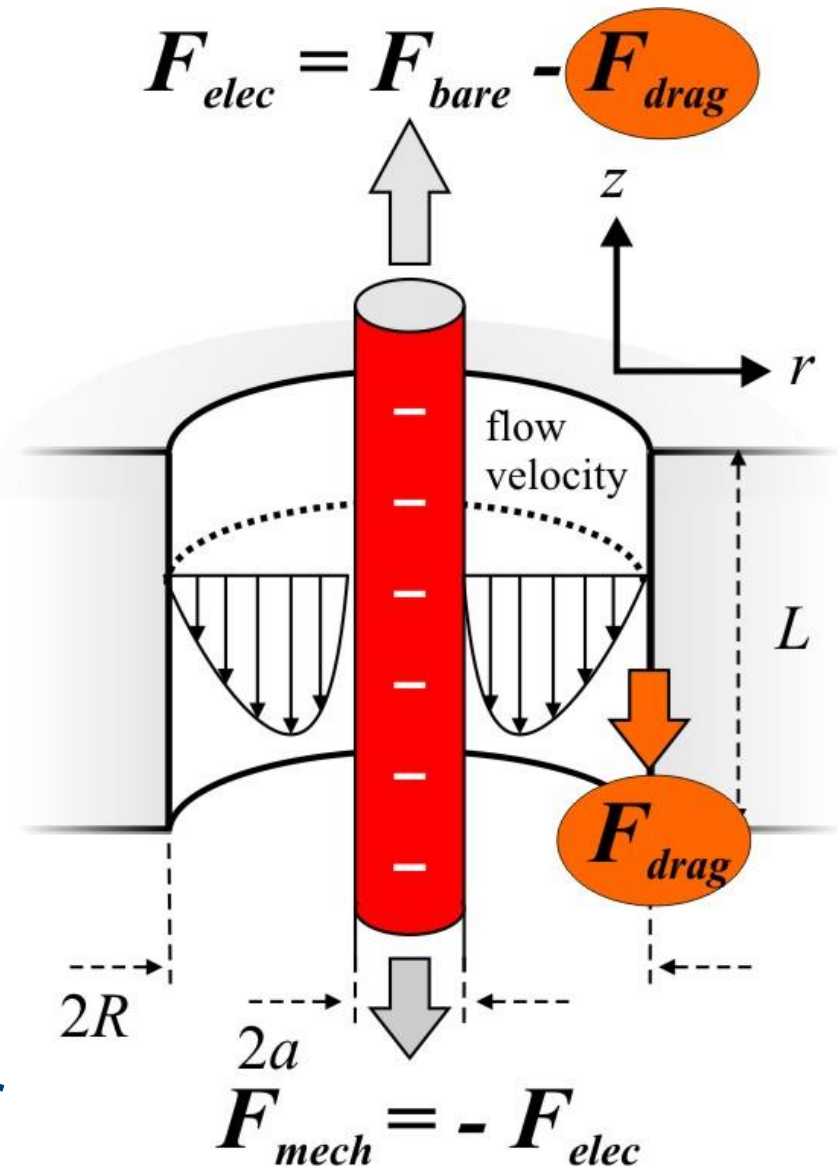
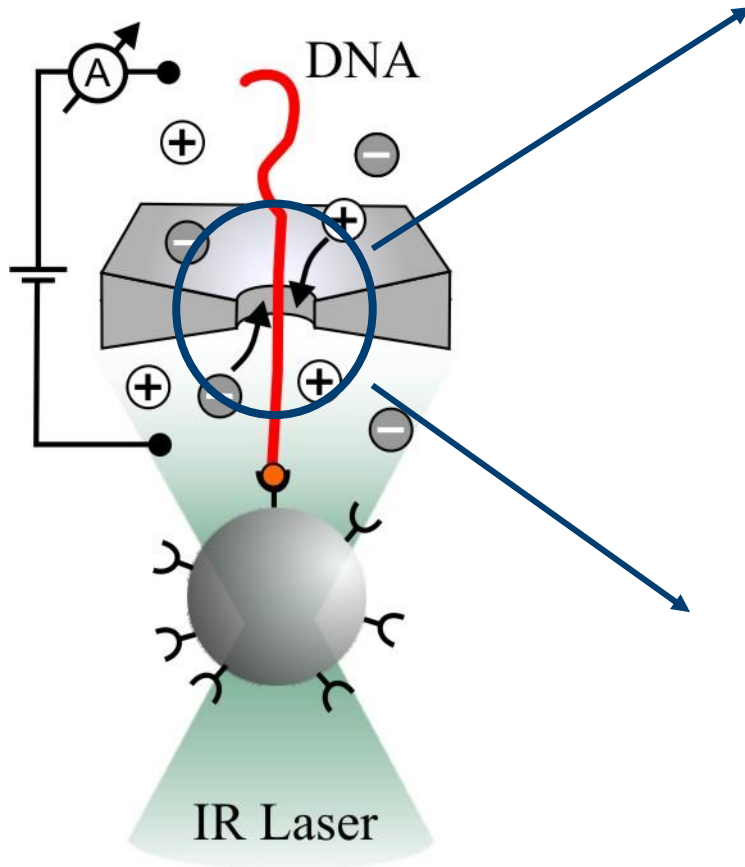
Force on DNA

(Keyser et al. 2006)



- Linear force-voltage characteristic as expected
- Absence of nonlinearities indicate that equilibrium formulae can be used
- Poisson-Boltzmann should work fine in this situation
- (Navier-)Stokes should also work
- Force does not depend on distance nanopore-trap
- Extract the gradient and vary salt concentration

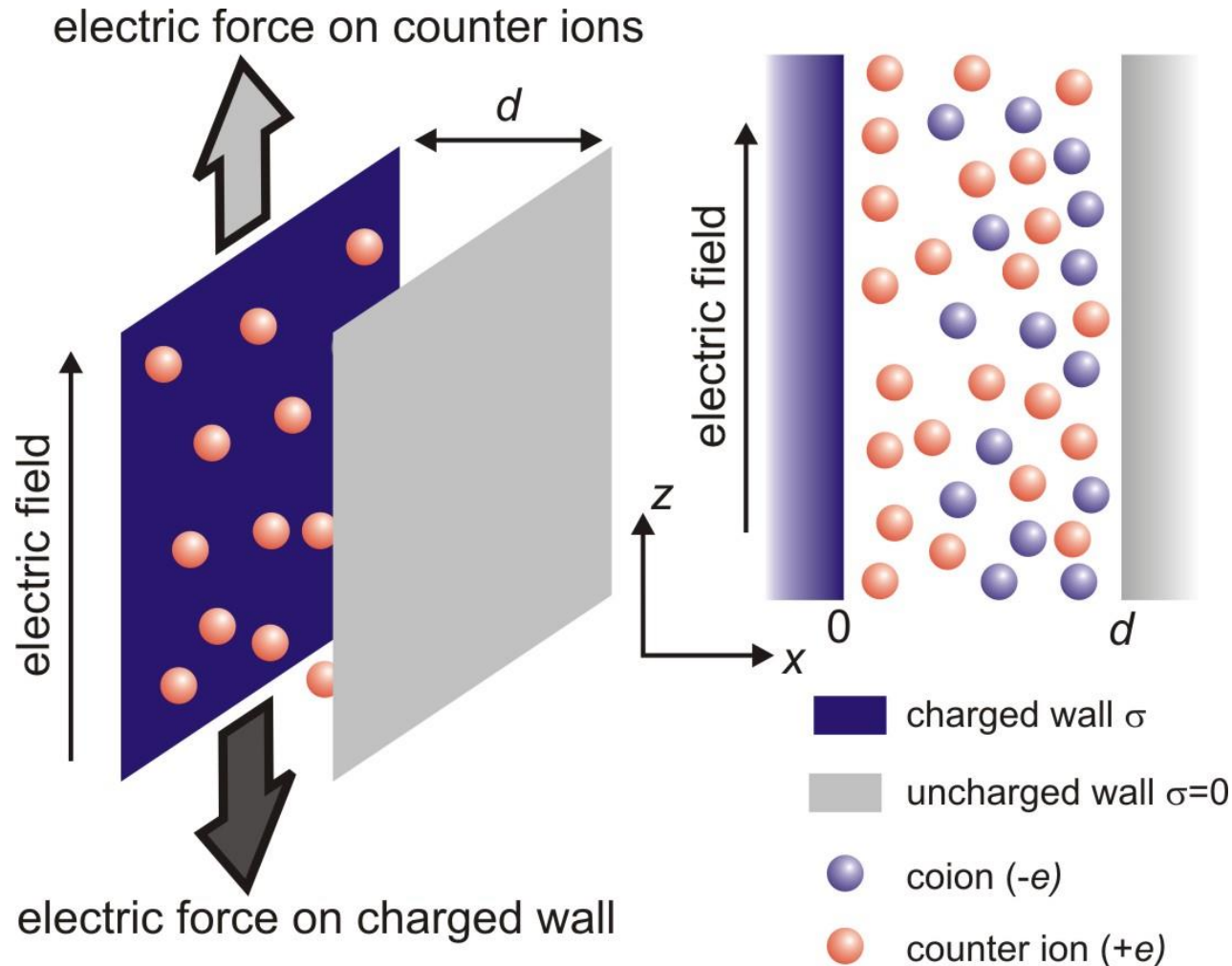
Hydrodynamics Should Matter



Hydrodynamic interactions matter

Force on a charged wall in solution?

(Keyser et al. 2010)



Poisson Boltzmann describes screening

(Keyser et al. 2010)

- Distribution of ions \Leftrightarrow Boltzmann distributed

$$n_{\pm}(x) = n_0 e^{\mp e\phi(x)/kT}$$

- When we have

$$|e\phi(x)/kT| \ll 1$$

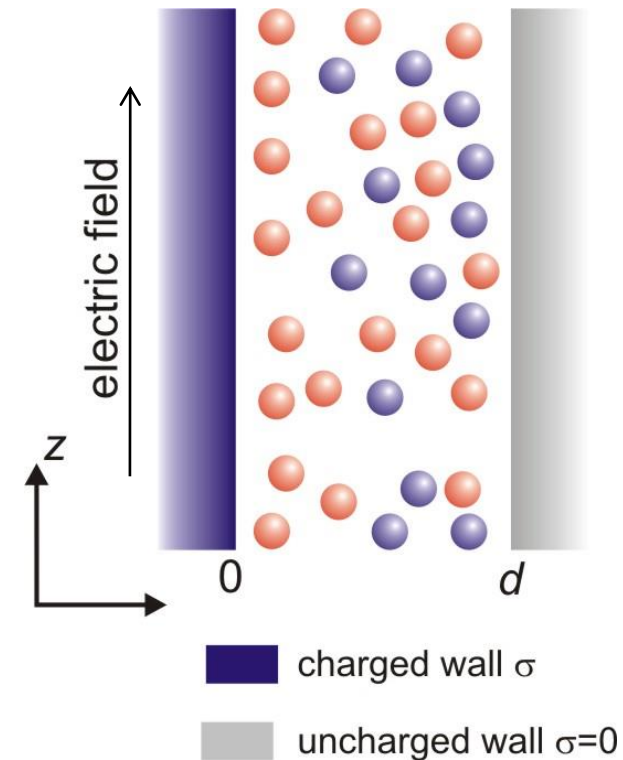
- Taylor expansion yields

$$n_{\pm}(x) = n_0 (1 \mp e\phi(x)/kT)$$

- Calculate $\phi(x)$ self consistently with the Poisson eq.

$$\nabla^2 \phi(\mathbf{r}) = -\rho(\mathbf{r}) / \epsilon_w$$

$$\rho(\mathbf{r}) = e[n_+(\mathbf{r}) - n_-(\mathbf{r})]$$



Poisson Boltzmann describes screening

(Keyser et al. 2010)

- This yields a simple differential equation

$$\frac{d^2 \phi(x)}{dx^2} = \frac{2e^2 n_0}{kT \epsilon_w} \phi(x) = \frac{\phi(x)}{\lambda^2}$$

- And we have the Debye screening length

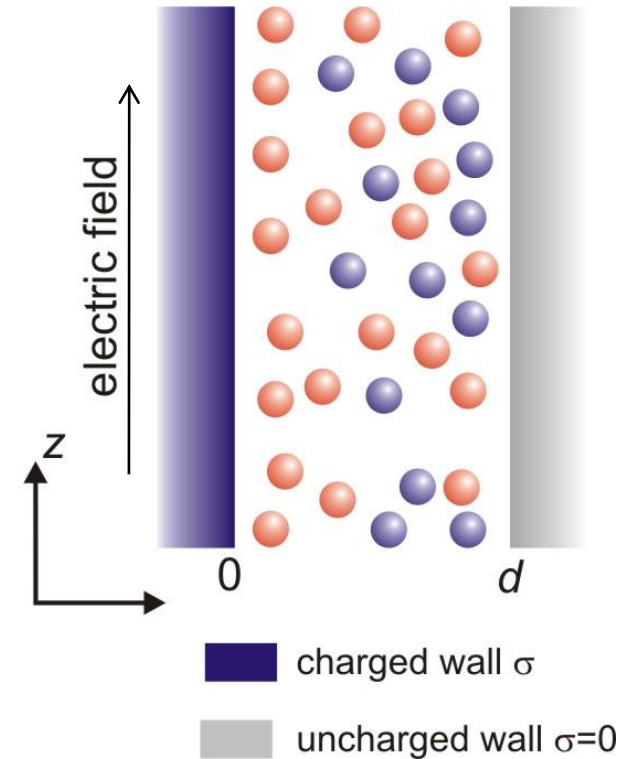
$$\lambda \equiv (kT \epsilon_w / 2e^2 n_0)^{1/2}$$

- Solution for the differential equation

$$\phi(x) = Ae^{-x/\lambda} + Be^{+x/\lambda}$$

– Boundary conditions:

$$\left. \frac{d\phi(x)}{dx} \right|_{x=0} = -\frac{\sigma}{\epsilon_w}; \quad \left. \frac{d\phi(x)}{dx} \right|_{x=d} = 0$$



Poisson Boltzmann describes screening

(Keyser et al. 2010)

- This yields the solution for $\phi(x)$

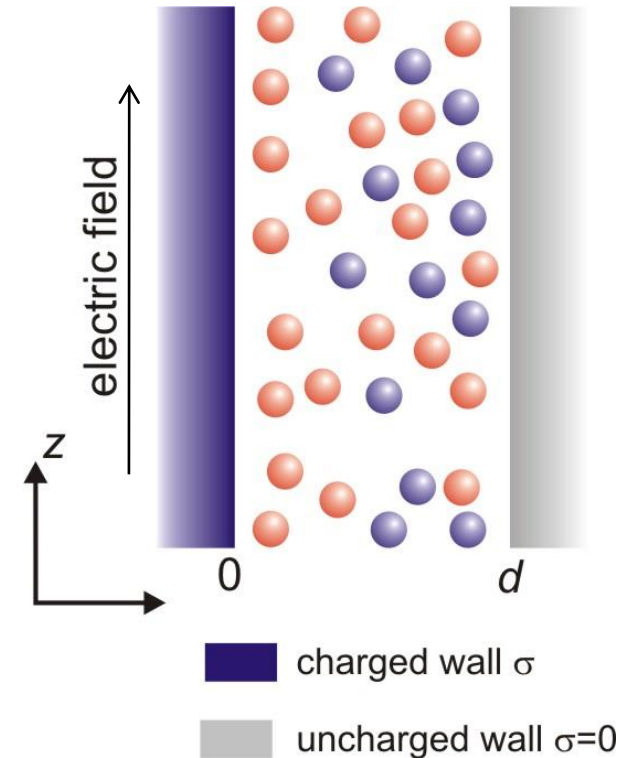
$$\phi(x) = \frac{\sigma\lambda}{\epsilon_w} \left(\frac{e^{-x/\lambda} - e^{-2d/\lambda} e^{x/\lambda}}{1 + e^{-2d/\lambda}} \right)$$

- Assuming that $d \gg \lambda$ we get

$$\phi(x) = \frac{\sigma\lambda}{\epsilon_w} e^{-x/\lambda} \quad (d \gg \lambda)$$

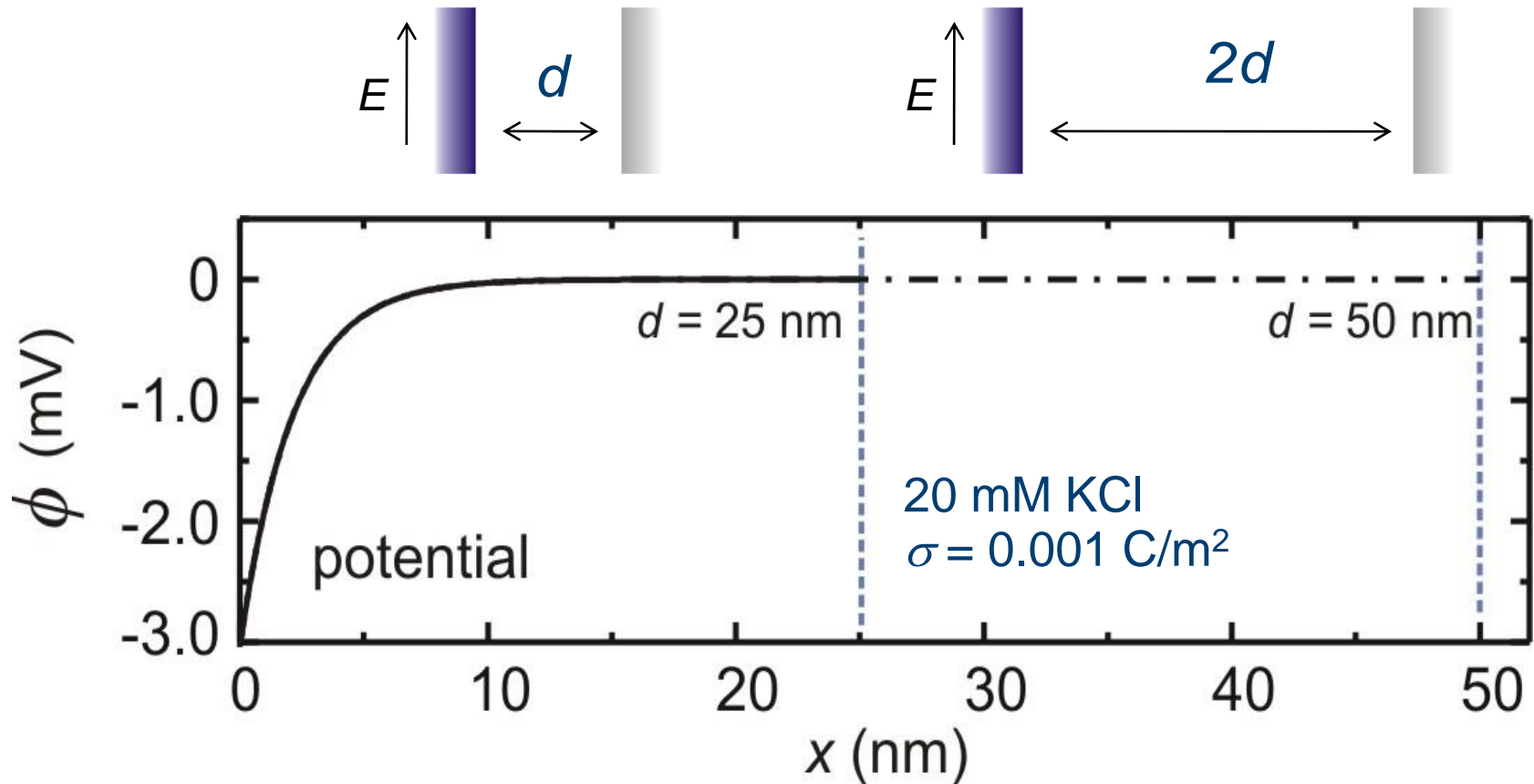
- Uncharged wall does not influence the screening layer!**

$$n_{\pm}(x) = n_0 \mp \frac{\sigma}{2e\lambda} e^{-x/\lambda}$$



Potential for a slightly charged wall

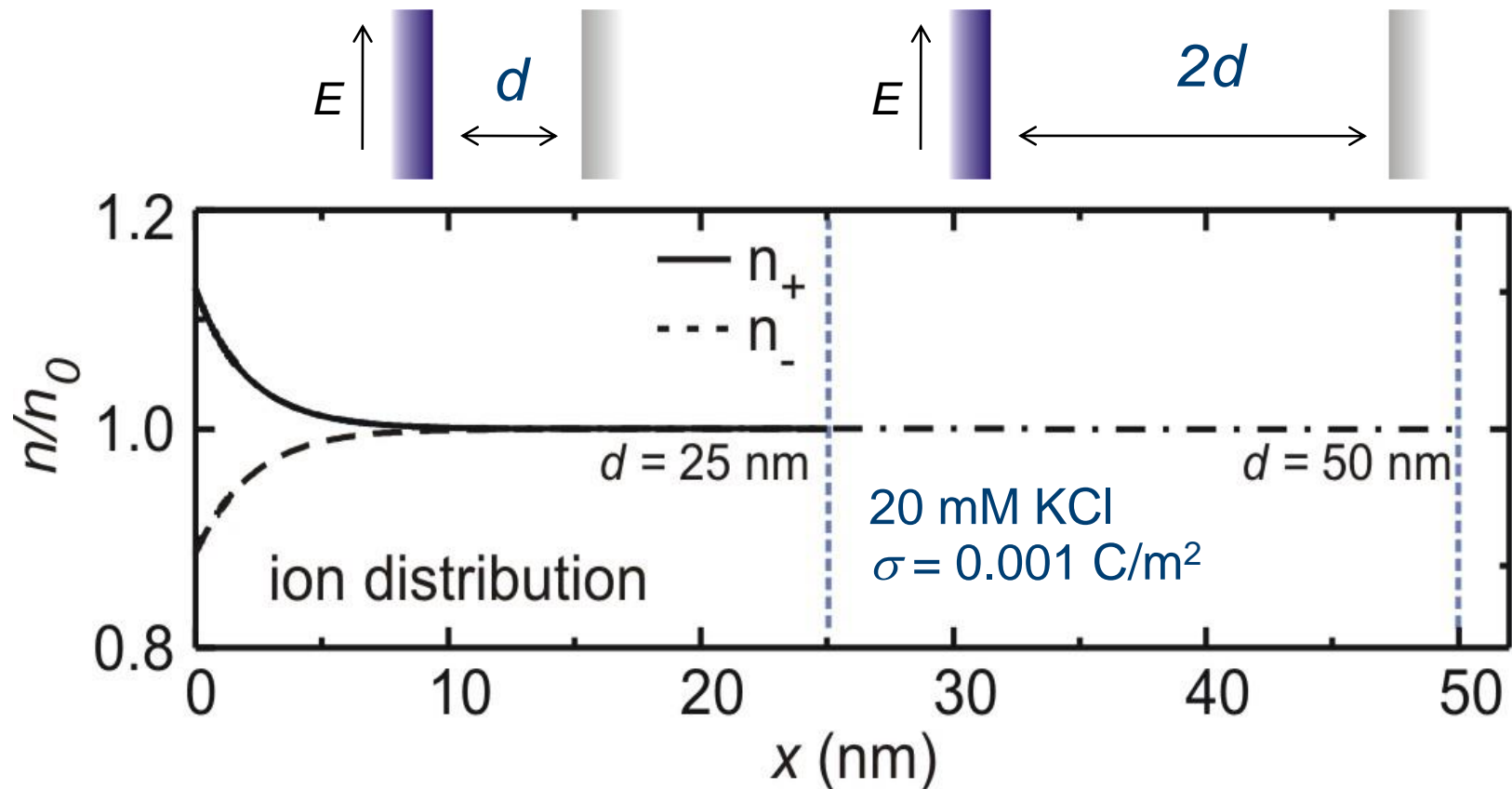
(Keyser et al. 2010)



- **Uncharged wall does not influence the screening layer!**

Ion distribution for a slightly charged wall

(Keyser et al. 2010)



- **Uncharged wall does not influence the screening layer!**

Electroosmotic flow along charged wall

(Keyser et al. 2010)

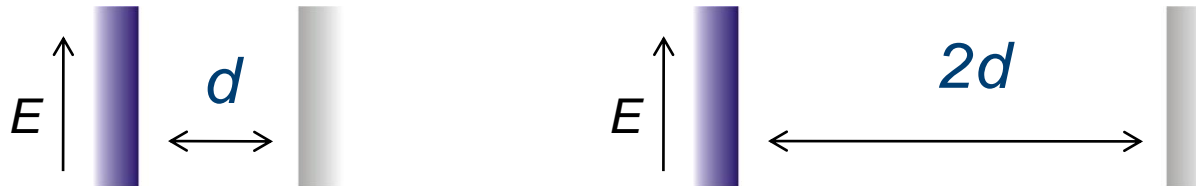
- Excess of counterions near surface leads to electroosmotic flow

$$\frac{d^2 v_z(x)}{dx^2} + \frac{\rho(x)E}{\eta} = 0$$

$\rho(x)E$ force exerted by electric field E , η viscosity of water

- This leads to velocity of water $v(x)$ assuming no-slip boundaries

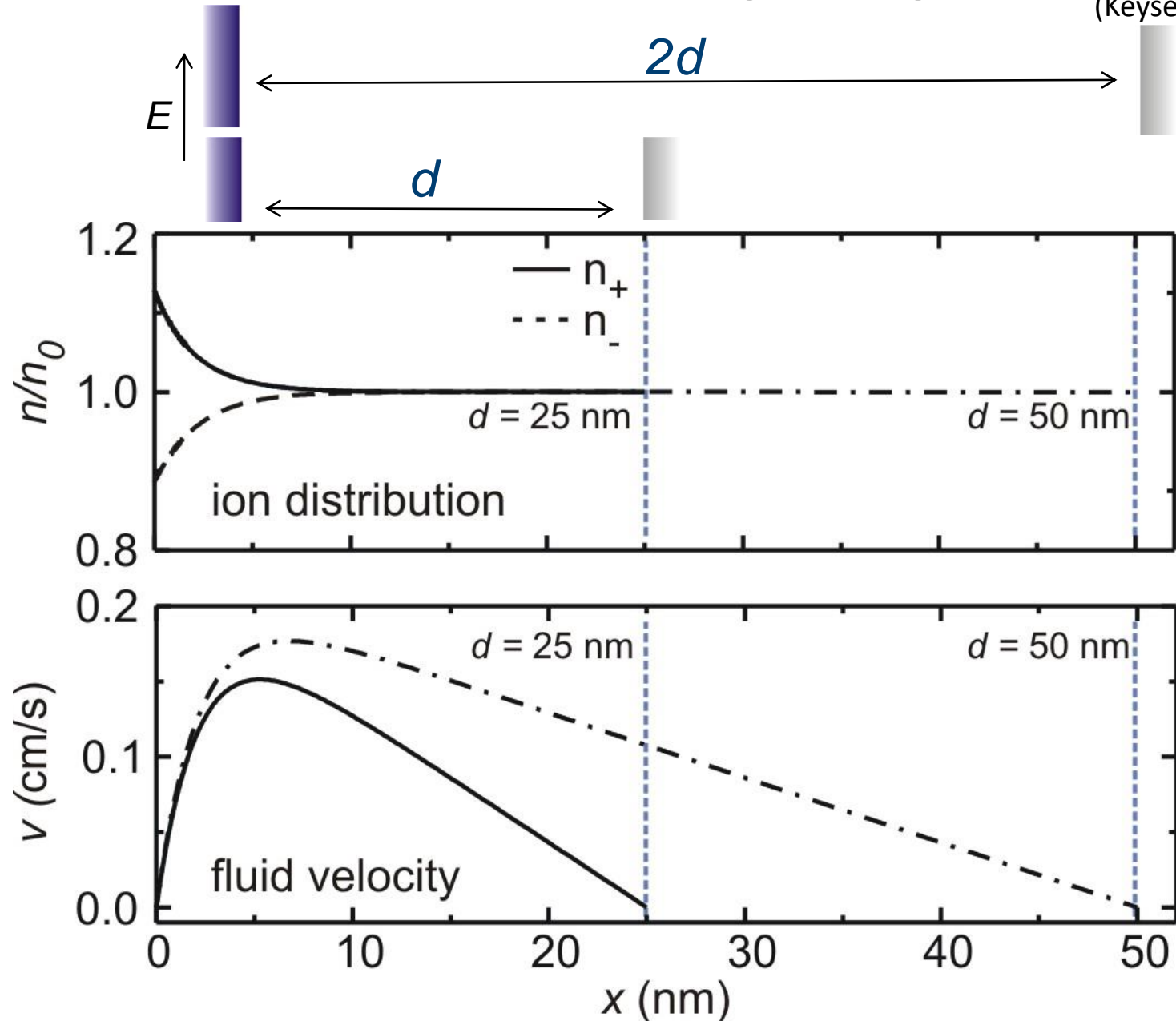
$$v(x) = -\frac{E\sigma\lambda}{\eta} \left(1 - e^{-x/\lambda} - \frac{x}{d} \right)$$



- Uncharged wall DOES influence electroosmotic flow!**

Electroosmotic flow along charged wall

(Keyser et al. 2010)



Forces on the DNA and Nanopore wall

(Keyser et al. 2010)

- Bare force F_{bare} is just product of area A , charge density and electric field E

$$F_{\text{bare}} = A\sigma E$$

- The drag force F_{drag} exerted by the flowing liquid

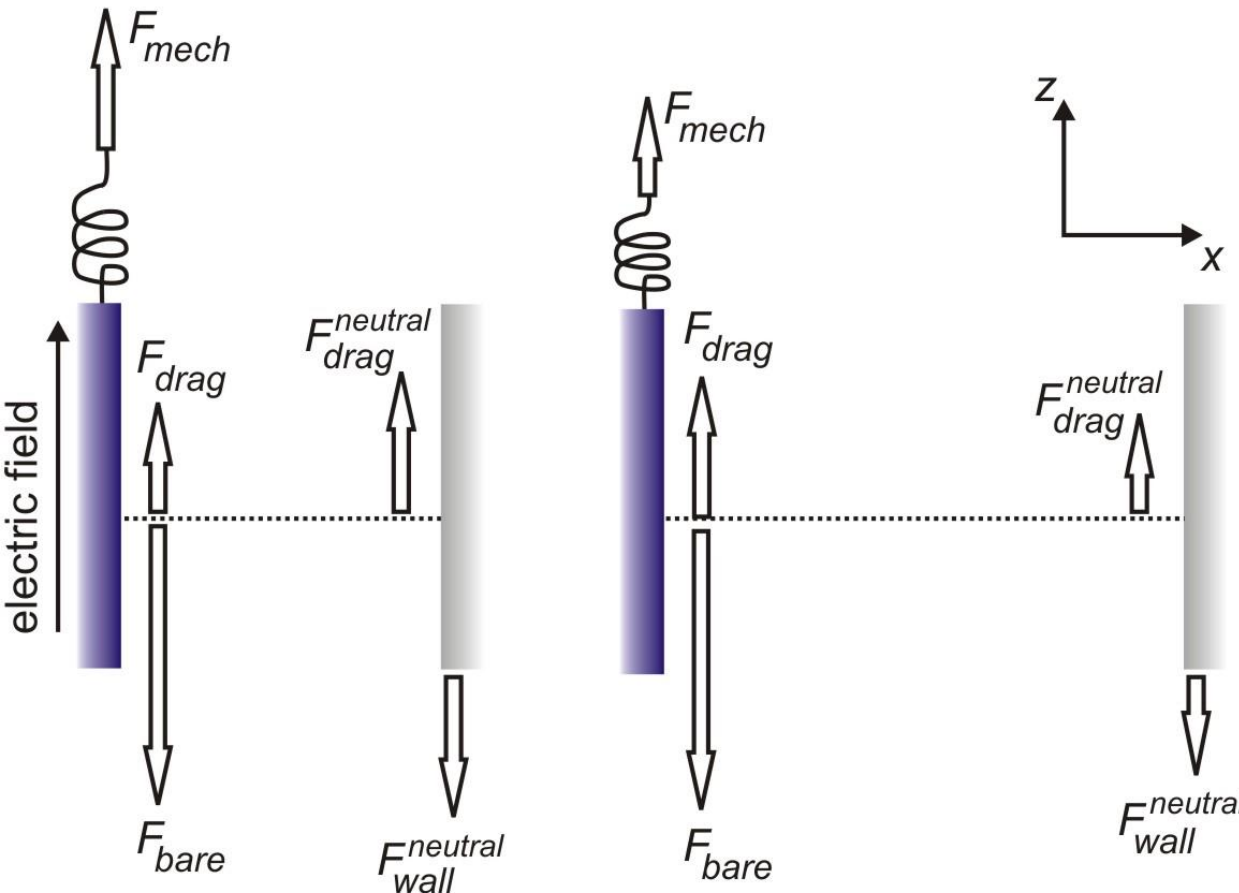
$$F_{\text{drag}} = A\eta \left| \frac{dv(x)}{dx} \right|_{x=0} = -AE\sigma \left(1 - \frac{\lambda}{d} \right) = - \left(1 - \frac{\lambda}{d} \right) F_{\text{bare}}$$

- The force required to hold the charged wall stationary is thus

$$F_{\text{mech}} = -F_{\text{elec}} = - \left(F_{\text{bare}} + F_{\text{drag}} \right) = -AE\sigma \frac{\lambda}{d}$$

Part of the force goes to the uncharged wall

(Keyser et al. 2010)



- F_{mech} depends on the distance d between the walls

■ charged wall σ ■ uncharged wall $\sigma=0$

DNA - High charge densities

(Keyser et al. 2010)

- For high charge densities linearized PB does not work:

$$\frac{d^2 \phi(x)}{dx^2} = \frac{2en_0}{\epsilon_w} \sinh\left(\frac{e\phi(x)}{kT}\right)$$

- With two infinite walls can still be solved:

$$\phi(x) = \frac{2kT}{e} \ln\left(\frac{1 + \gamma e^{-x/\lambda}}{1 - \gamma e^{-x/\lambda}}\right)$$

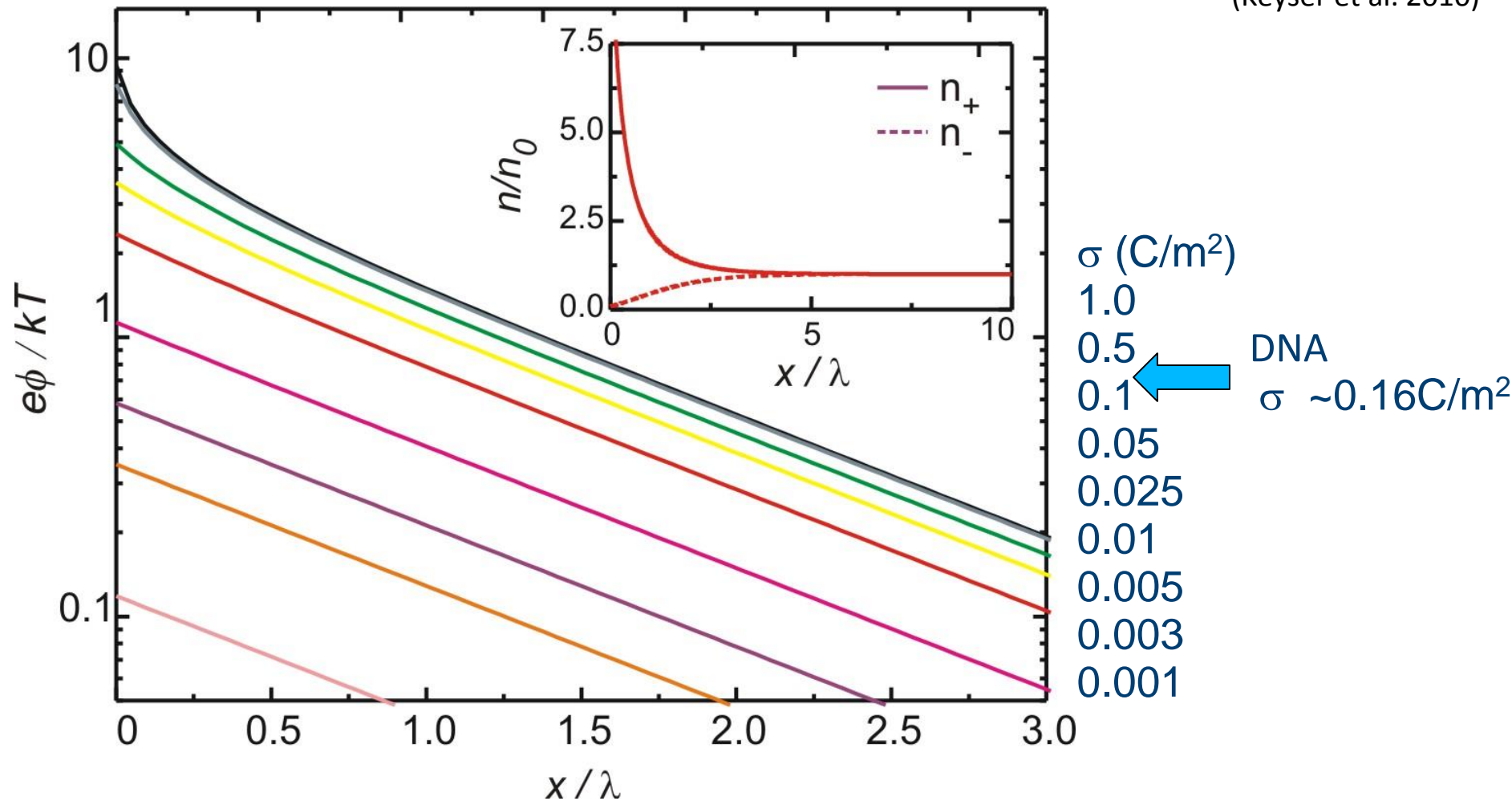
$$\gamma = -\lambda_{GC} / \lambda + \left(1 + \lambda_{GC}^2 / \lambda^2\right)^{1/2}$$

- Introducing the Gouy-Chapman length

$$\lambda_{GC} = 2kT\epsilon_w / e |\sigma|$$

Gouy-Chapman solution of PB equation

(Keyser et al. 2010)



PB in cylindrical coordinates \Leftrightarrow nanopore, DNA

(Keyser et al. 2010)

- Electrostatic potential Φ and distribution of ions n_{\pm} :

$$\nabla^2 \bar{\Phi}(\mathbf{r}) = \lambda_D^{-2} \sinh \bar{\Phi}(\mathbf{r}) \quad n_{\pm}(\mathbf{r}) = n_0 e^{z_{\pm} \bar{\Phi}(\mathbf{r})}$$

with $\bar{\Phi} = -e\Phi/k_B T$ as normalized potential

- Boundary conditions:

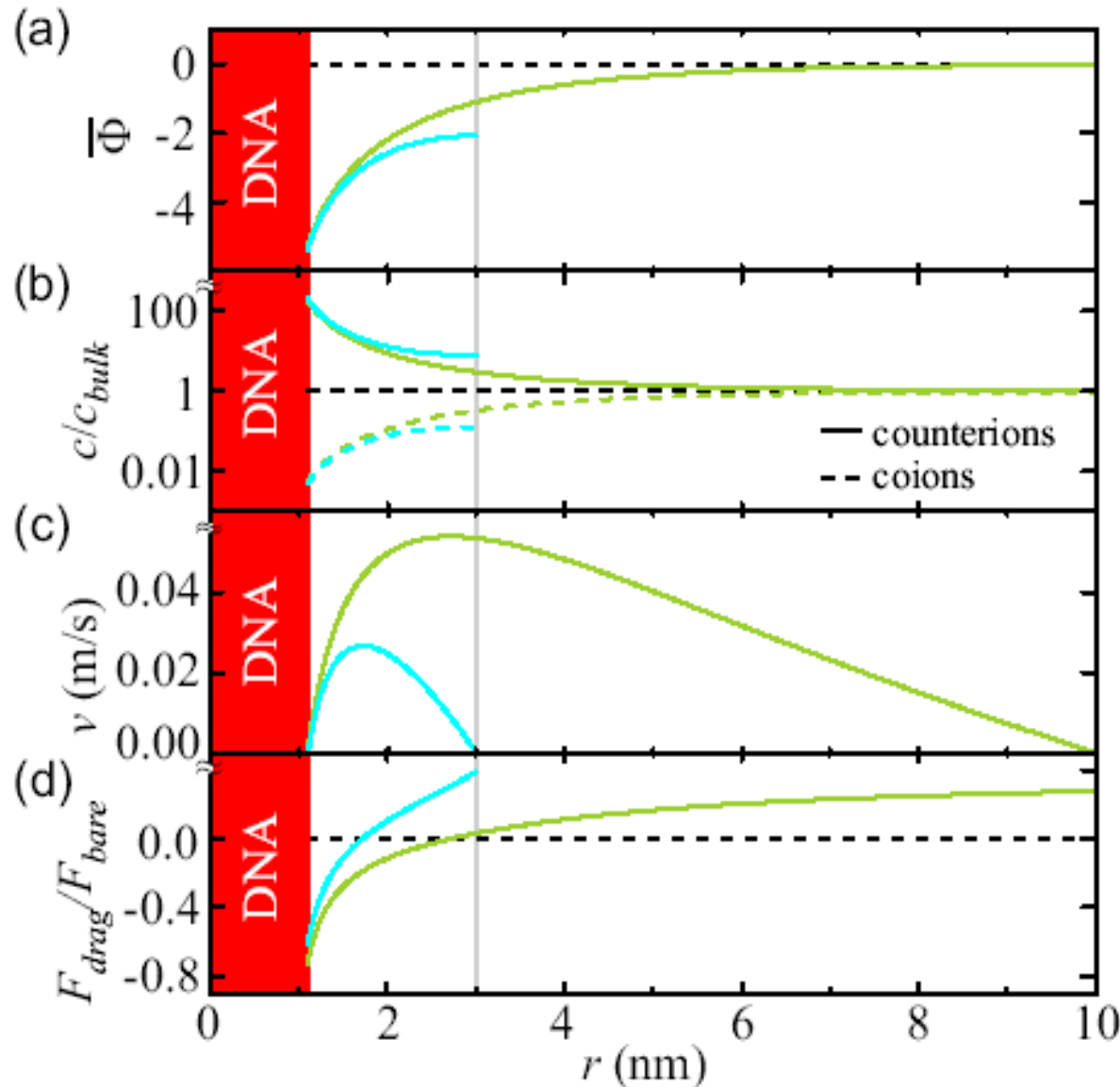
$$d\Phi/dr = 0 \quad \text{Insulating nanopore walls (uncharged)}$$

$$d\Phi/dr = -\lambda_{bare}/2\pi a\epsilon \quad \text{on DNA surface}$$

- Simplification: access resistance is neglected
- Only possible to solve numerically

Finite Element Calculation

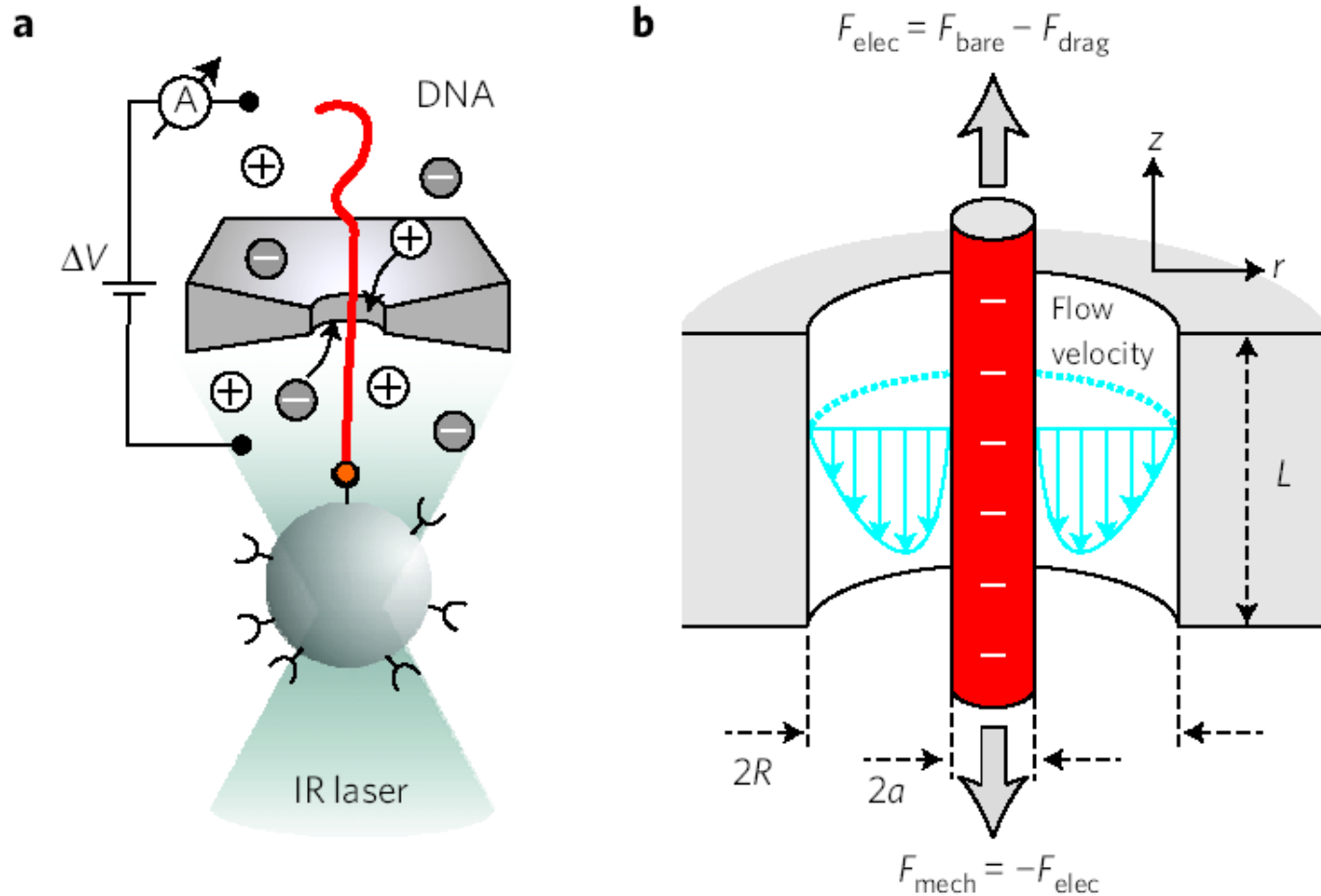
(Keyser et al. 2009)



- Combining Poisson Boltzmann and Stokes
- Main result: Force on DNA depends on pore diameter
- Change in pore diameter by factor 10 increases drag by a factor of two

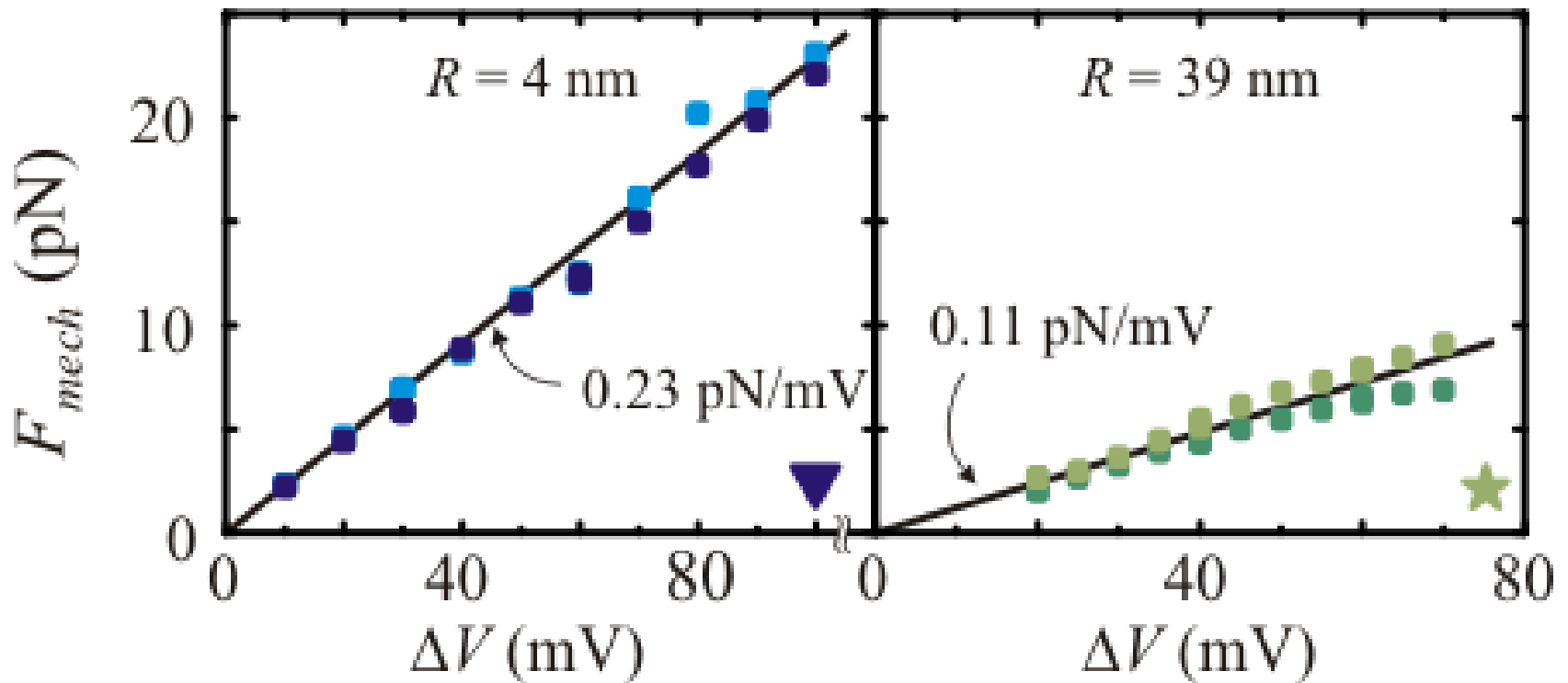
Hydrodynamics Should Matter Here!

(Keyser et al. 2009)



- Test hydrodynamic interactions by increasing nanopore diameter

Force Dependence on Nanopore Radius



- Force is proportional to voltage as expected
- For larger nanopore force is roughly halved as expected from model
- Measure for a range of nanopore sizes and compare with numerical results

Membranes and proteins

- Membrane proteins and ion channels
- Rotary motors in cell membranes
- Rotary motors for swimming bacteria

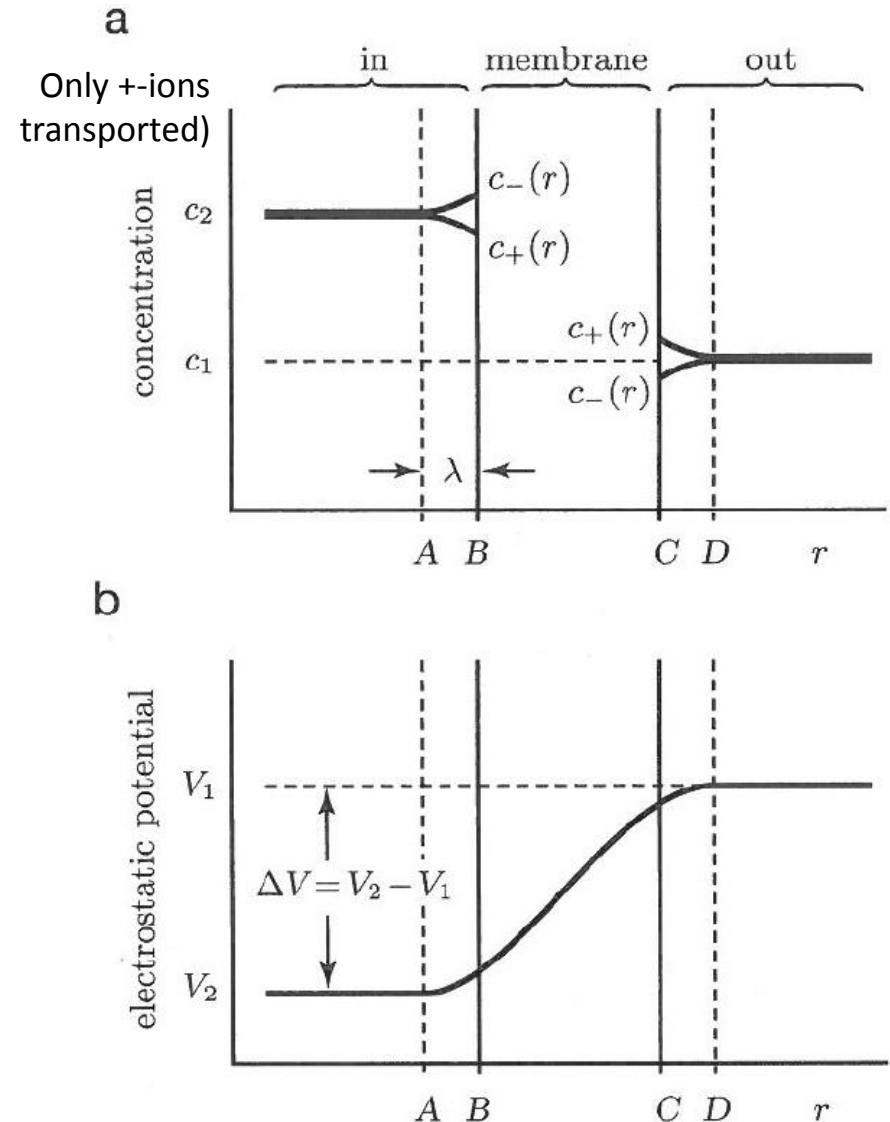
Molecular Machines – Ion Pumps/Motors

(Nelson 2006)

- Ion concentration differences lead to potentials across cell membranes, Nernst equation
- In case the membrane is slightly selective for one of the ions we get a current until a stable double layer is formed
- Thus with the Nernst equation we have a membrane potential ΔV in equilibrium which is given by

$$\Delta V = V_2 - V_1 = V_{Nernst} = -\frac{k_B T}{ze} \ln \left(\frac{c_2}{c_1} \right)$$

- Membrane potentials can be measured by patch-clamping



Molecular Machines – Ion Pumps/Motors

(Nelson 2006)

- Donnan equilibrium, in the case of more than a single ionic species we have to take into account all their concentrations
- With Na, K, Cl in and out of the cell we have for outside (c_1) and inside (c_2) of the cell because of charge neutrality

$$c_{1,Na} + c_{1,K} - c_{1,Cl} = 0$$

$$c_{2,Na} + c_{2,K} - c_{2,Cl} + \rho_{macro} / e = 0$$

taking into account the charged macromolecules in the cell ρ_{macro}/e

- In the cell the concentration c_2 will be different from outside, in addition we have the membrane potential ΔV to take into account
- All three species have to obey the Nernst equation so we get the Gibbs-Donnan relations with ΔV now the Donnan potential

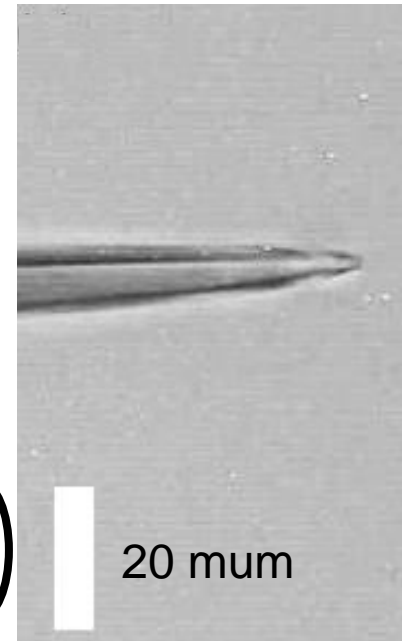
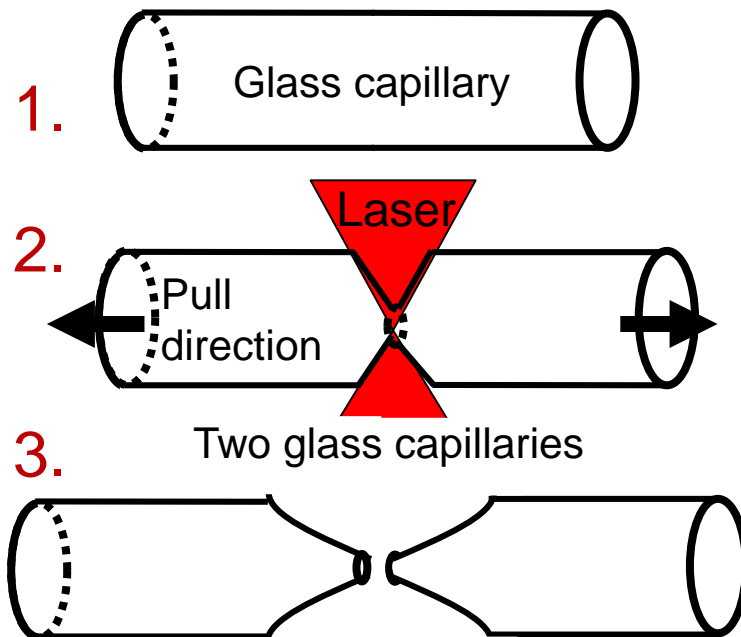
$$const = \left(\frac{c_{1,Na}}{c_{2,Na}} \right) = \left(\frac{c_{1,K}}{c_{2,K}} \right) = \left(\frac{c_{1,Cl}}{c_{2,Cl}} \right) = \dots \text{ and } \Delta V = -\frac{k_B T}{e} \ln \left(\frac{c_{1,Na}}{c_{2,Na}} \right) = \dots$$

- Membrane potentials can be measured by patch-clamping
http://www.damtp.cam.ac.uk/user/gold/teaching_biophysicsIII.html

*Fabrication of Glass Microcapillaries**

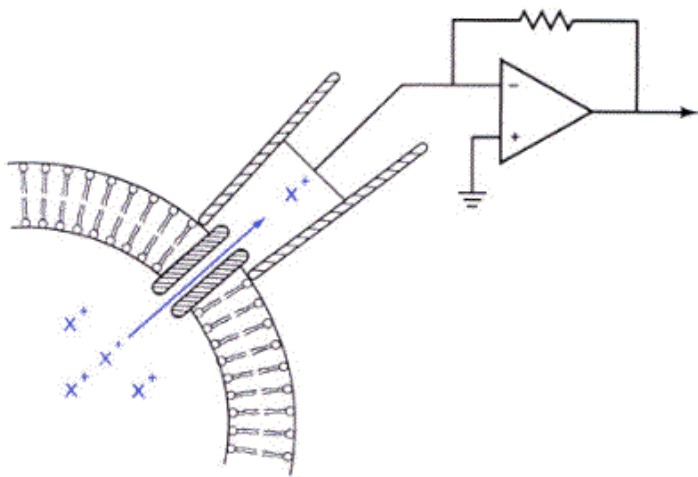
1. Glass capillary placed in puller
2. Laser heats up capillary and force applied to both sides: Glass softens and shrinks
3. Strong pull separates glass in two parts

Sutter P-2000

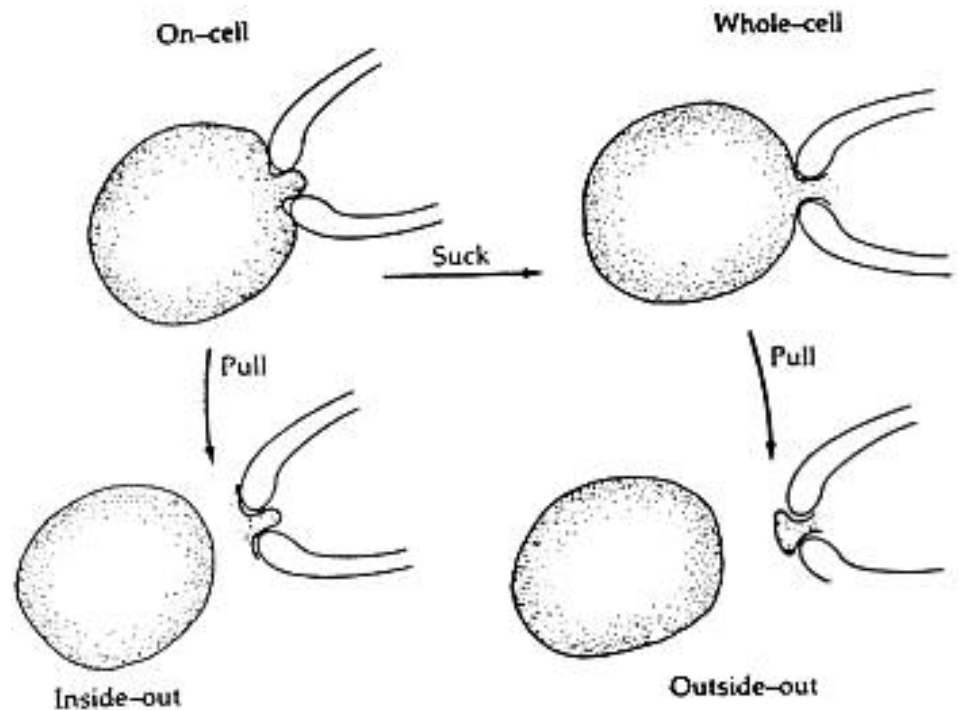


Patch clamping

Current measurement through a SINGLE membrane pore possible



Patch-clamping modes of operation



Detection of Biological Membrane Potentials

(E. Neher Nobel lecture)

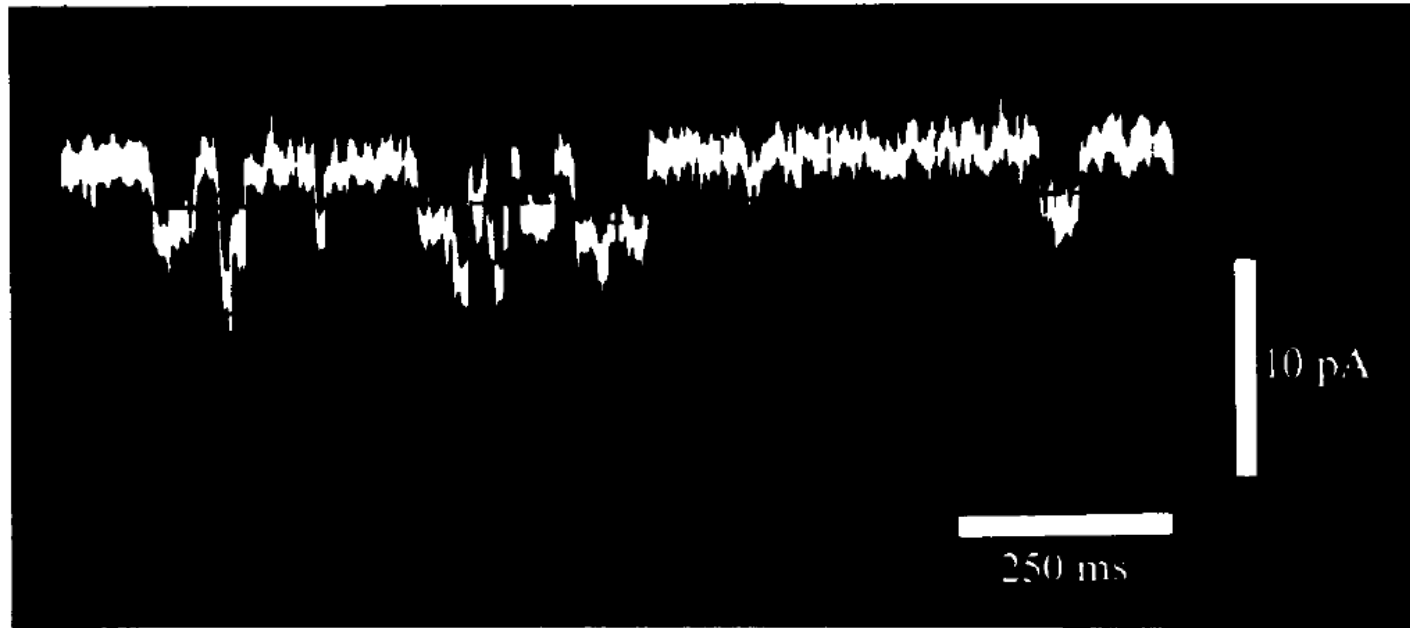


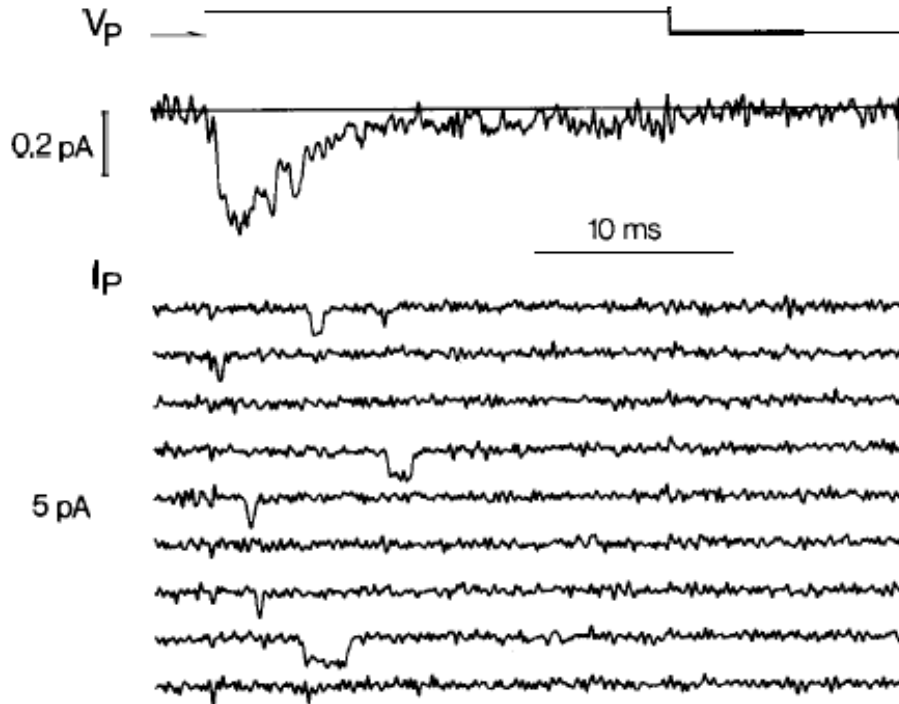
Figure 2. Early single-channel currents from denervated frog (*Rana pipiens*) cutaneous pectoris muscle. The pipette contained 0.2 μ M suberyldicholine, an analogue of acetylcholine which induces very long-lived channel openings. Membrane potential -120 mV; temperature 8°C . Reproduced from Neher & Sakmann 1976.

- Glass capillary is pulled into a small tip with diameters of a few 10s-100s of nm and attached to the surface of the cell
- First true single-molecule measurements – done in the early 1970s!

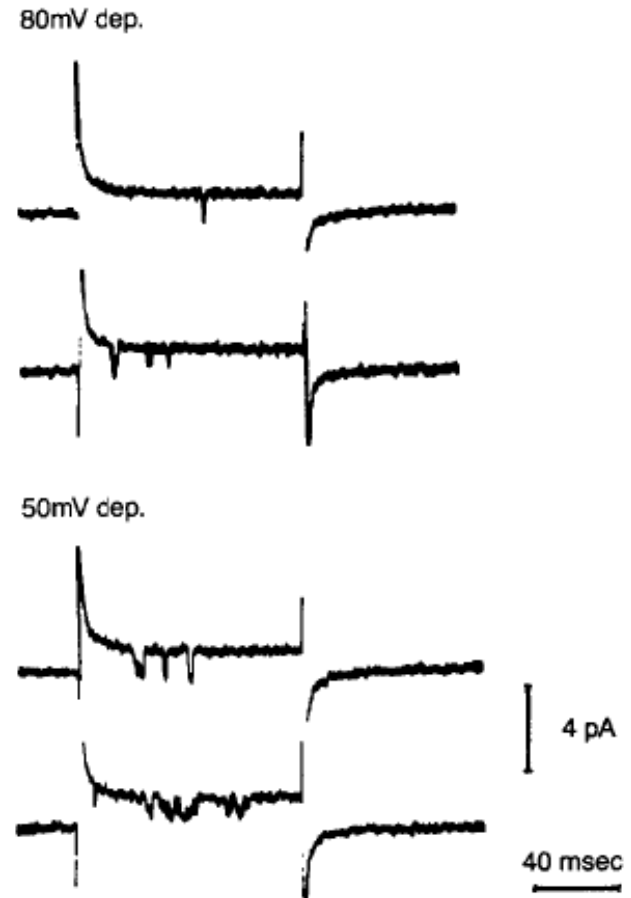
Patch Clamping – Membrane Potentials

(E. Neher Nobel lecture)

Na-channels



Ca-channels

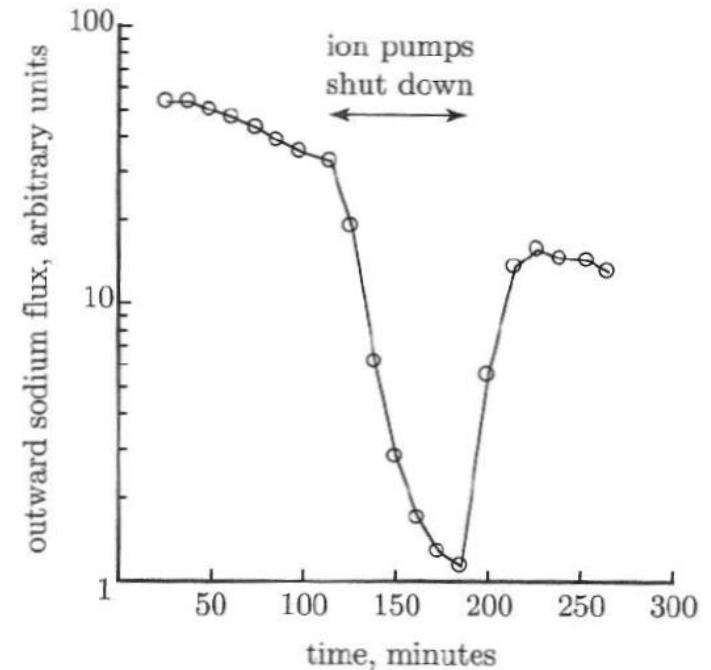
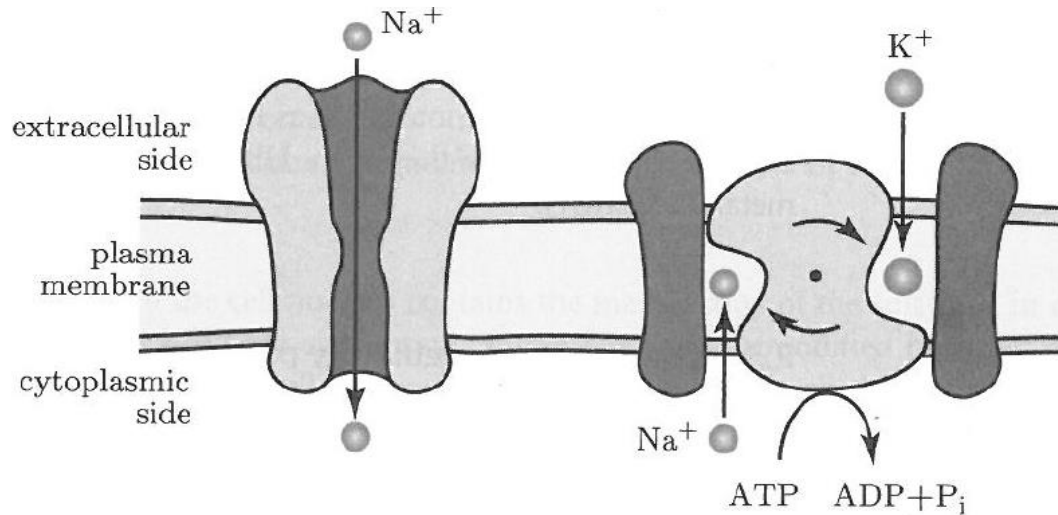


Patch clamping was a true scientific revolution allowing for studies of voltage gating in single protein channels, nerve transduction and many other biological phenomena. One of the papers of Sakmann and Neher is cited more than 16,000 times!

http://www.damtp.cam.ac.uk/user/gold/teaching_biophysicsIII.html

Donnan equilibrium and membrane potential

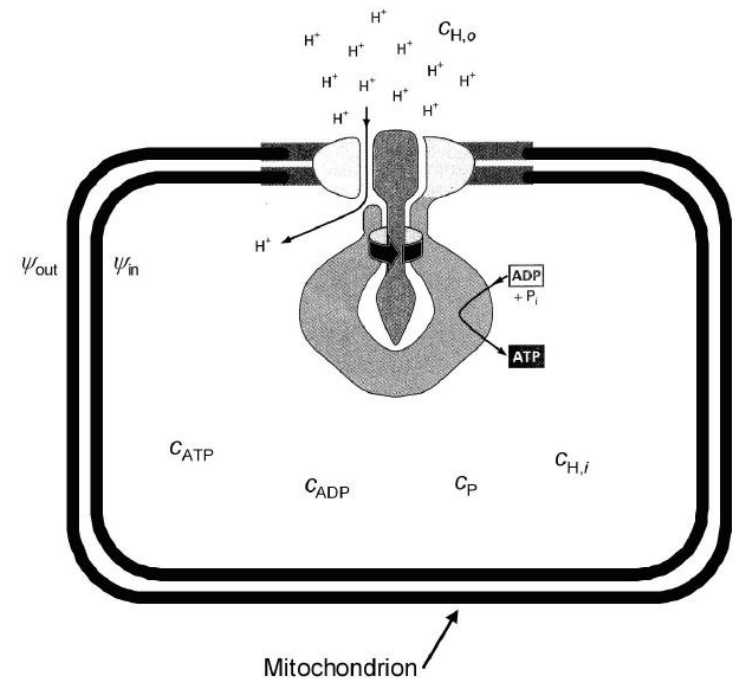
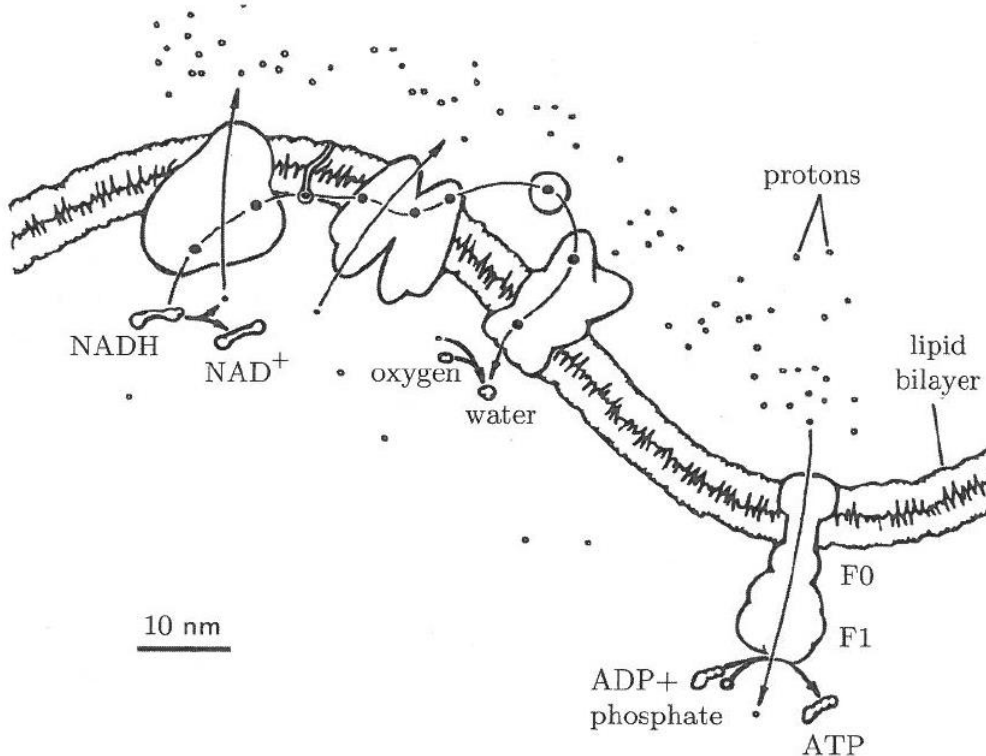
(Nelson 2006)



- Membrane potential for sodium is not explained by the Donnan equilibrium \Leftrightarrow active process (energy) needed to keep this membrane potential up
- Ion pumps use ATP to pump sodium out of the cell while the same pump (ATP driven) import potassium into the cells, hence sodium-potassium pump was discovered
- Function can be tested in the same lipid bilayer systems as described for the nanopores for DNA detection

Generating ATP in mitochondria

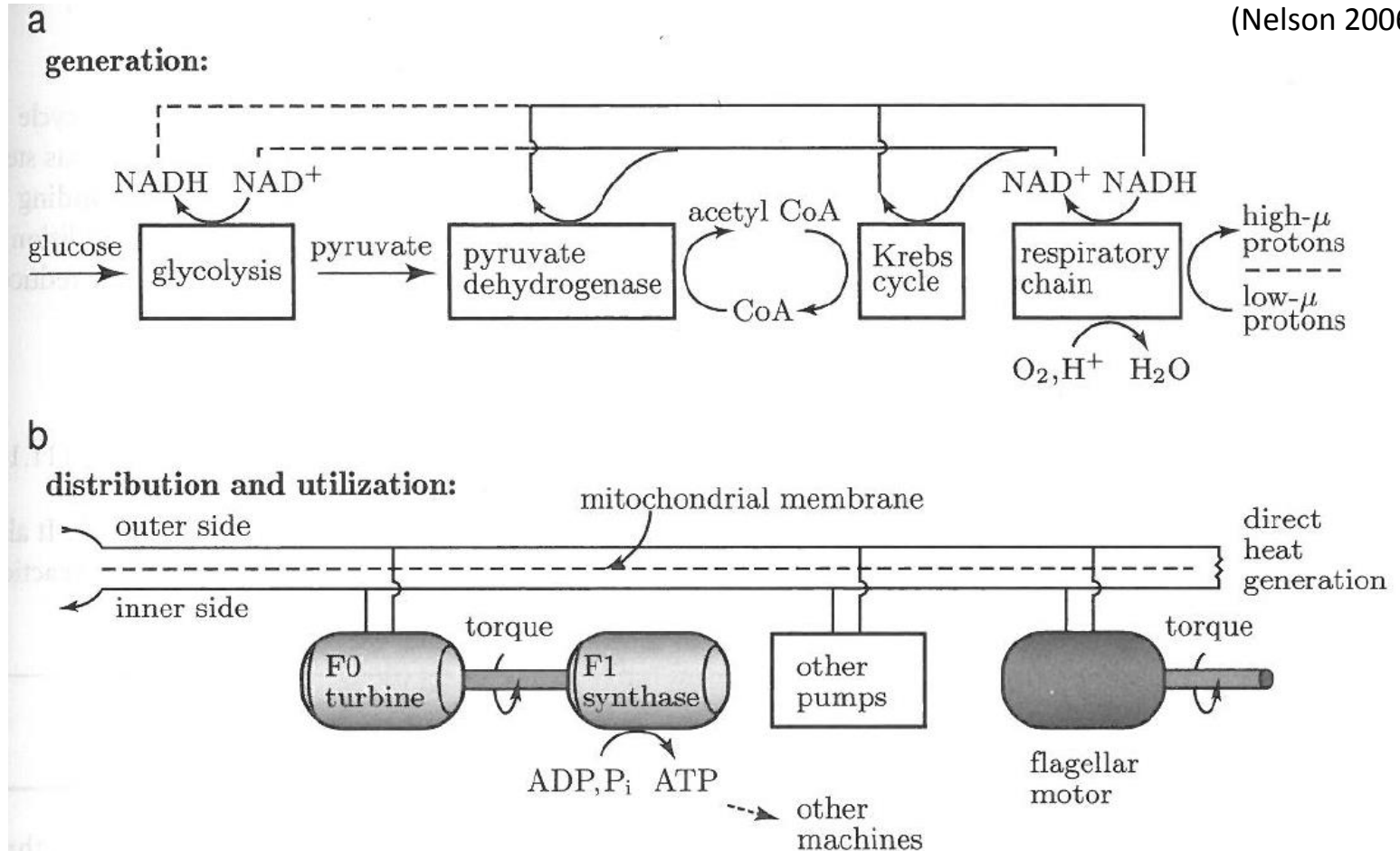
(Nelson 2006)



- ATP is the main energy carrier in the cell, it is also used to make DNA and can be easily changed into GTP
- Mitochondria convert a proton gradient into the rotary motion of a transmembrane protein called F₀F₁ATPase
- Lipid membrane is needed to uphold the proton gradient which is created by deprotonation of NADH and generation of water

Molecular Machines – Ion Pumps/Motors

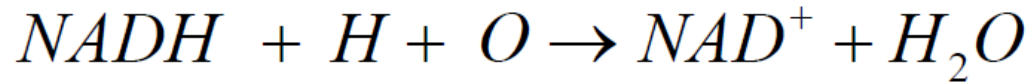
(Nelson 2006)



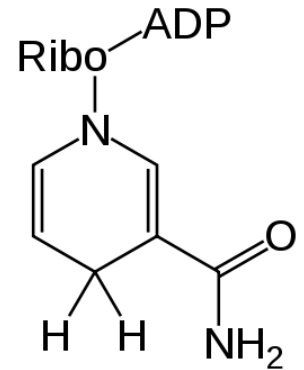
- ATP production process is very close to energy production in power plants
- Free energy ΔG is provided here by the proton gradient
- There are several chemical sub-steps involved which are not explained here but can be found for instance in Nelson chapter 11.3

Hydrogen and Oxygen to water

- After a number of reactions three educts yield water, NADH (Nicotinamide adenine dinucleotide), protons, oxygen



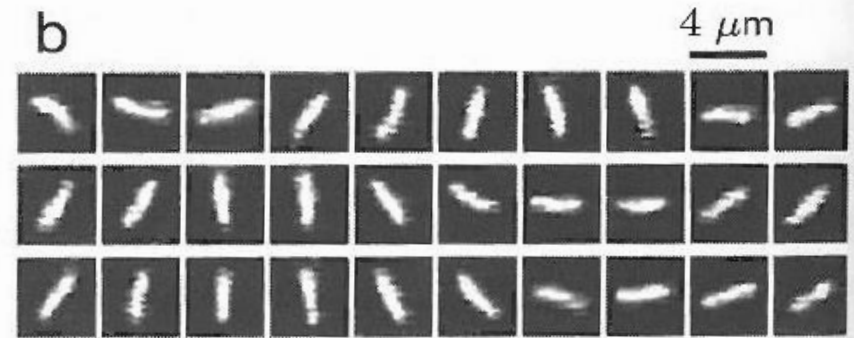
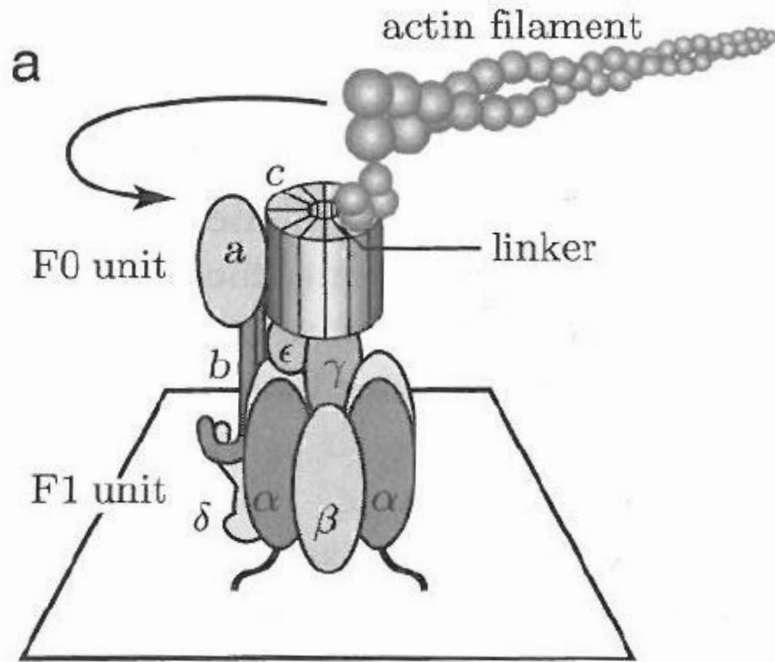
- It can be measured that DG of this reaction is up to $-88k_B T$ which is obviously an upper bound as in the real system we have to take the concentrations of the molecules and thus their chemical potentials into account adjusting DG
- This cycle keeps the proton gradient over the mitochondria membrane up and thus provides the energy for F_0F_1 ATPase which finally generates ATP from ADP and
- Interestingly this process can also be reversed – in the absence of a protein gradient this F_0F_1 ATPase burns ATP and creates ADP



NADH

Molecular Machines – Ion Pumps/Motors

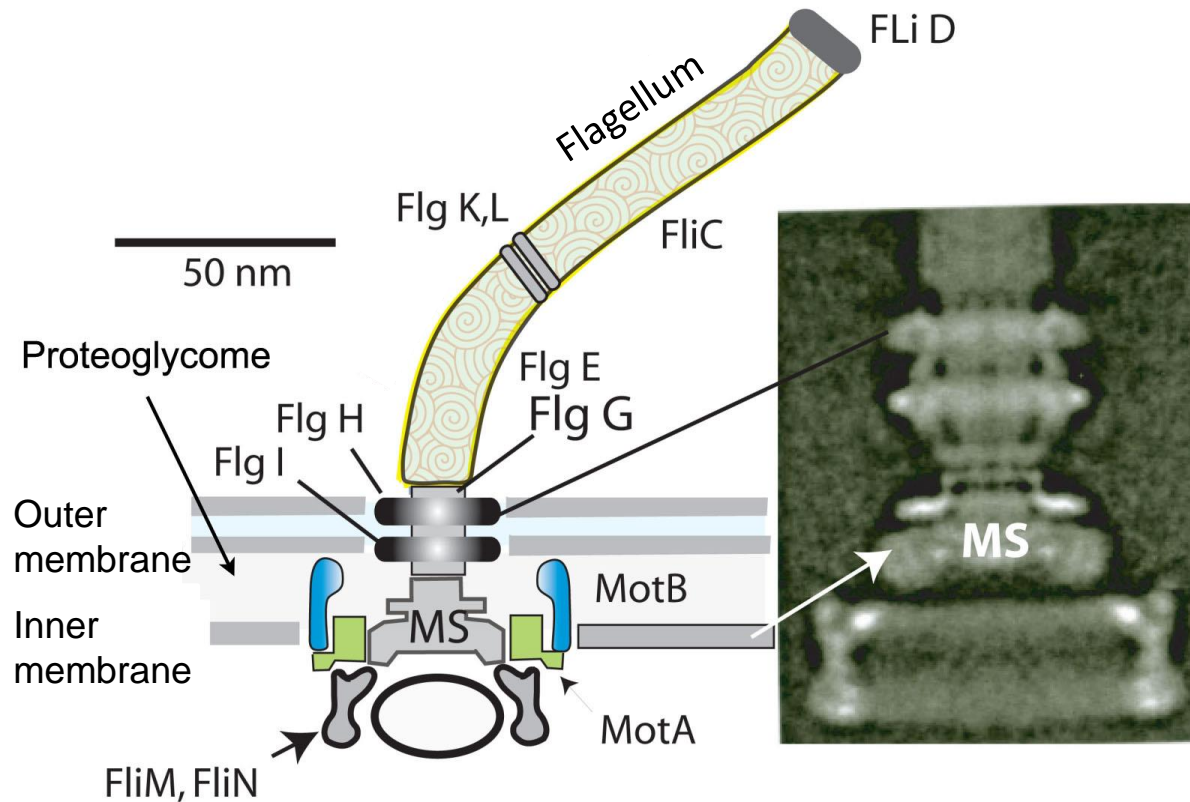
(Nelson 2006)



- It is possible to image the rotary motion of the F₀F₁ATPase by attaching an actin filament which is fluorescently labelled to the top of the motor
- Rotary motion in three steps can be observed
- Highly efficient molecular machine with efficiency close to 1!

Proton-driven Flagellum Motor of E.coli

(Berg 2003)



Stator:

Motor proteins:
MotA, MotB

Rotor:

Protein ring MS composed
of 26 FliG, FliF

Direction control:

FliM, FliN

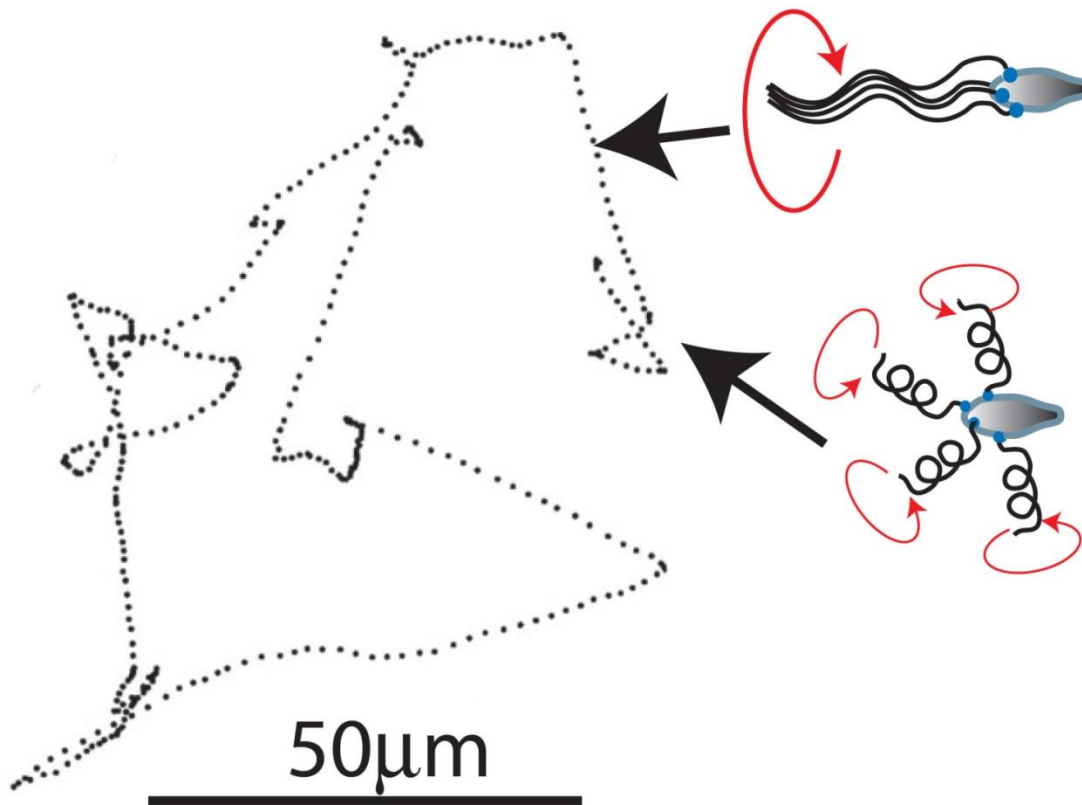
Motor is driven by a *proton gradient* over the inner and outer membranes.

MotA and MotB are proton channels allowing for the passage and converting the electric energy into rotational motion.

Bacteria use not ATP but ion currents for driving their rotary motors.

Change of Flagellum during Swimming/Tumbling

(Berg 2003)



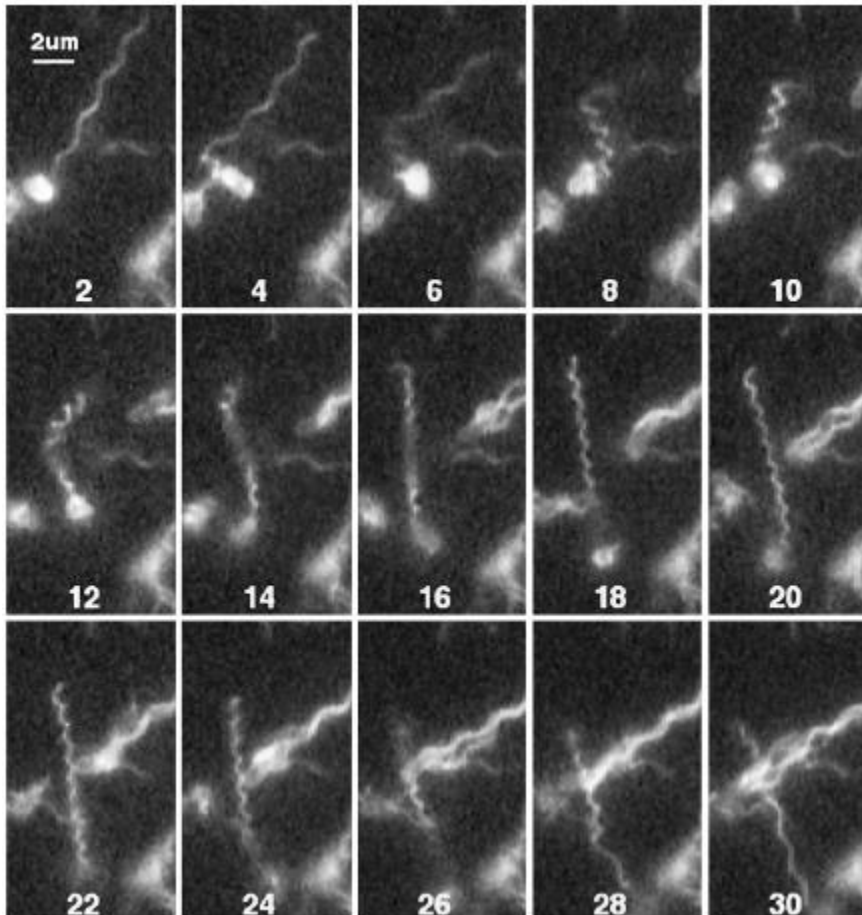
E.Coli swims in straight lines with intermittent tumbling motion.

During straight line swimming the motors rotate counter clockwise (CCW) and during tumbling clockwise (CW).

Flagella conformation depends on rotation direction. In CCW the flagella form a bundle while in CW they rotate separately.

Change of Flagellum during Swimming/Tumbling

(Berg 2003)



Single flagellar filament of E.Coli, imaged by fluorescent microscopy.

Frame numbers indicate video frame numbers with ~17ms between frames.

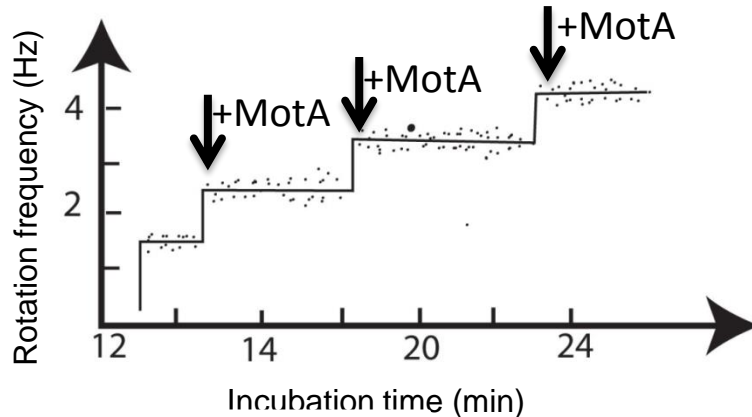
Direction switches from CCW to CW after frame 2, changing conformation to semi coiled (frame 10) and then to the 'curly' helix.

Switch back to CCW (after frame 26) leads to transformation back to the normal helical confirmation (see 2).

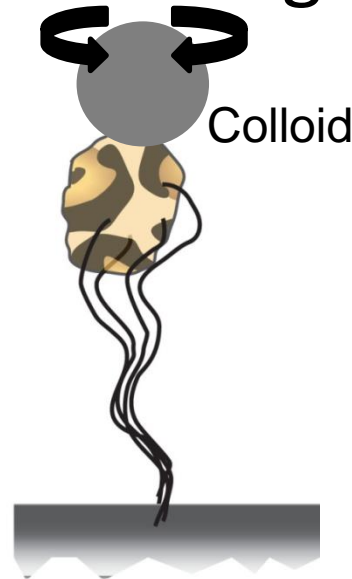
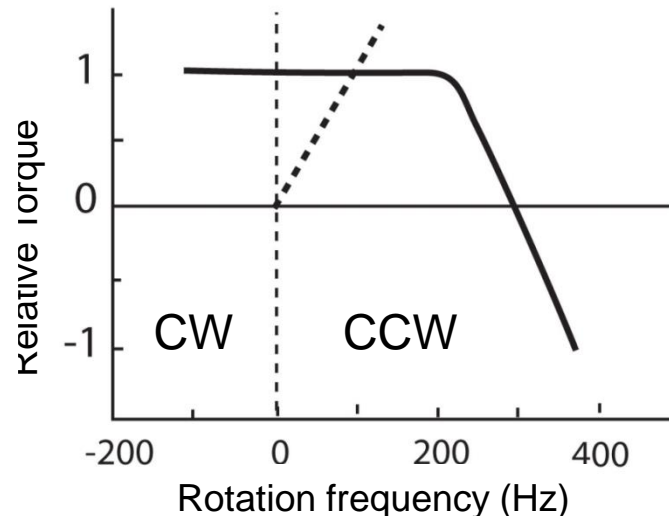
Characteristics of the Flagella Motor

(Berg 1993)

MotA is important for motor function.



Using a deletion mutant of E.coli, i.e. removing the protein from the genome, it can be shown that MotA is the relevant subunit. It can be reincorporated by gene transfer using bacteriophages. Each additional motor unit increases the rotation frequency in quantized steps.



Determine motor characteristics by attaching a single bacterium to a surface. Attaching a colloid of known diameter you can determine the rotation frequency and use drag force to extract torque M .

$$M = \gamma_{colloid} \omega \approx 3 \cdot 10^{-18} \text{ Nm}$$

Change of colloid diameter can be used to measure torque, as direct torque measurements are difficult with MT. The torque is independent over a wide range of frequencies.